

JAN 2022 DIAGNOSIS LIST

22-0101: somatic yolk sac tumor (uterus; GYN path)

22-0102: BCOR sarcoma (spinal cord; soft tissue pathology)

22-0103: “Solid tubulocystic” variant of cholangiocarcinoma (“cholangioblastic” variant)
(liver; GI path)

22-0104: membranoproliferative pattern glomerulonephritis with mixed
cryoglobulin (kidney; medical renal path)

22-0105: basal cell carcinoma (prostate; GU path)

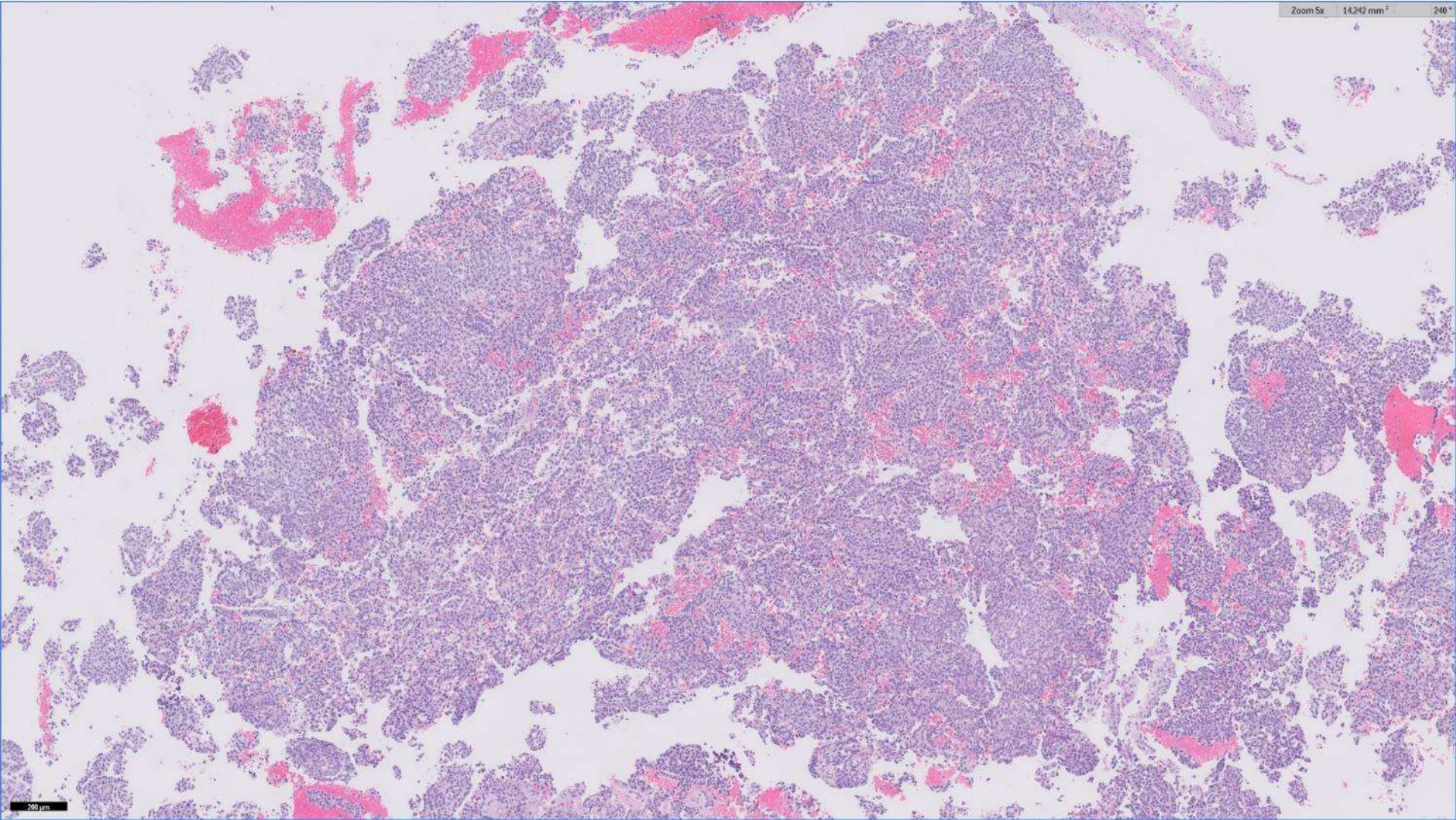
22-0106: brain (IgG4-related disease; neuropath & hemepath)

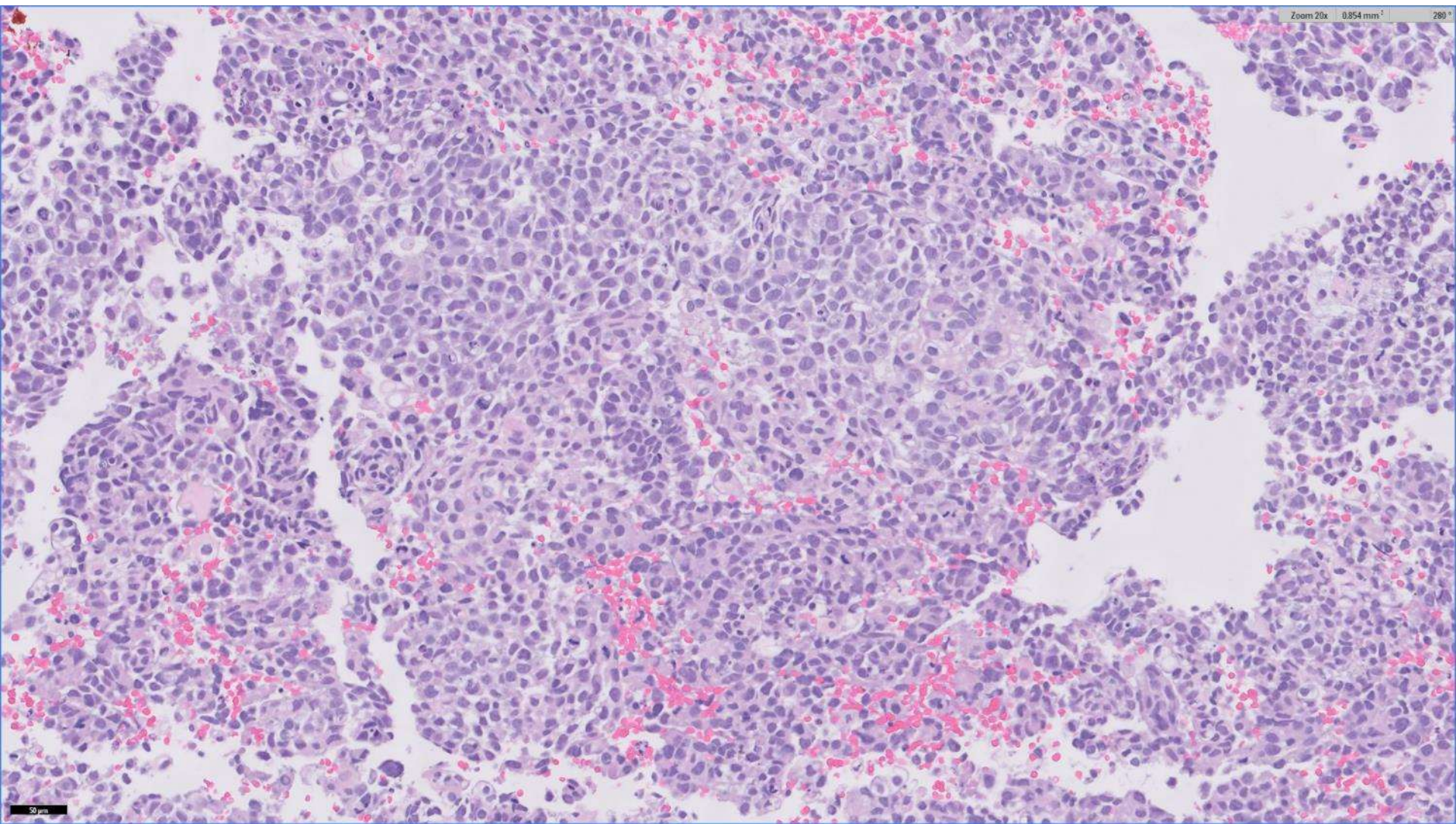
22-0107: sarcomatoid acquired cystic disease associated renal cell carcinoma
(kidney; GU path)

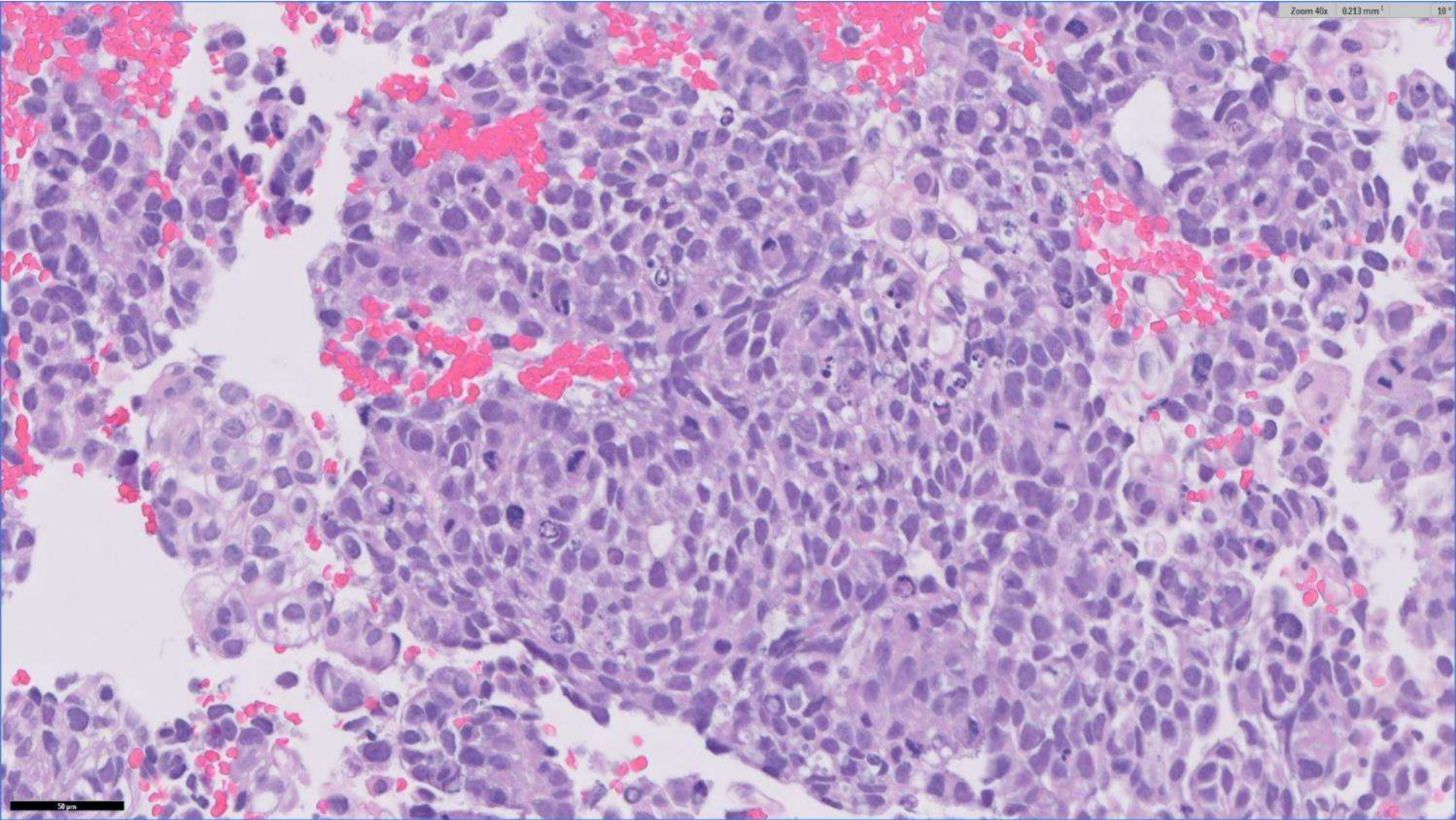
22-0101

Amanda Borgen/Nicholas Ladwig; UCSF

82-year-old F with post-menopausal bleeding and an enlarged uterus who underwent endometrial biopsy.

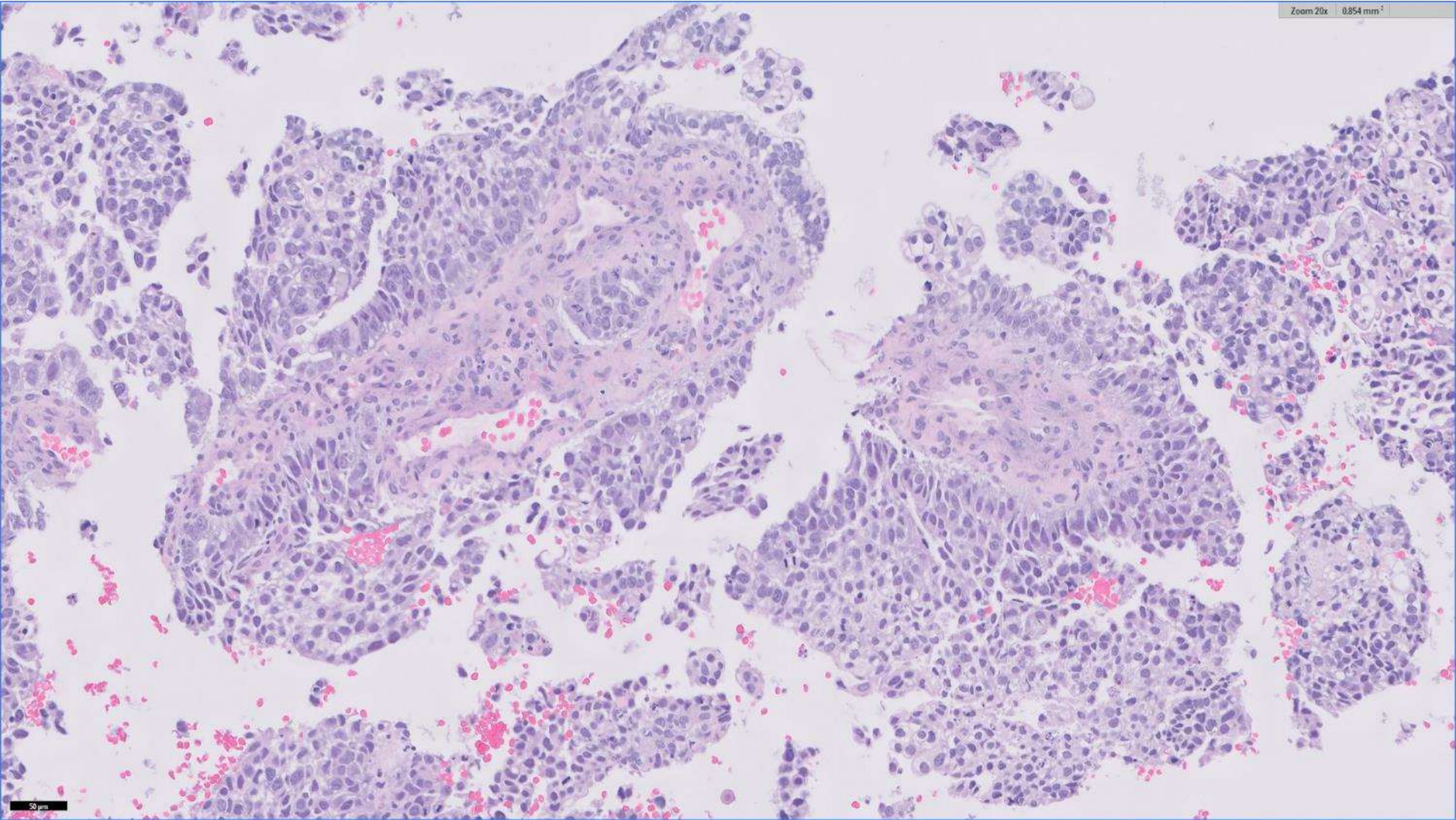






Zoom 40x 0.213 mm² 10°

50 µm



FISH testing

- Negative for *SS18* and *BCOR* rearrangements

NGS Panel

- Positive for *BCOR-CCNB3* fusion

Sarcoma with *BCOR* alteration

- Recently defined undifferentiated sarcoma, predominately arising in children
 - *BCOR-CCNB3* age range is 2-44 years, median 15 years
 - *BCOR-MAML3* and *BCOR-ZC3H7B* fusions more frequent in adults (median age 39 years, range 5-70 years)
 - *BCOR*-ITD and primitive myxoid mesenchymal tumor of infancy occur within 1st year of life
- Male predominance (M:F ~4.5:1)
- *BCOR-CCNB3* sarcoma
 - Frequently arise in bones of the pelvis/sacrum and lower extremities
 - Other locations reported include kidney and soft tissues of the head and neck, trunk, and extremities
- Sarcoma with *BCOR* internal tandem duplication
 - More often occur in soft tissues of the trunk, retroperitoneum, and head and neck
 - Includes primitive myxoid mesenchymal tumor of infancy
- 5-year survival of 72-80%
 - Sites of metastases include lung, bone, liver

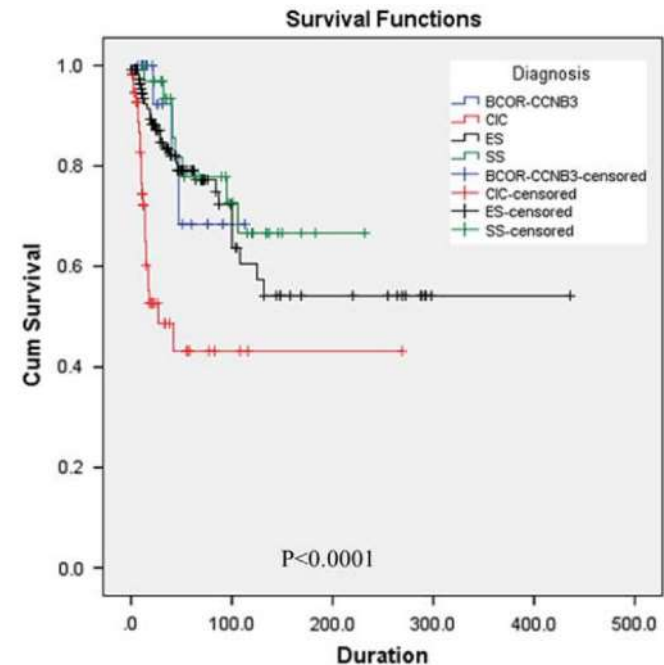


FIGURE 7. OS of 22 BCS (blue), 121 ES (black), 34 SS (green), and 57 *CIC*-rearranged sarcomas (red). BCS was associated with a more favorable outcome compared with *CIC*-rearranged sarcoma ($P=0.005$), whereas no significant survival difference was noted between BCS and ES ($P=0.738$) or BCS and SS ($P=0.802$). Duration is shown in months.

Histology and immunohistochemistry

- Proliferation of cells with hyperchromatic nuclei and eosinophilic to clear cytoplasm arranged in sheets with varied architecture and morphology including:
 - Round cells
 - Spindle cells arranged in fascicles
 - Myxoid background
 - Collagenous stroma
 - Whorl formation
 - Perivascular condensation
 - Delicate capillary network
- Mitotic activity is variable; necrosis may be present
- IHC: BCOR, SATB2, TLE1, BCL1+, PAX7, CD99+ ~50% of cases
 - CyclinB3+ in cases with *BCOR-CCNB3*
 - S100, Sox10, CK negative; EMA typically negative
- DDx
 - Ewing Sarcoma
 - Monophasic synovial sarcoma
 - Desmoplastic small round cell sarcoma
 - Rhabdomyosarcoma
 - Malignant peripheral nerve sheath tumor
 - Small cell osteosarcoma
 - *CIC-DUX4* sarcoma

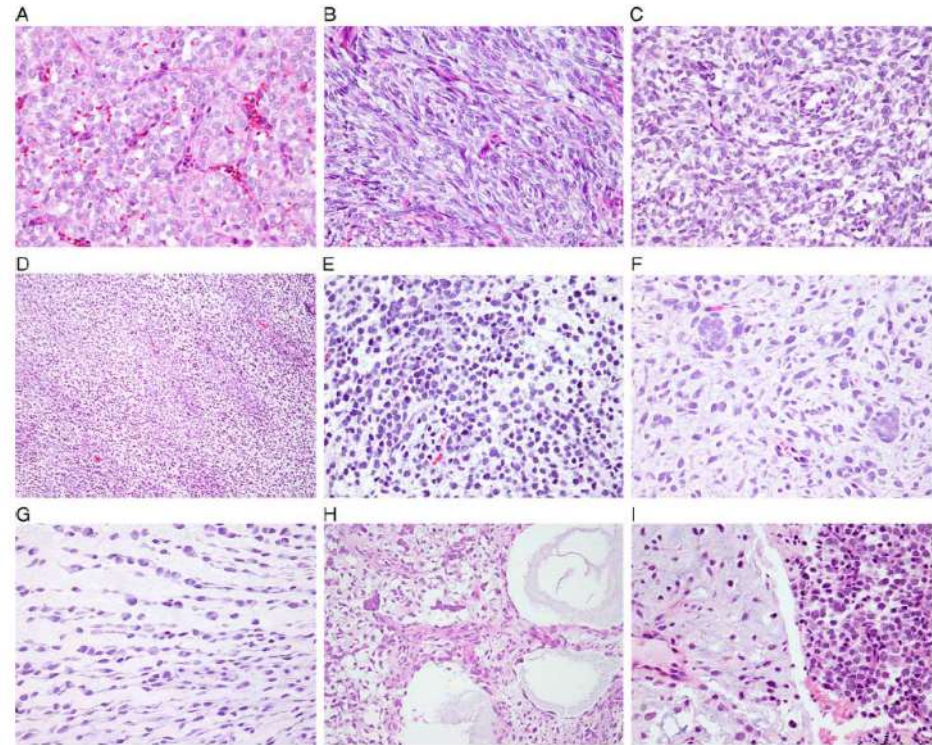


FIGURE 1. Histologic spectrum of BCS with round to spindle cells and occasional myxoid stroma. A, A predominant round cell morphology with uniform nuclei, fine chromatin pattern, and delicate vascular network. B, Monomorphic spindle cell morphology arranged in a fascicular pattern, reminiscent of SS. C, Short spindle to ovoid cells with vague whorling pattern. D, Alternating hypercellular and hypocellular areas, mimicking MPNST. E, Small amount of myxoid stroma between loosely arranged tumor cells is a common finding. Less common features includes: cell clustering (F), cord-like arrangement (G), and microcystic formation (H). I, Sharp contrast of hypercellular round cell component and hypocellular myxoid area.

BCOR-CCNB3

- BCOR is a corepressor associated with BCL6 and a component of the polycomb complex PRC1.1, associated with chromatin remodeling and histone modification
 - *BCOR* is located at Xp11.4
 - Fusions frequently involve exon 15, which includes a binding domain responsible for protein-protein interaction and complex formation
 - Internal tandem duplications frequently involve the PUFD domain
- CCNB3 is a cyclin B protein involved in cell cycle control, primarily found in developing testicular germ cells
 - *CCNB3* also located on X chromosome; fusion results from paracentric inversions
 - Fusion to 3' end results in loss of an N-terminal destruction box motif

Other *BCOR*-altered tumors

- High-grade endometrial stromal sarcoma: *BCOR* ITD, *JAZF1-BCOR*, *EPC1-BCOR*, *ZC3H7B-BCOR*
- CNS tumor with *BCOR* internal tandem duplication: *BCOR* ITD
- Clear cell sarcoma of the kidney: *BCOR* ITD
- Primitive myxoid mesenchymal tumor of infancy: *BCOR* ITD
- Ossifying fibromyxoid tumor (aggressive subtypes): *ZC3H7B-BCOR*
- Acute myeloid leukemia: *BCOR-RAR α*

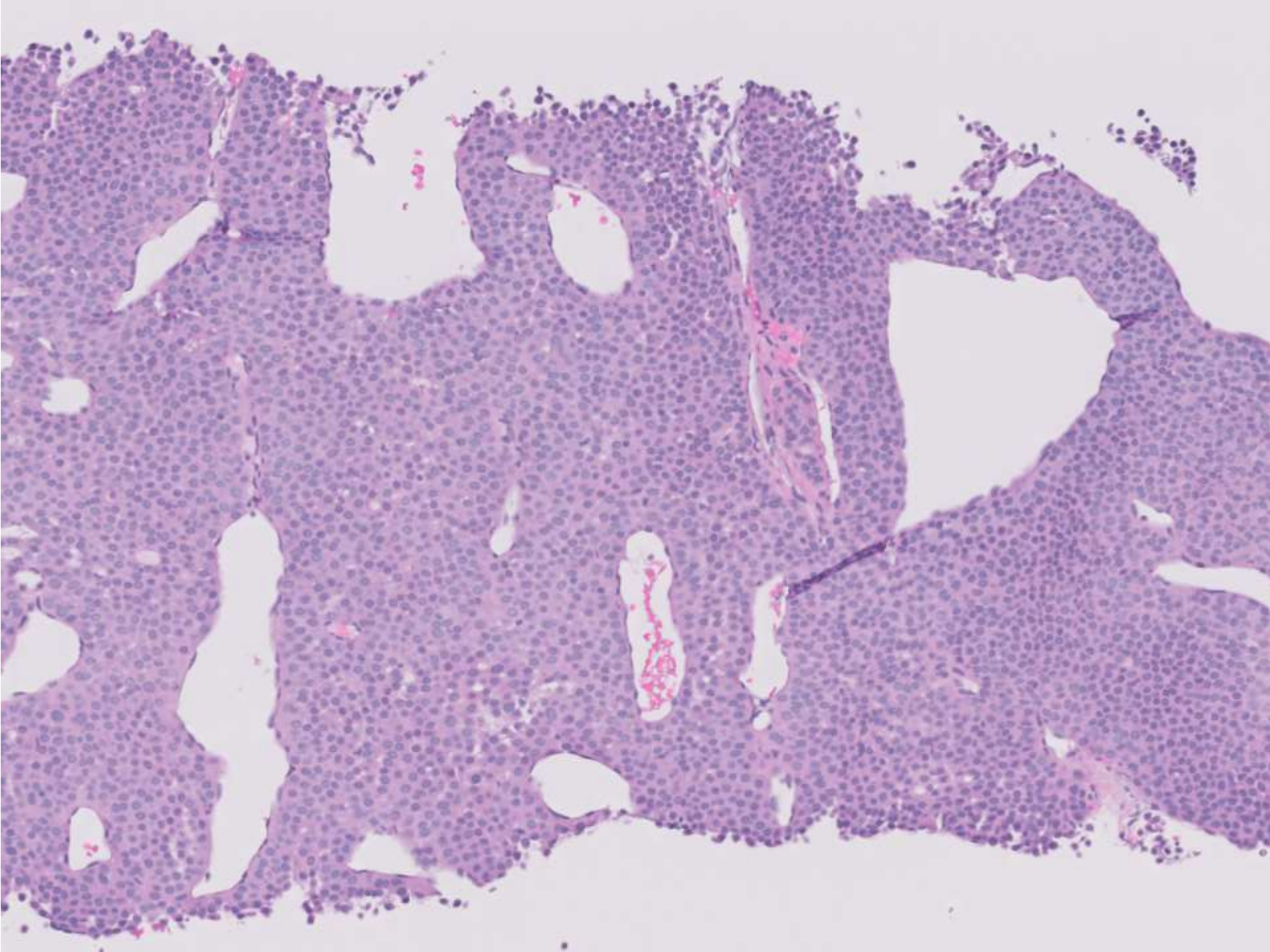
References

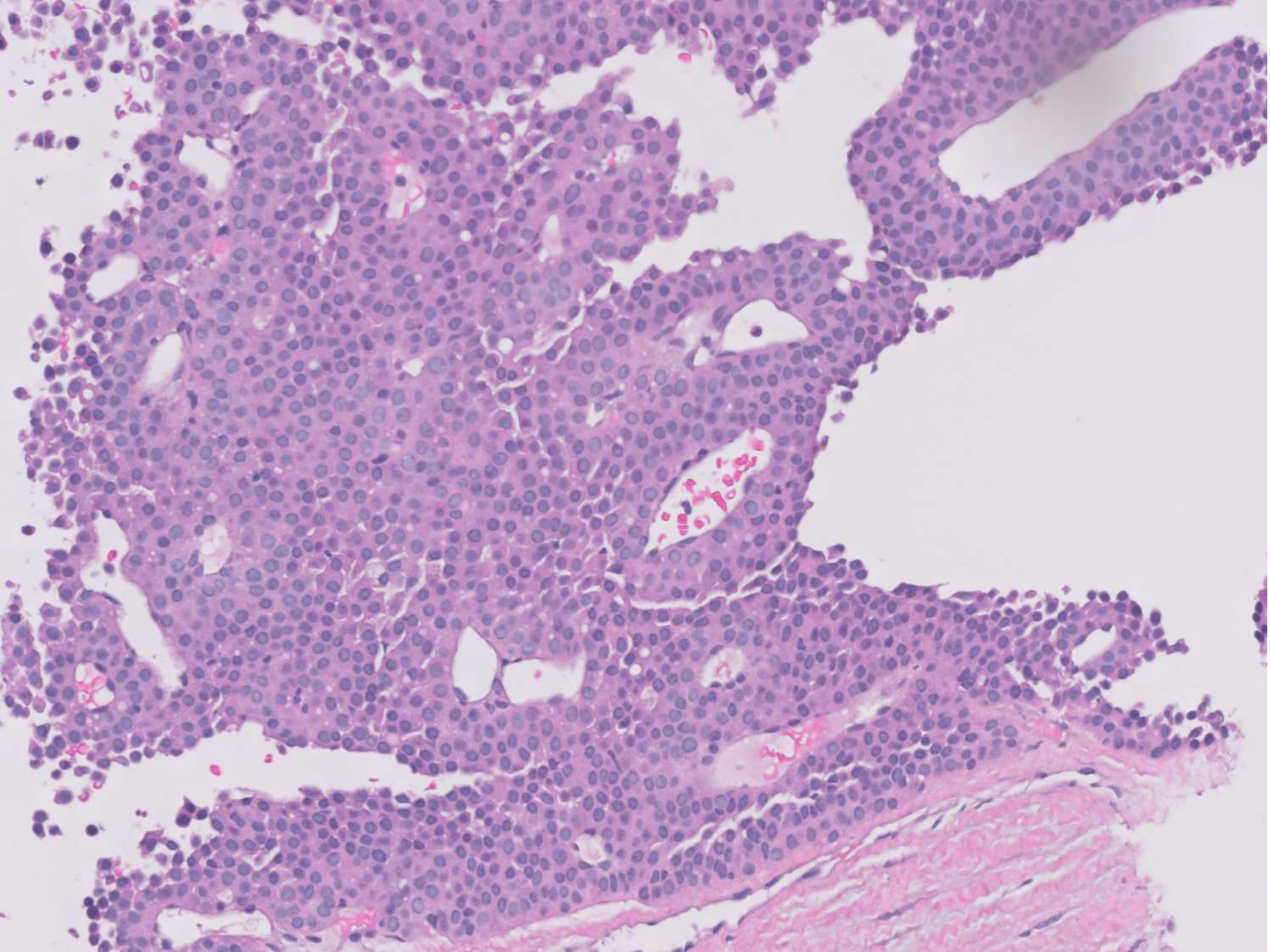
- Kao YC, Owosho AA, et. al. BCOR-CCNB3 Fusion Positive Sarcomas: A Clinicopathologic and Molecular Analysis of 36 Cases With Comparison to Morphologic Spectrum and Clinical Behavior of Other Round Cell Sarcomas. *Am J Surg Pathol*. 2018 May;42(5):604-615.
- Specht K, Zhang L, et. al. Novel BCOR-MAML3 and ZC3H7B-BCOR Gene Fusions in Undifferentiated Small Blue Round Cell Sarcomas. *Am J Surg Pathol*. 2016 Apr;40(4):433-42.
- Machado I, Navarro S, Llombart-Bosch A. Ewing sarcoma and the new emerging Ewing-like sarcomas: (CIC and BCOR-rearranged-sarcomas). A systematic review. *Histol Histopathol*. 2016 Nov;31(11):1169-81.
- Toki S, Wakai S, Sekimizu M, et. al. PAX7 immunohistochemical evaluation of Ewing sarcoma and other small round cell tumours. *Histopathology*. 2018 Oct;73(4):645-652.

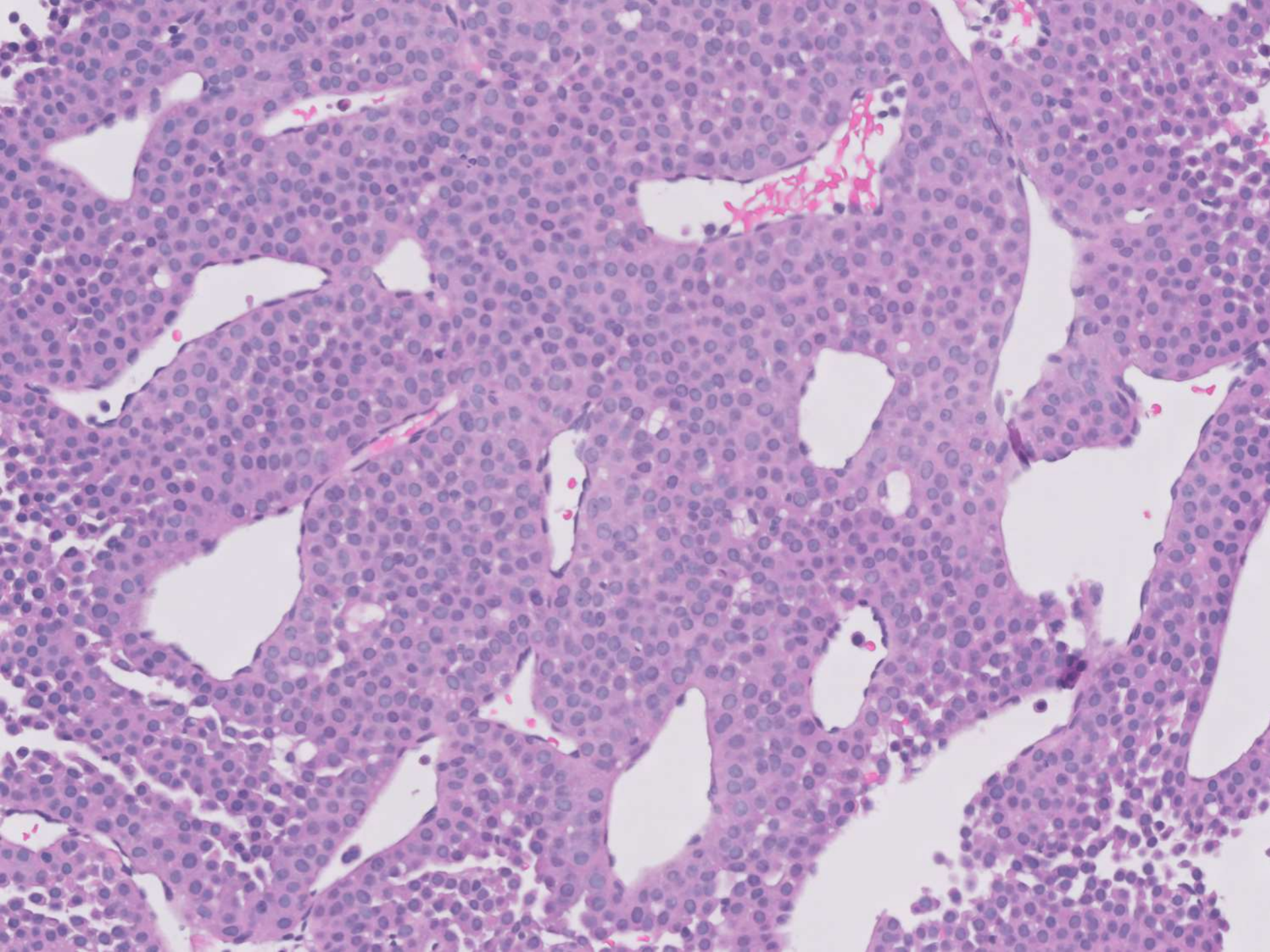
22-0103

Sanjay Kakar; UCSF

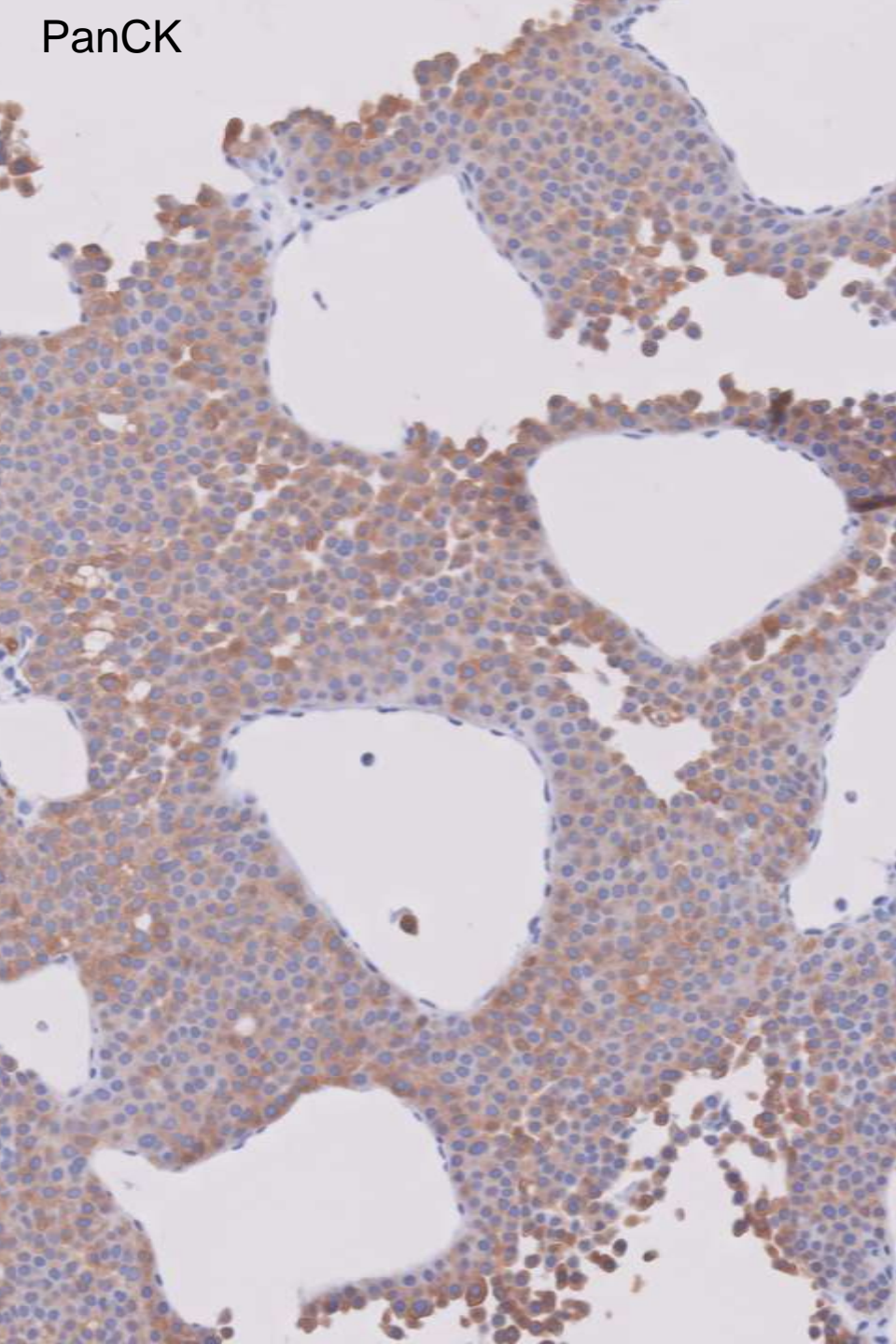
23-year-F with multiple liver masses in segments 7 and 8, largest measuring 23cm (others 4-5cm), without extrahepatic mass and no history of liver disease.



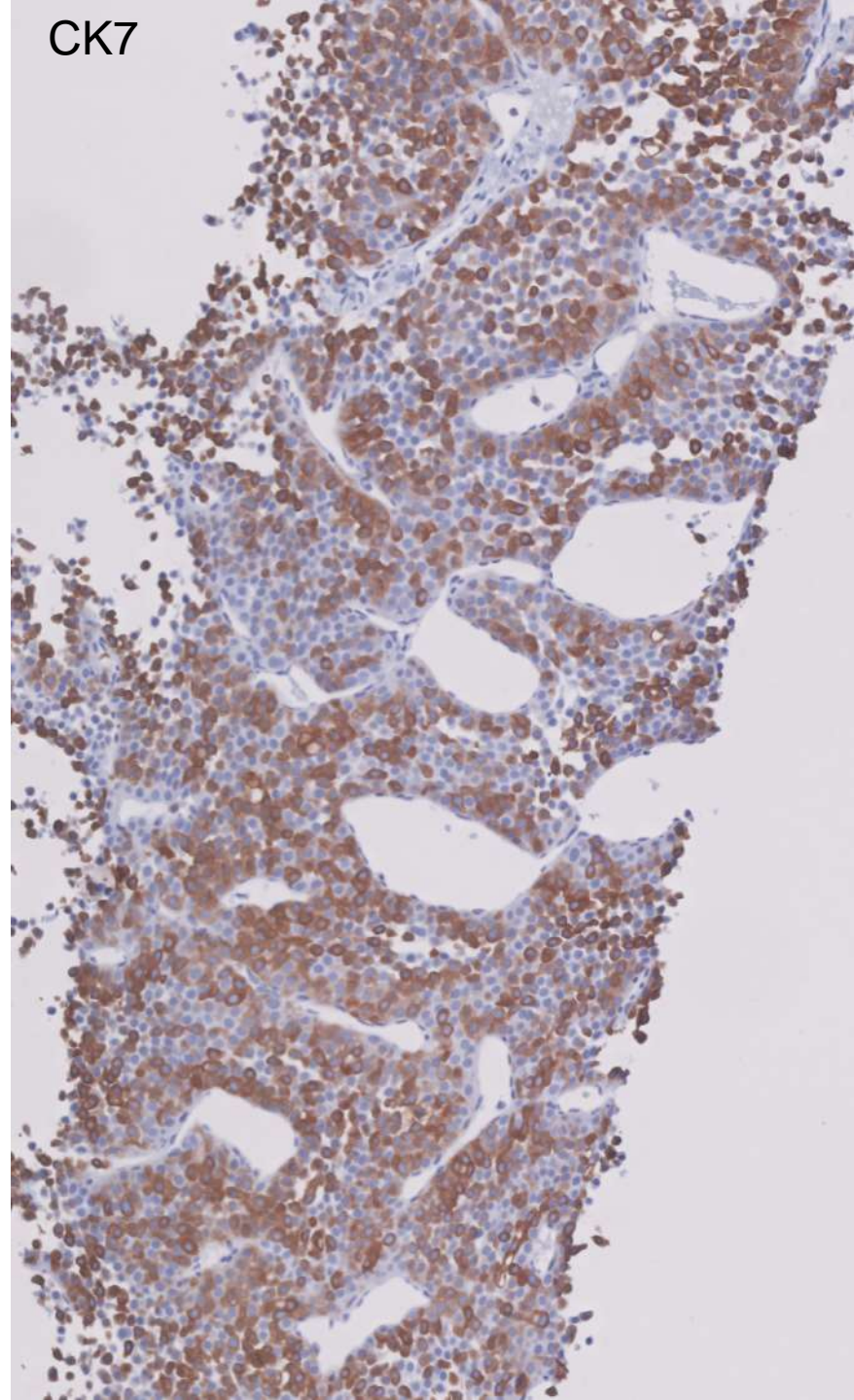




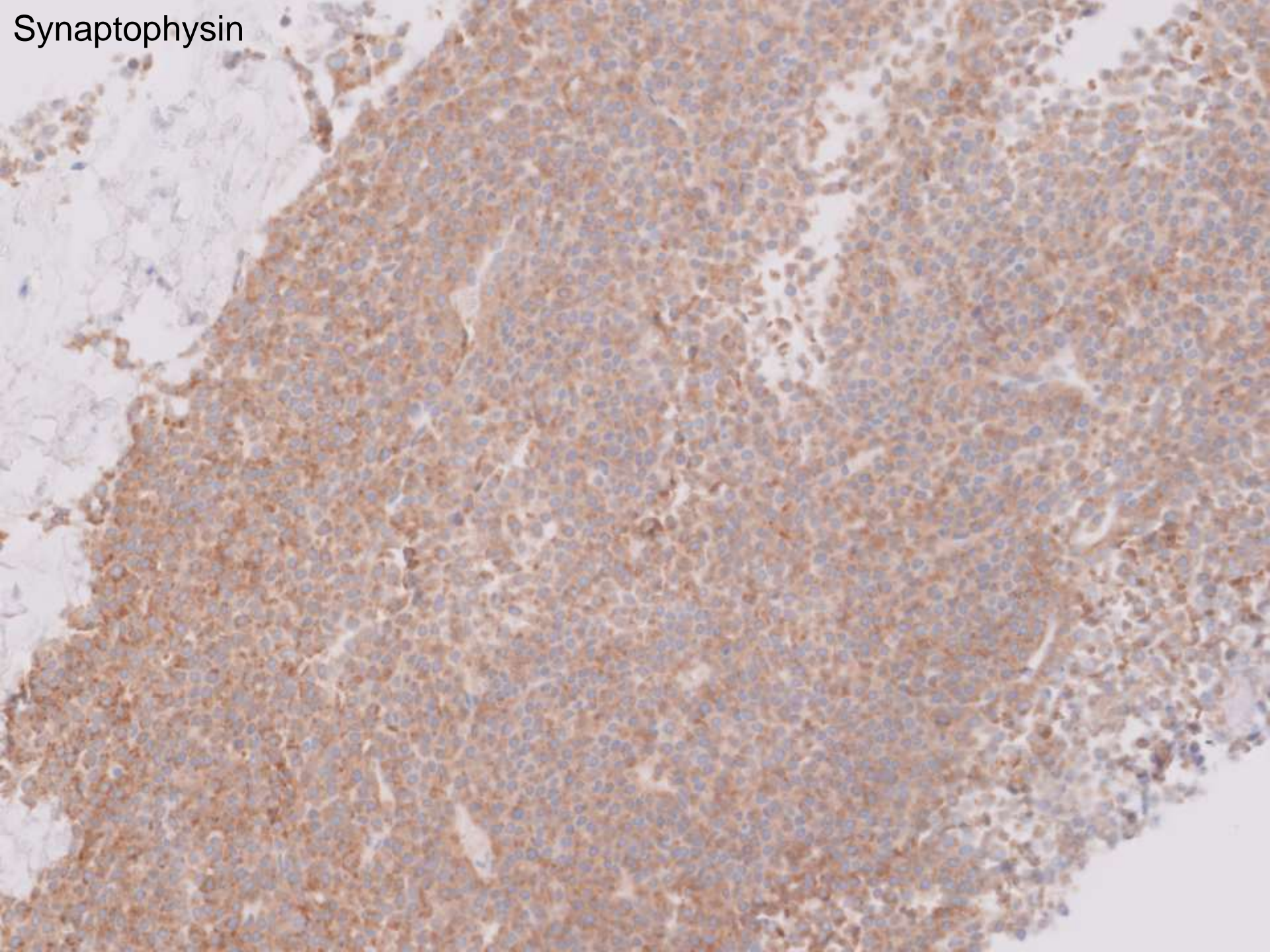
PanCK



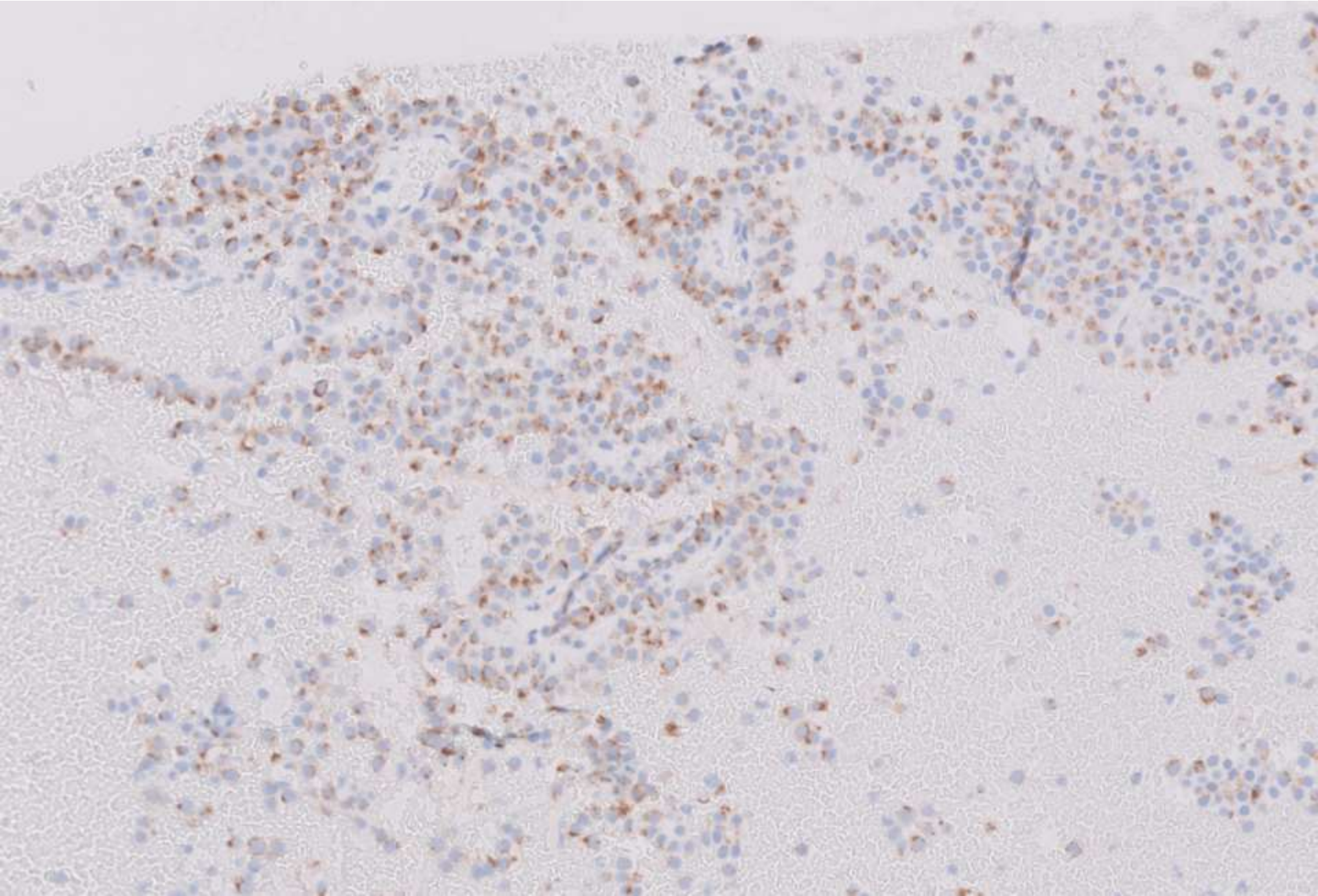
CK7



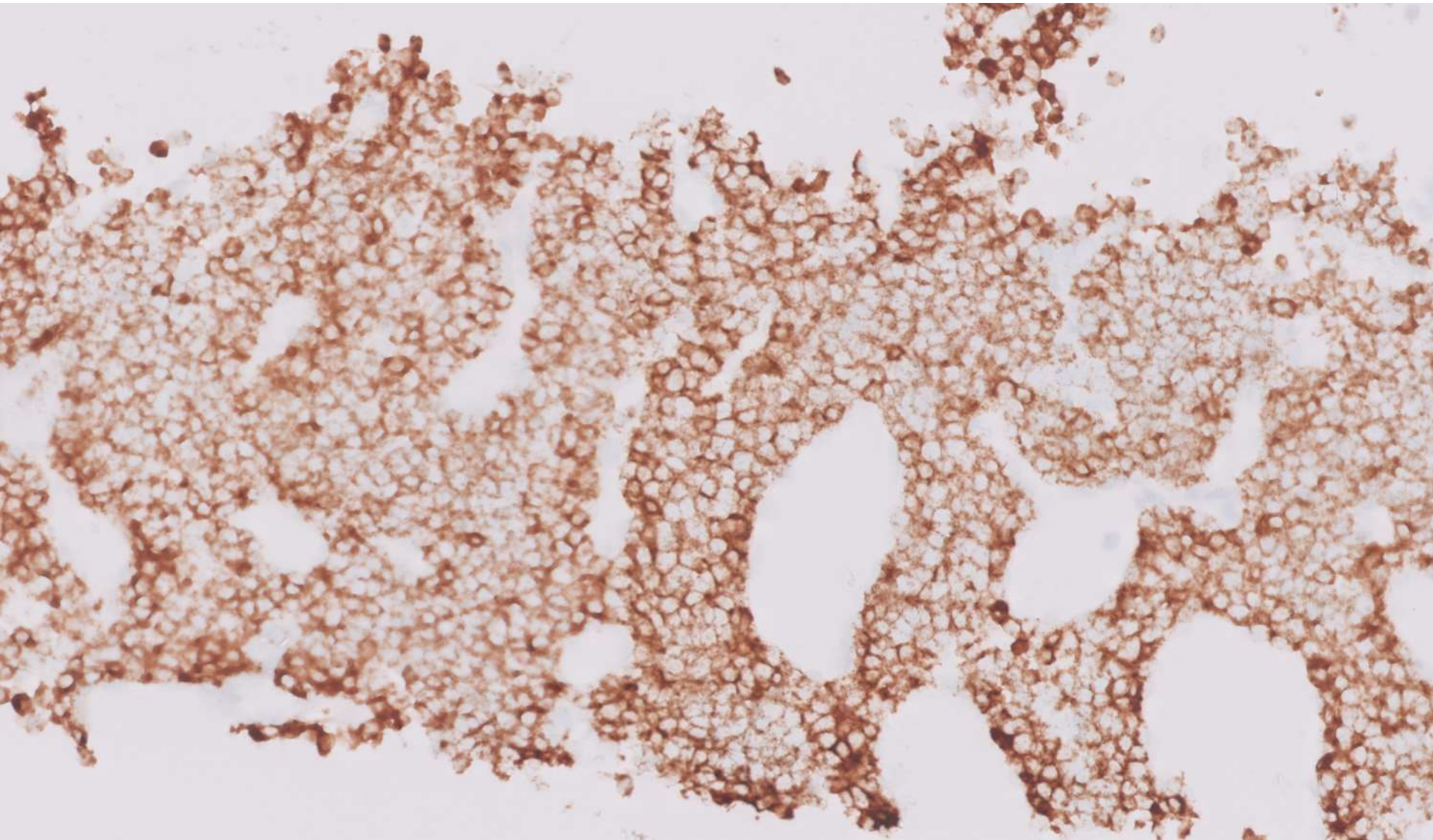
Synaptophysin



Chromogranin (cell block)



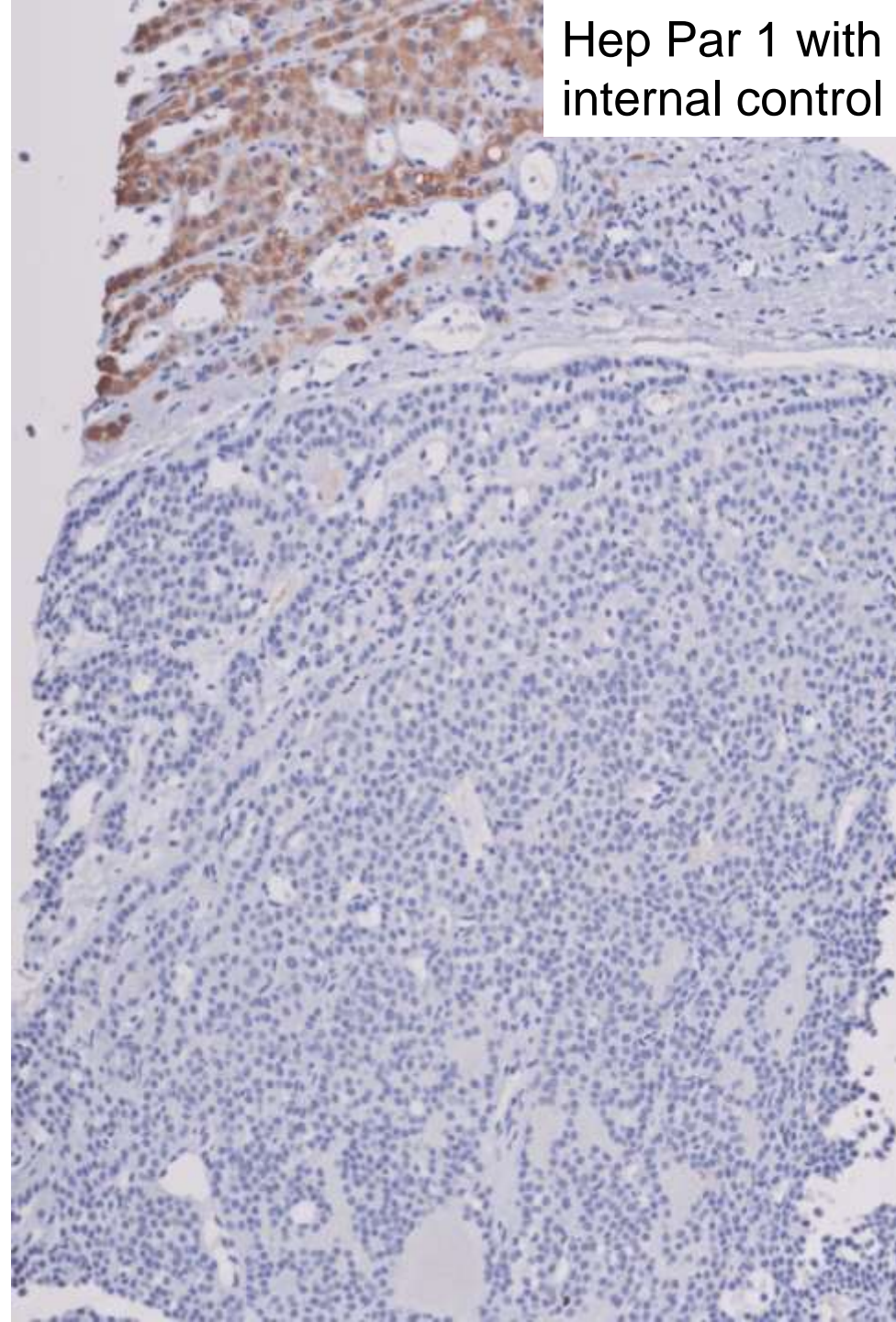
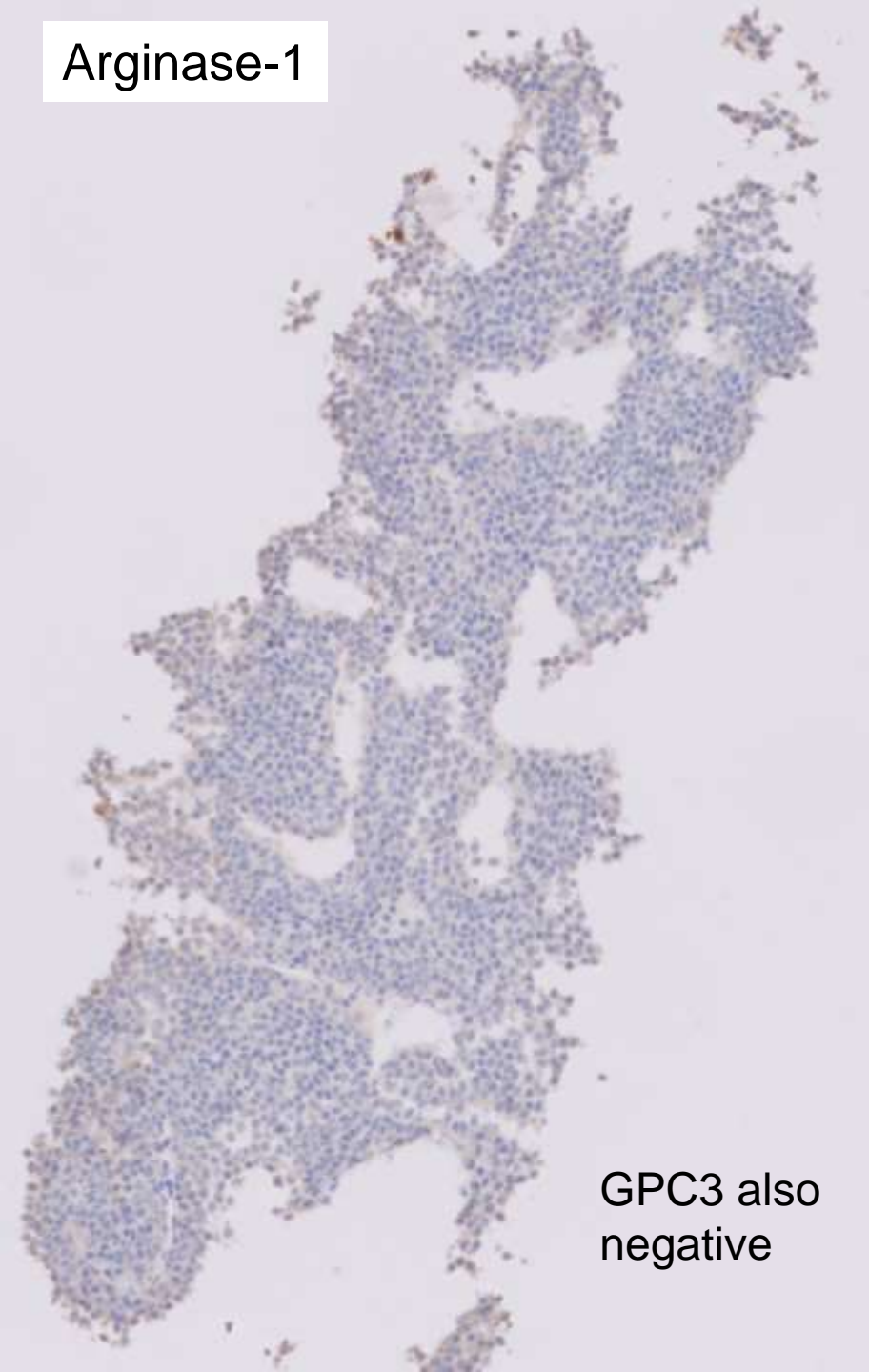
Albumin ISH

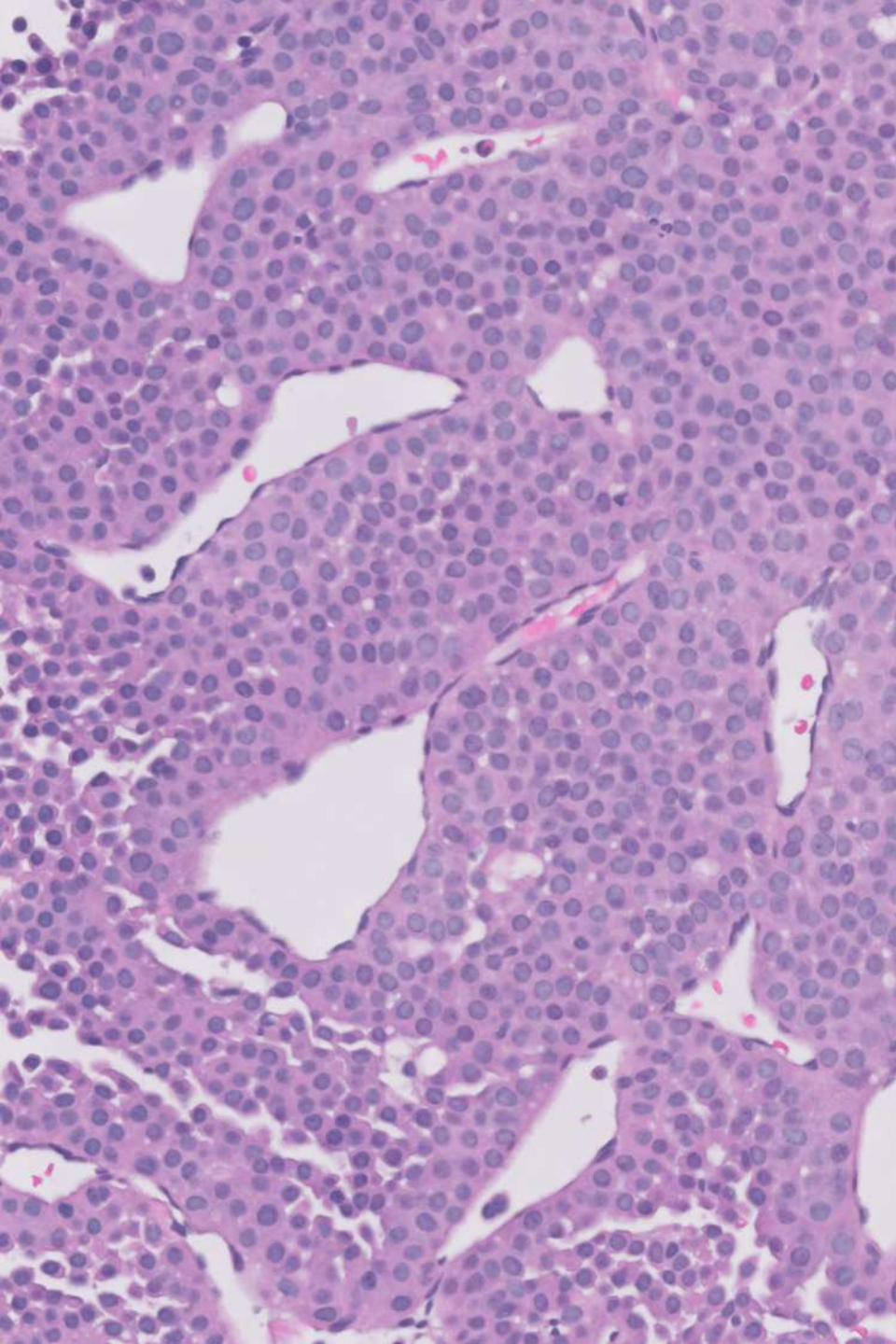


Arginase-1

GPC3 also
negative

Hep Par 1 with
internal control



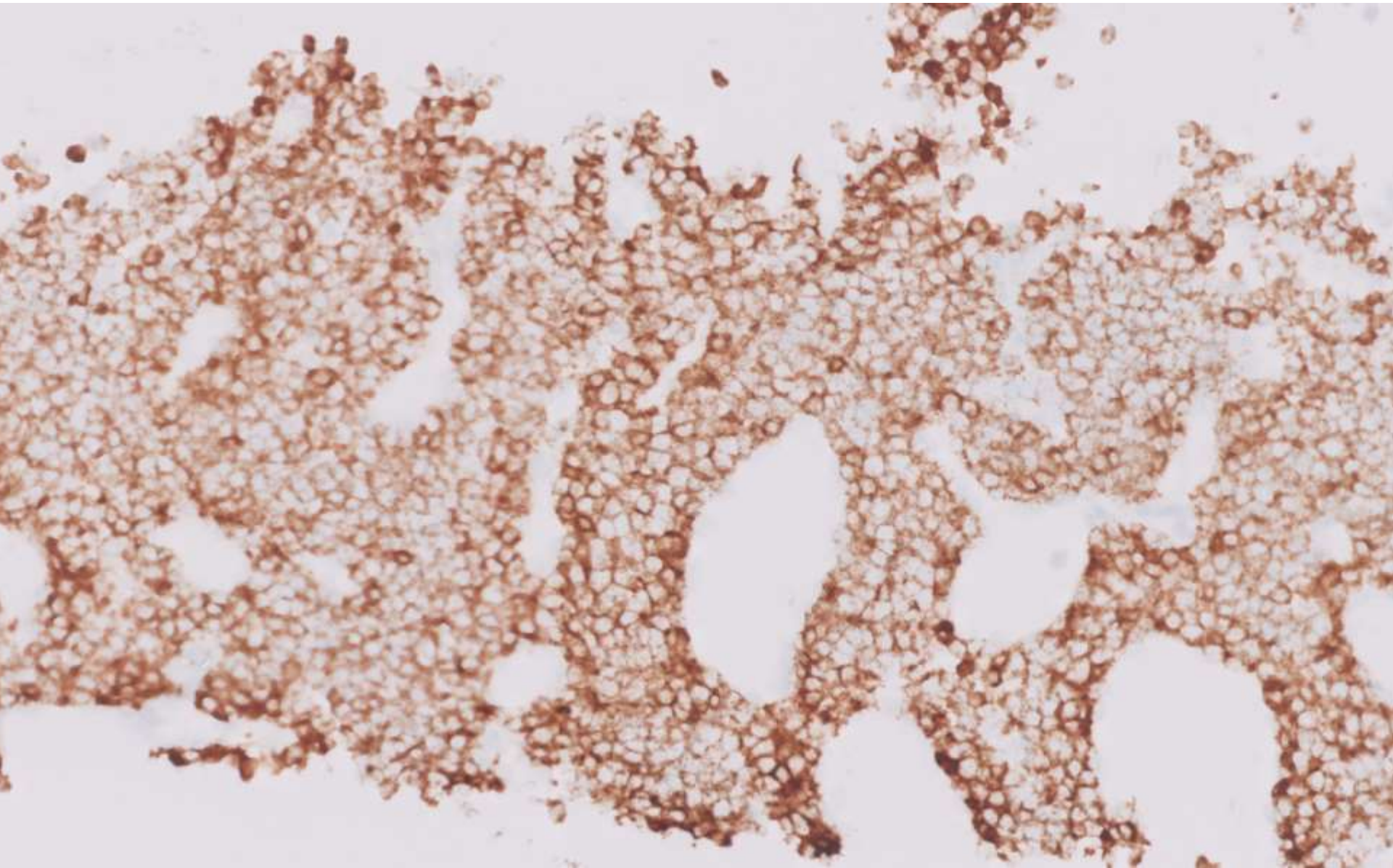


Differential diagnosis

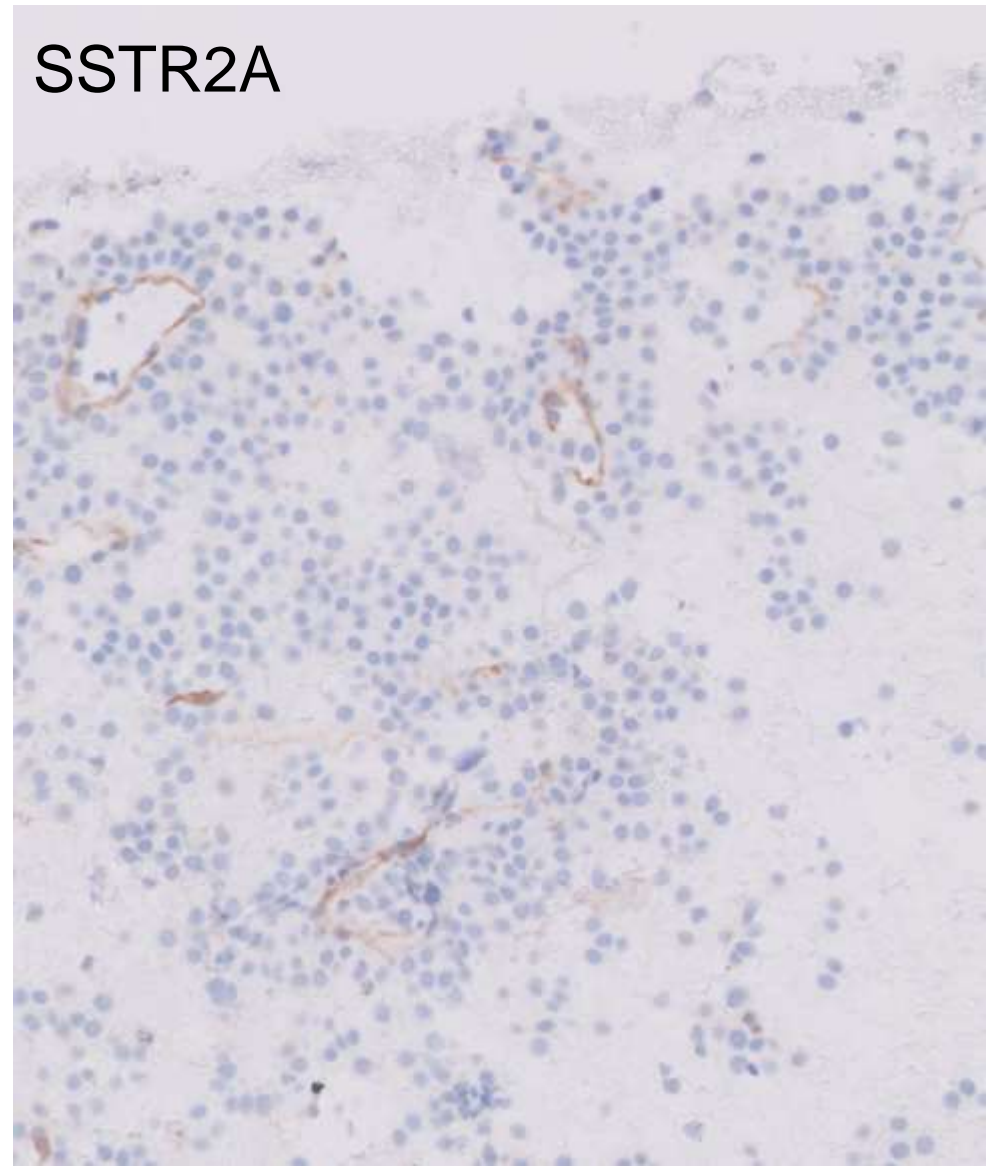
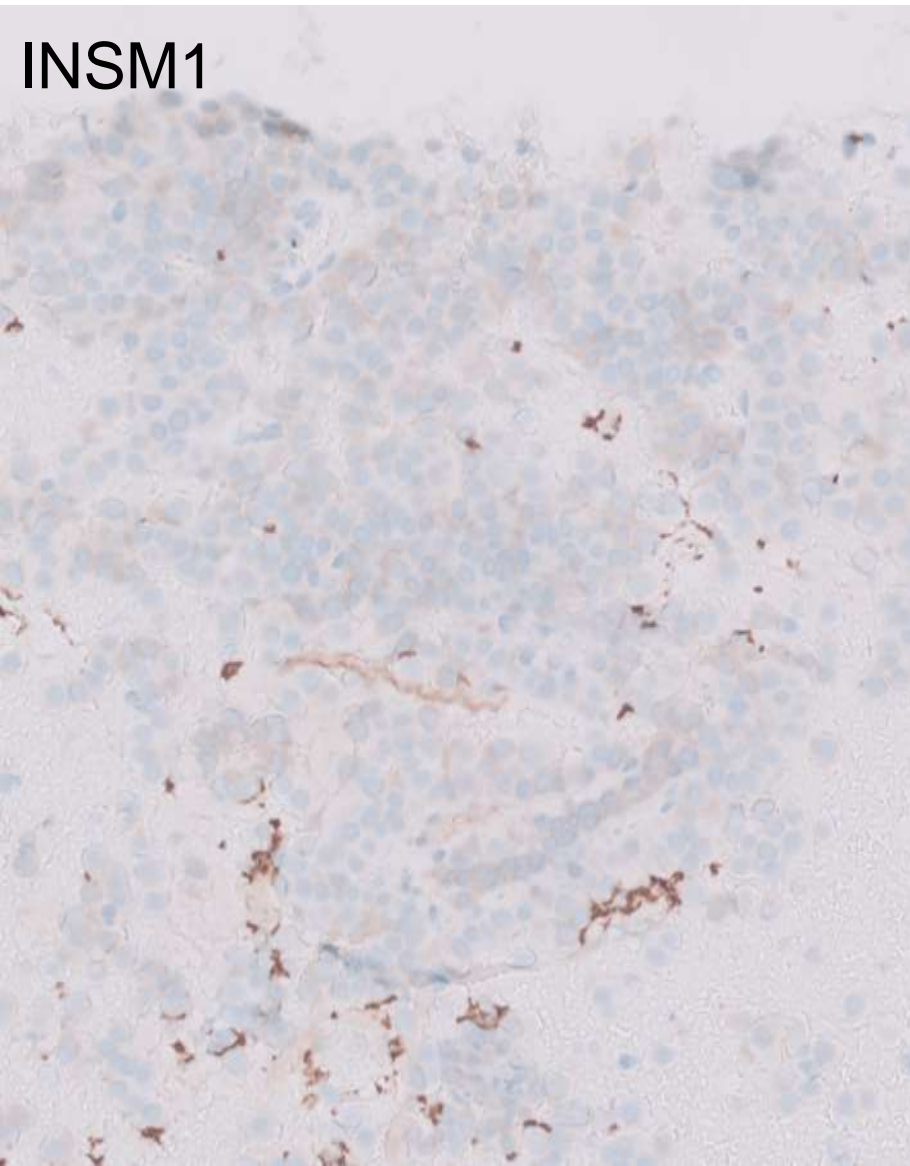
- Neuroendocrine neoplasm
- Hepatocellular carcinoma

Marker	Result
PanCK, CK7, CK19	Positive
Synapto Chromogranin	Patchy positive
Hep Par 1 Arginase Glypican-3	Negative

Albumin in situ hybridization



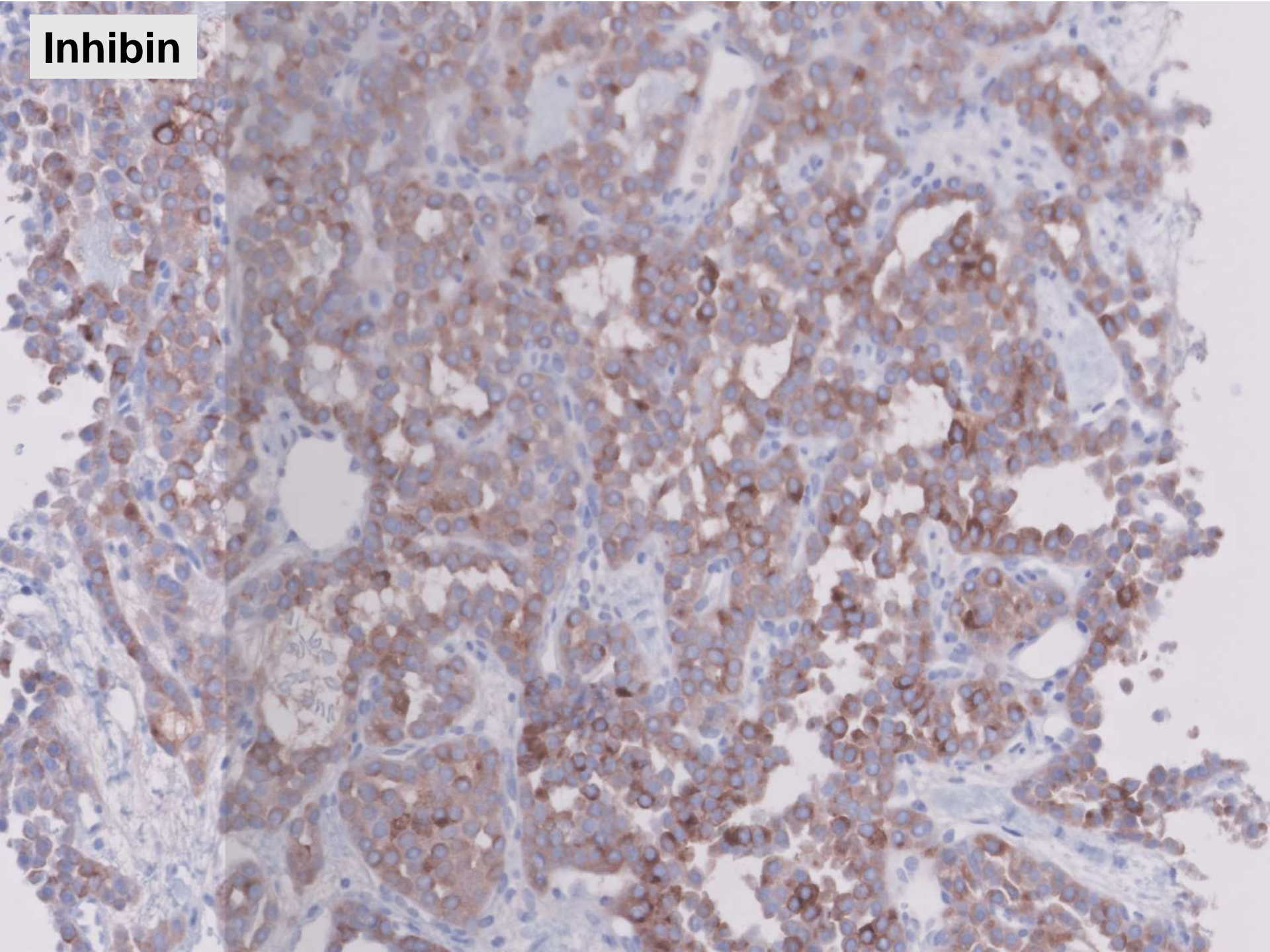
INSM1, SSTR2A: negative
No extrahepatic primary



Additional negative work-up

Category	Antibodies
Adrenocortical	SF1
Acinar cell carcinoma	Chymotrypsin
Mesothelial	WT1, calretinin
Other carcinomas	CDX2, GATA3, TTF1, PAX8
Mesenchymal	KIT, desmin, SOX10

Inhibin



Sex Cord Stromal Tumor

- Inhibin: positive
- Other markers: negative
FOXL2, calretinin, WT-1, SF-1
No ovarian/uterine mass

Albumin ISH+ve

Primary Liver Carcinoma

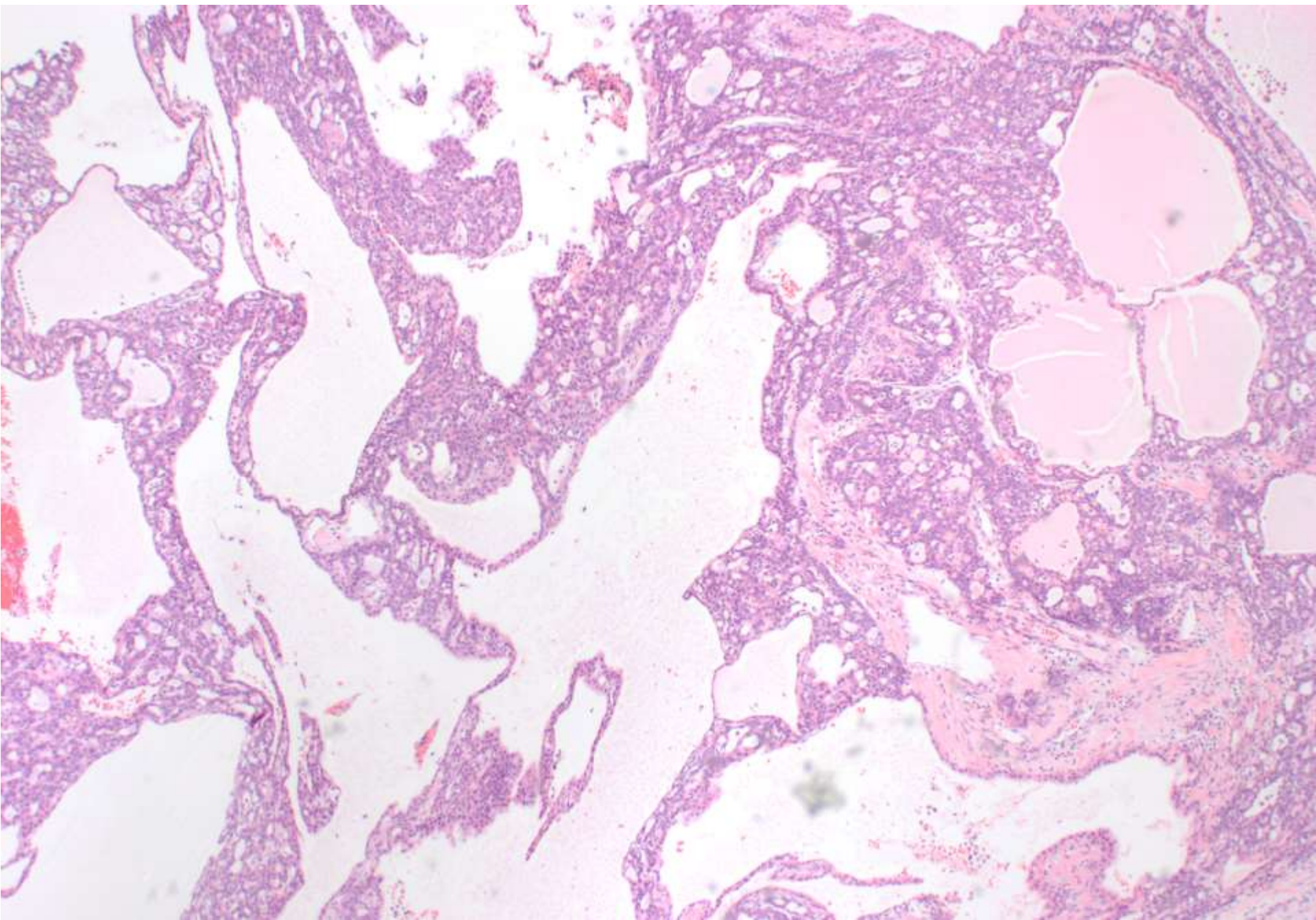
Primary Liver Carcinoma	IHC results
Hepatocellular carcinoma	Hep Par 1, arginase-1, glypican-3: negative
Intrahepatic cholangiocarcinoma (iCCA)	CK7, CK19: positive

Inhibin+ cholangiocarcinoma

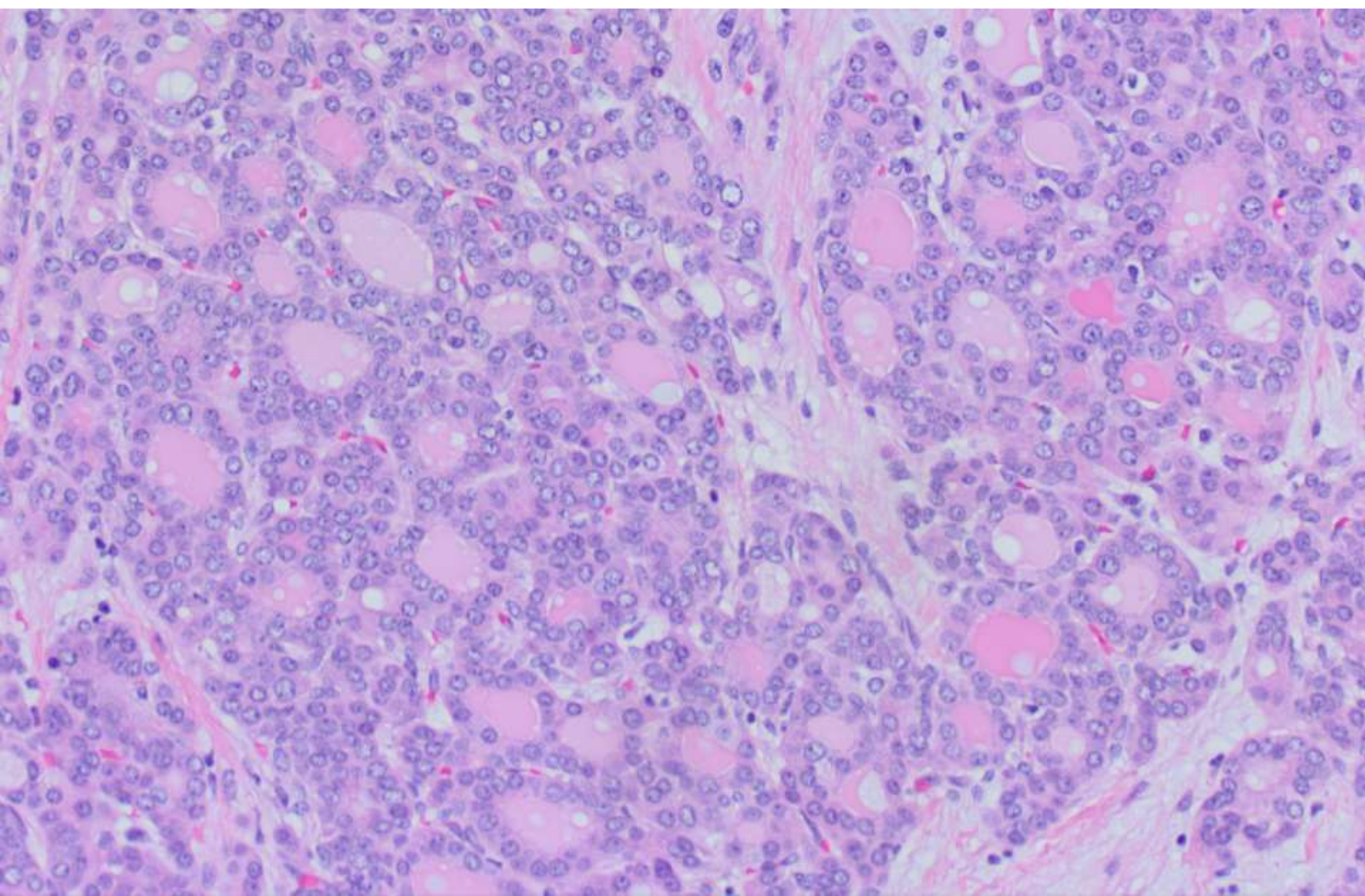
- Thyroid-like
- ‘Cholangioblastic’
- Solid-tubulocystic variant

Braxton, Hum Pathol 2017
Wen/Kakar, Hum Pathol 2021

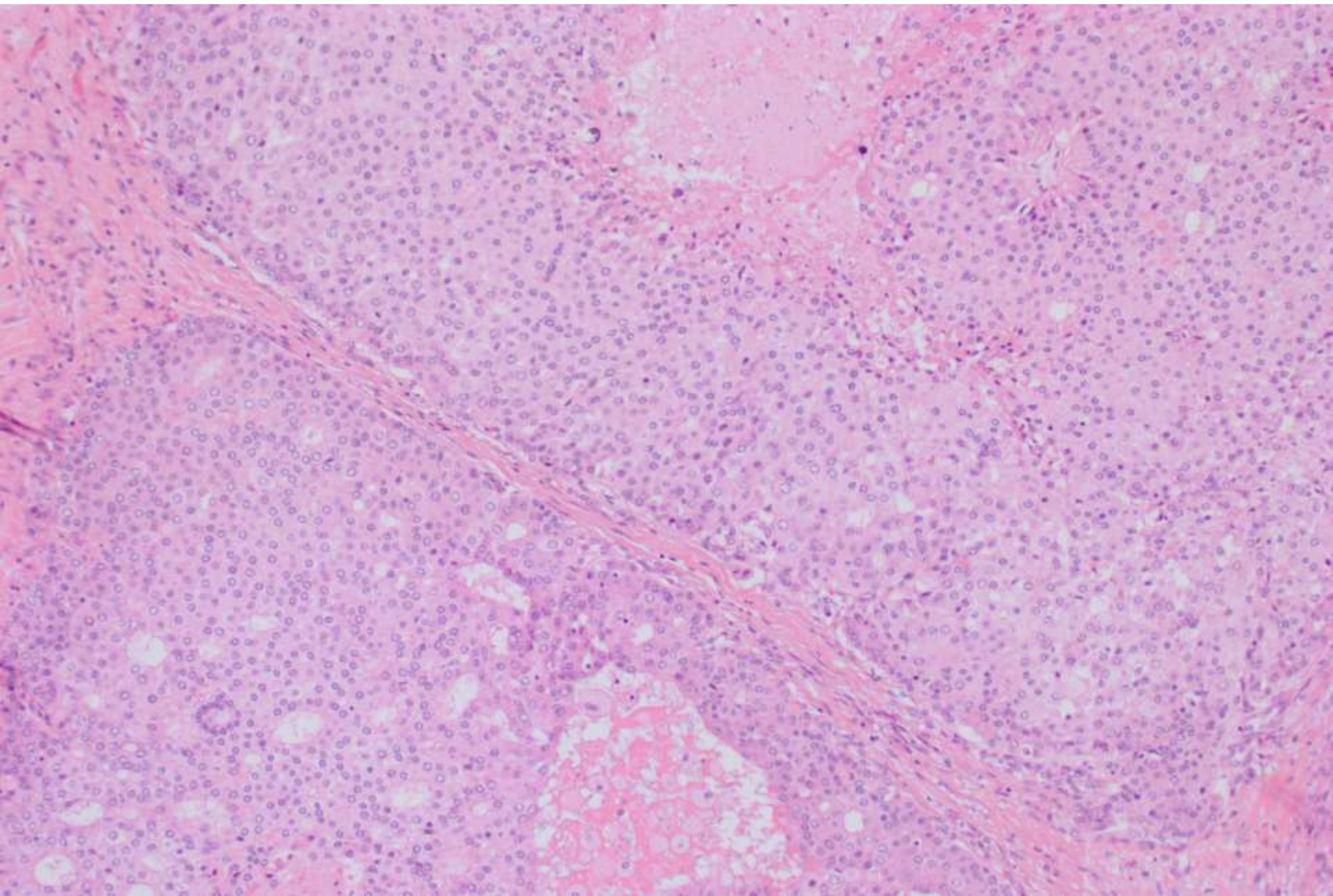
Tubular (thyroid-like) and cystic patterns



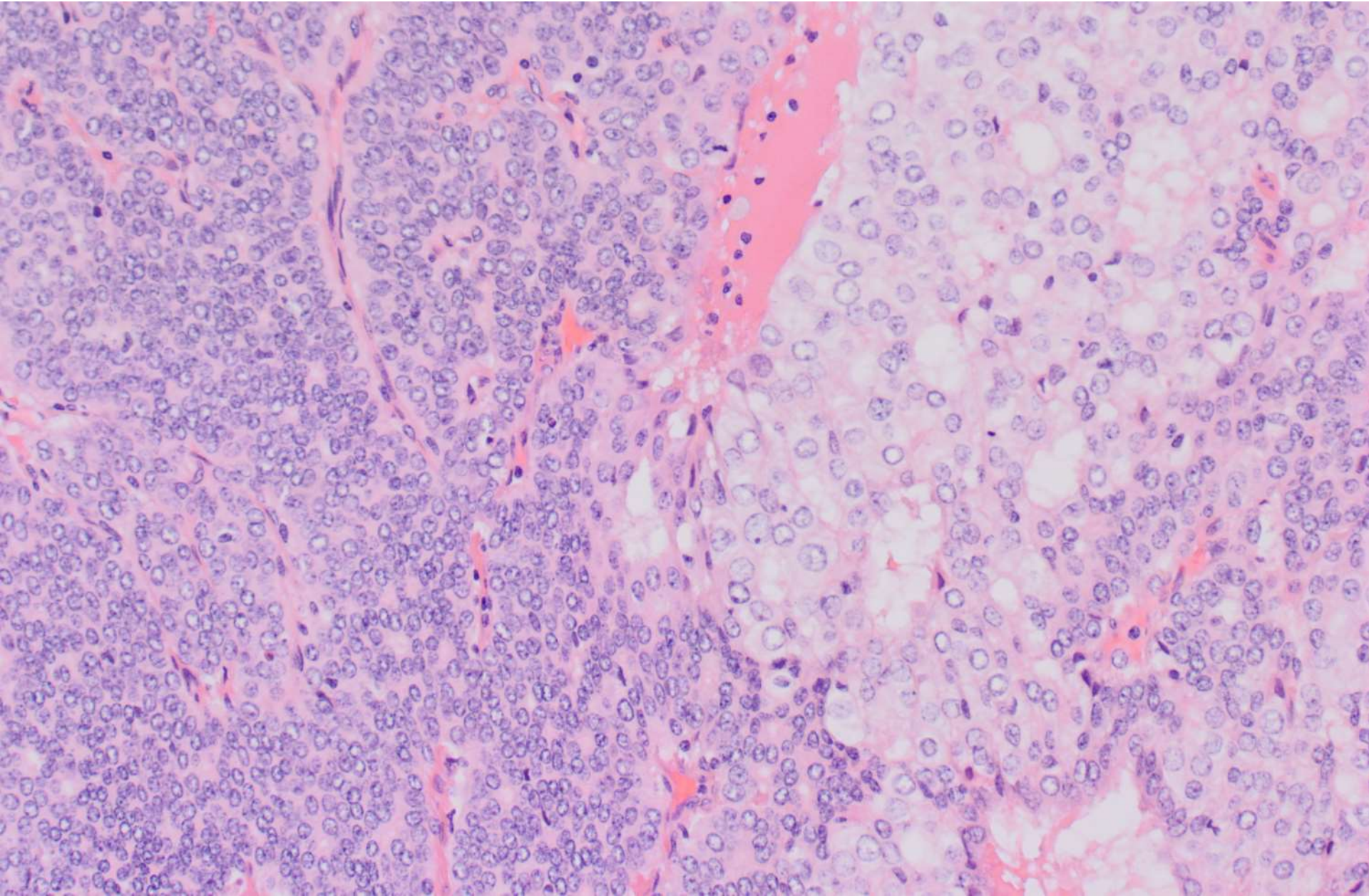
Tubular architecture: thyroid-like

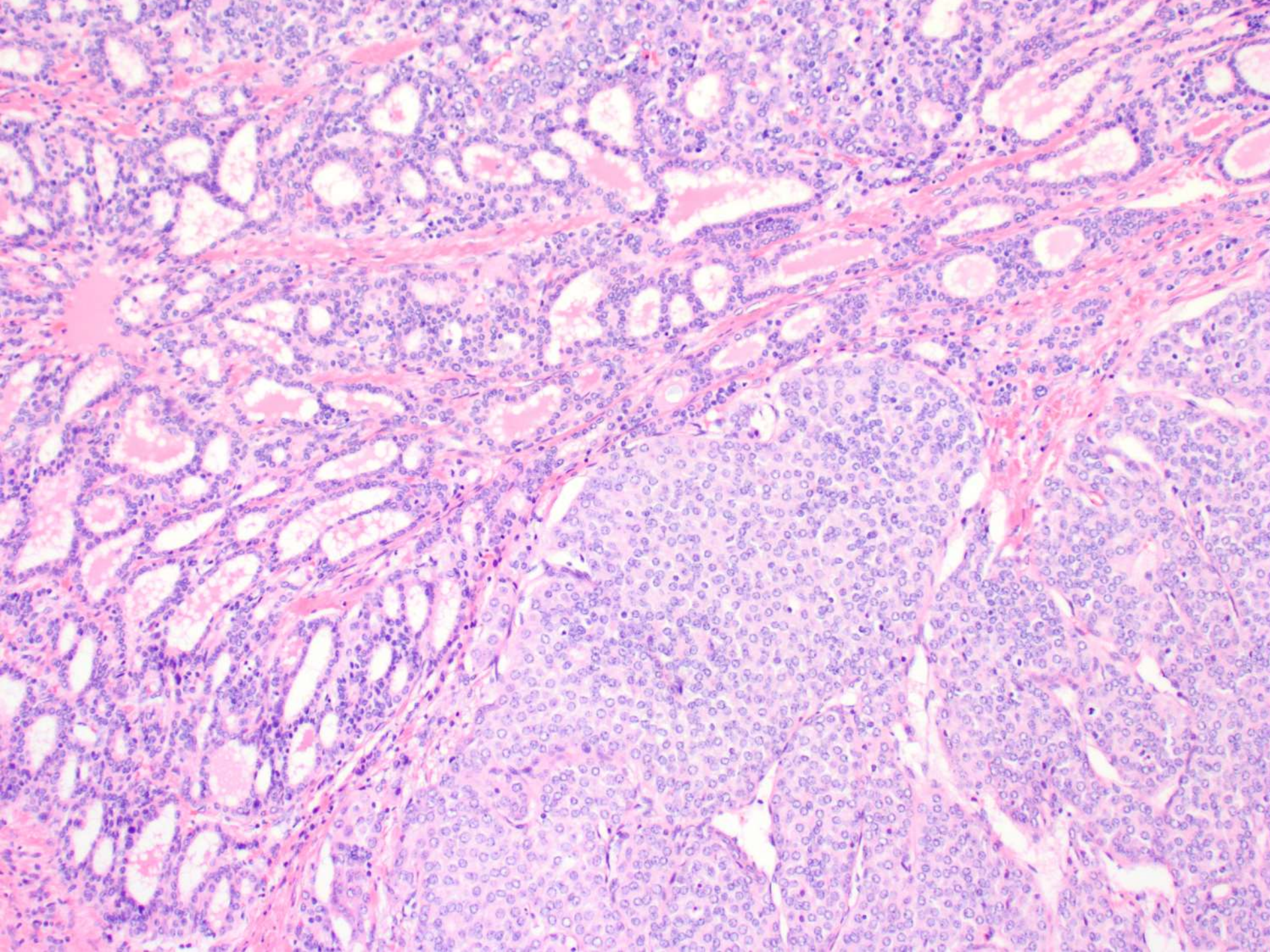


Solid (HCC-like) area



“Primitive” component and HCC-like area





Inhibin+ iCCA: Clinical course

Series	Outcome
Braxton, Hum Pathol 2017 (n=3)	2 had metastatic disease on follow-up, died within 4 years of diagnosis
UCSF series (n=6)	Recurrence/metastasis in 3 (50%) cases

Braxton, Hum Pathol 2017
Wen/Kakar, Hum Pathol 2021

Molecular changes in iCCA

Molecular changes	Frequency
<i>IDH1/IDH2</i>	12-36%
<i>BAP1</i>	19-25%
<i>PBRM1</i>	11-17%
<i>FGFR2</i> fusion	13%

None of these changes in inhibin-positive iCCA

Inhibin+ cholangiocarcinoma

Case Reports

> Am J Surg Pathol. 2021 Nov 1;45(11):1550-1560.

doi: 10.1097/PAS.0000000000001729.

A Novel NIPBL–NACC1 Gene Fusion Is Characteristic of the Cholangioblastic Variant of Intrahepatic Cholangiocarcinoma

- Novel *NIPBL-NACC1* gene fusion: 3 cases
- UCSF series: present in all 4 cases tested (unpublished data)

Diagnosis

- RNAseq: *NIPBL-NACC1* fusion
- Diagnosis: "Solid-tubulocystic variant of intrahepatic cholangiocarcinoma"
- Lung metastasis on further work-up
- Gemcitabine/cisplatin chemotherapy

Summary

"Solid-tubulocystic variant of intrahepatic cholangiocarcinoma"

- "Cholangioblastic": not preferred
- Large tumors in young women
- Albumin ISH, inhibin positivity
- Syn/Chr patchy+, INSM1 negative
- *NIPBL-NACC1* fusion; lacks typical molecular changes of iCCA

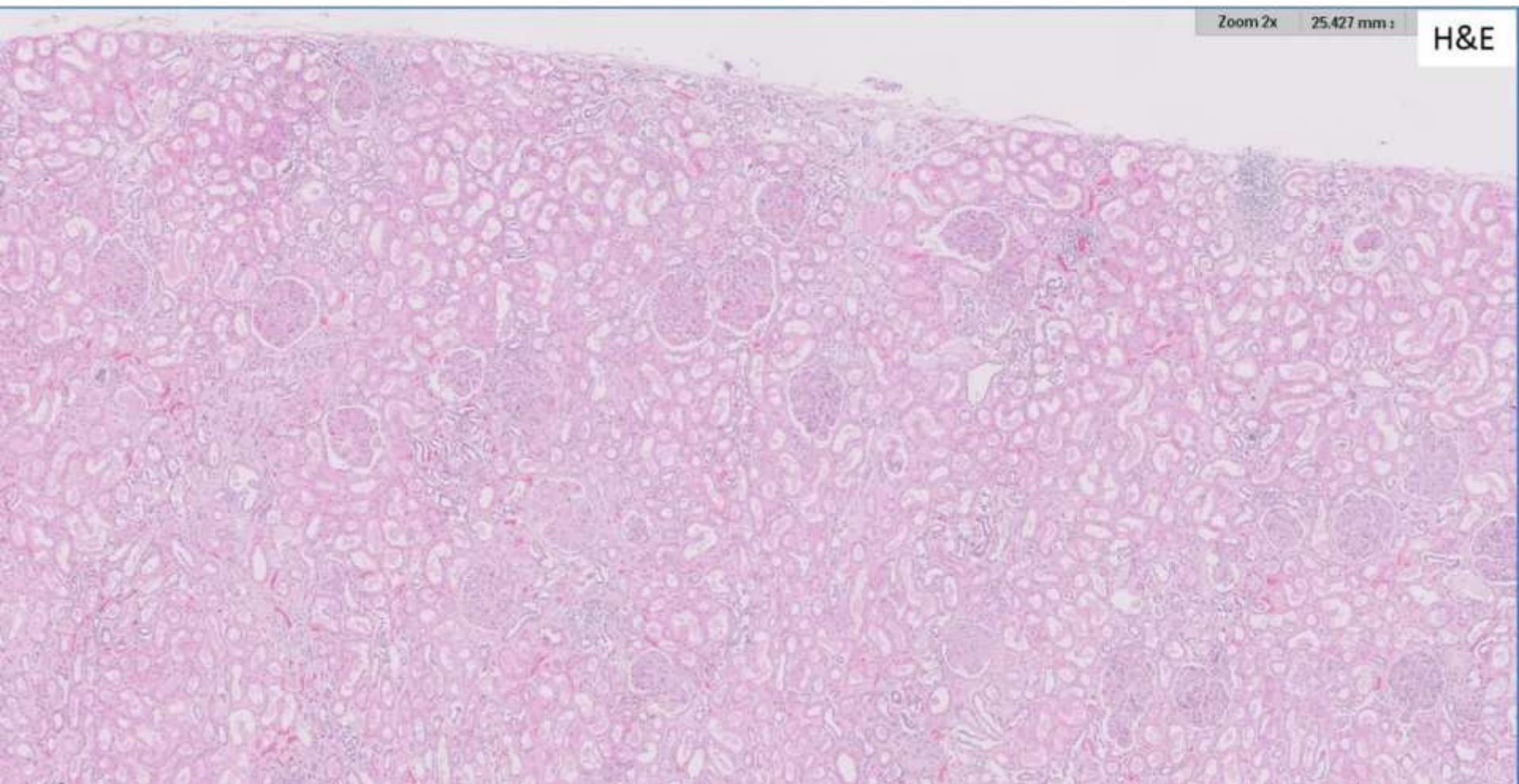
22-0104

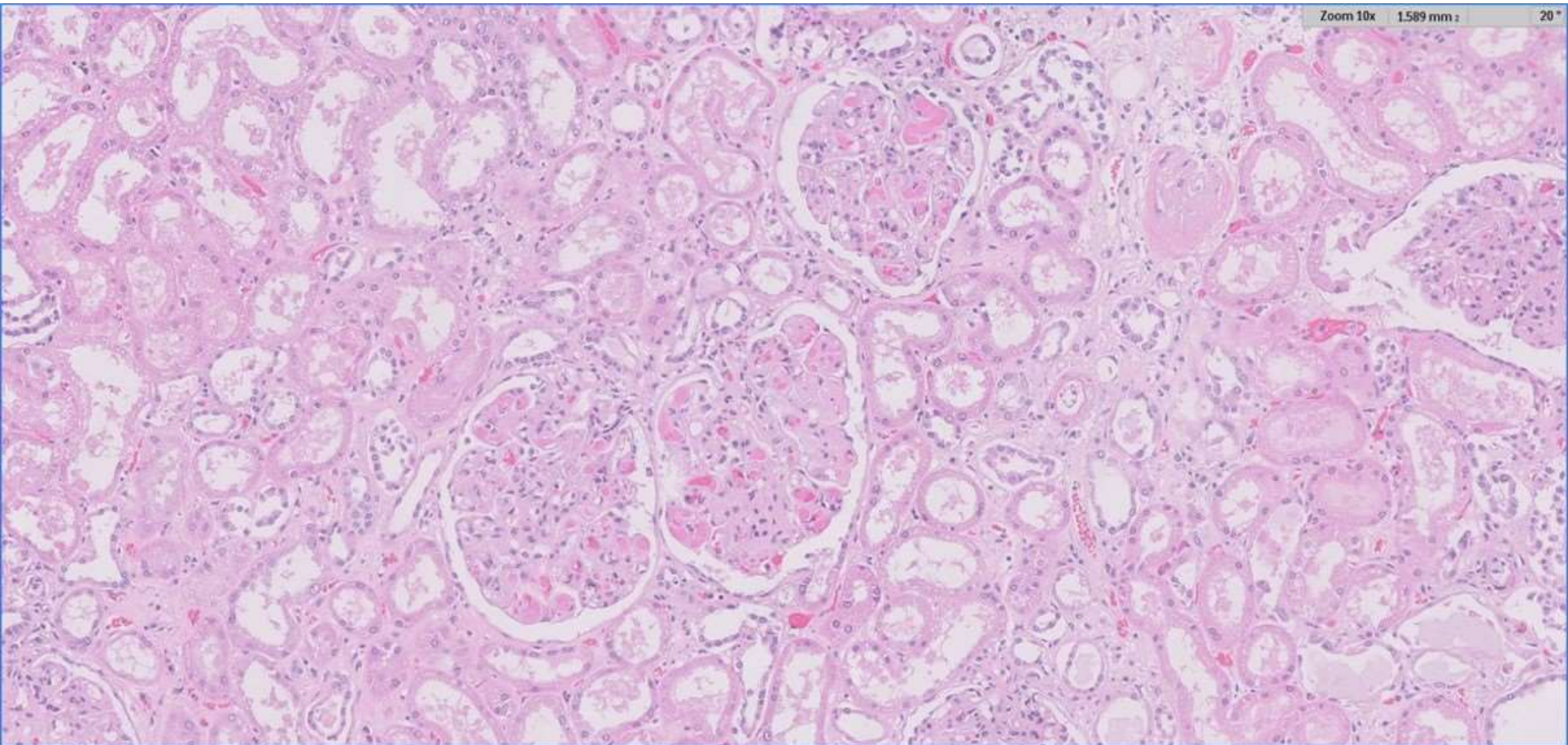
Alexandra Chang-Graham/Megan Troxell; Stanford

Elderly year-old woman with history of rheumatoid arthritis, on methotrexate, with months of abdominal pain. She developed a skin rash and presented to a hospital where she was determined to have new-onset acute renal failure requiring dialysis. She developed pancytopenia and acute hypoxic respiratory failure. Her status declined and she passed away.

Zoom 2x 25.427 mm:

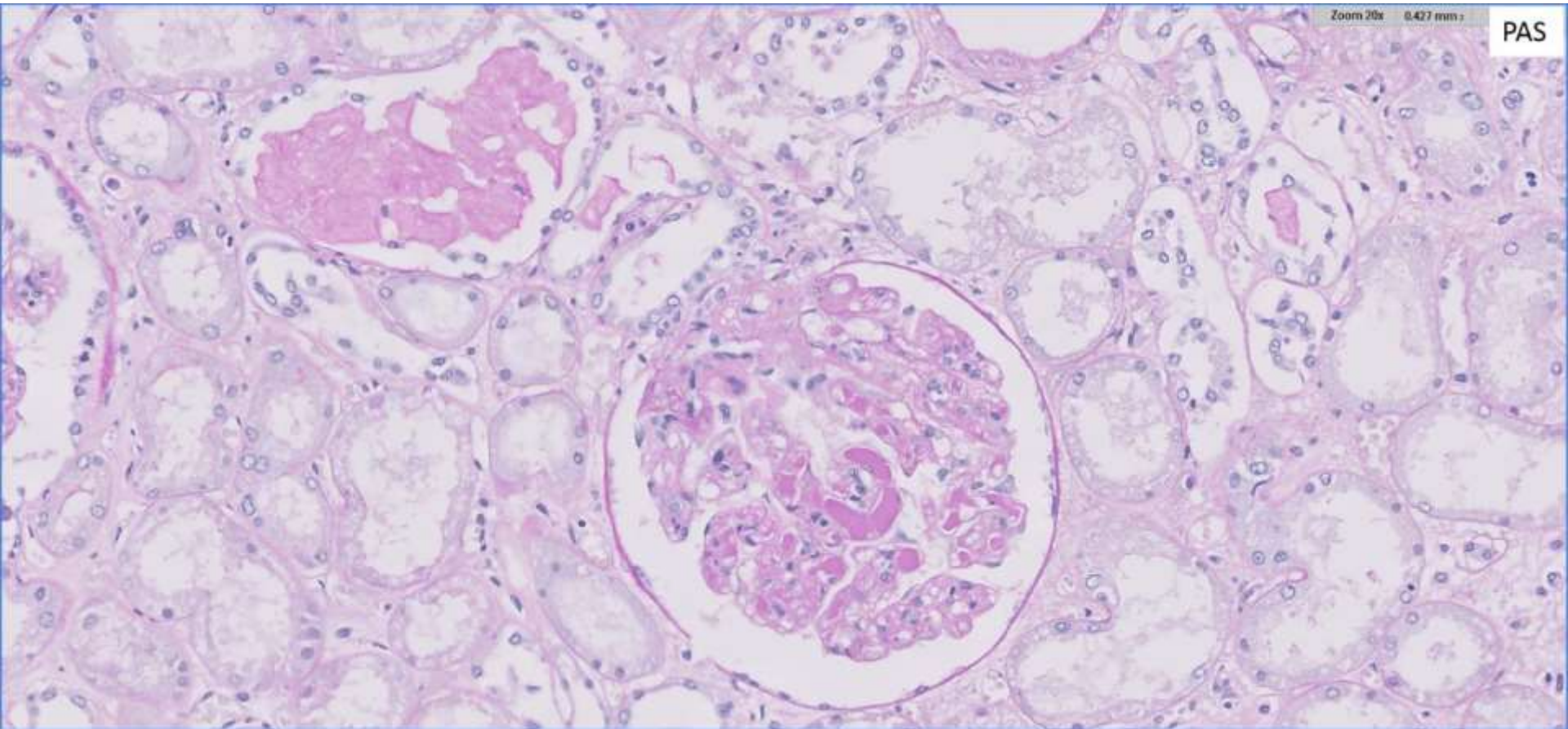
H&E

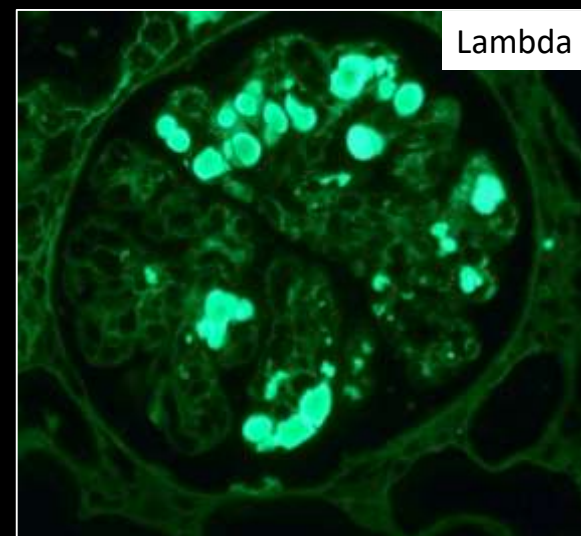
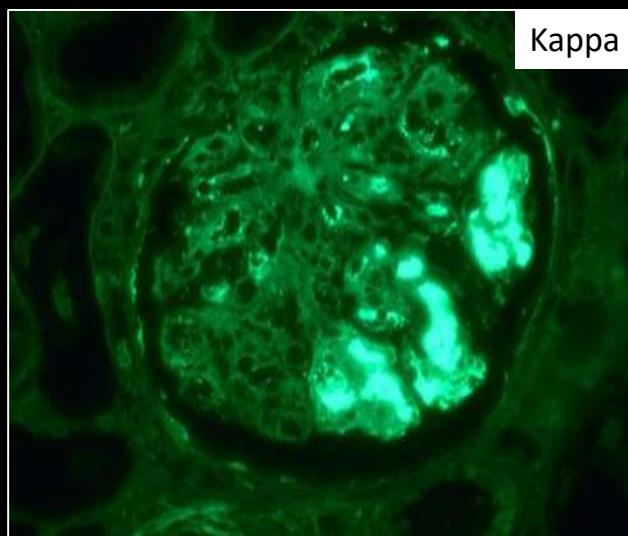
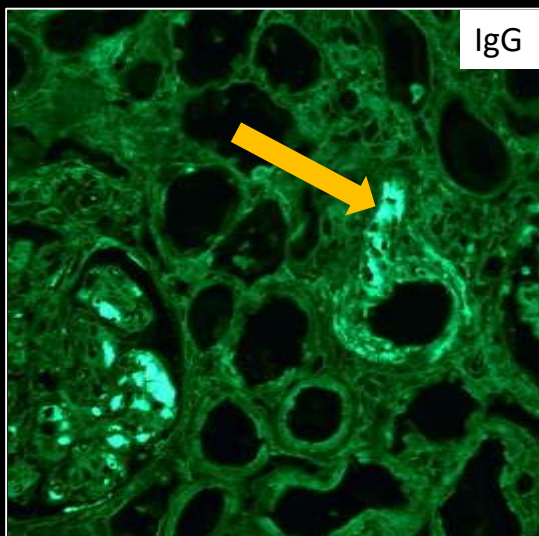
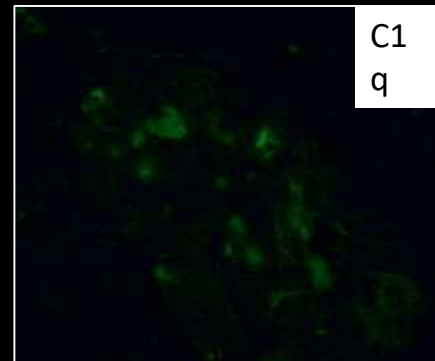
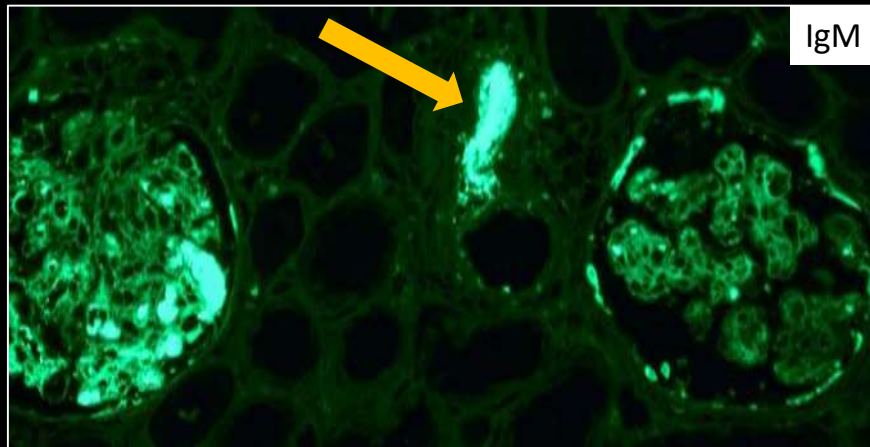
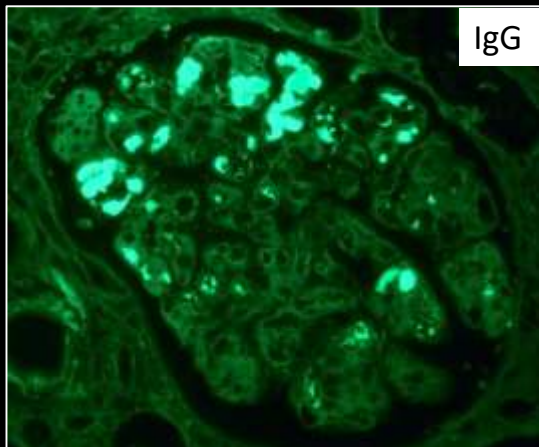


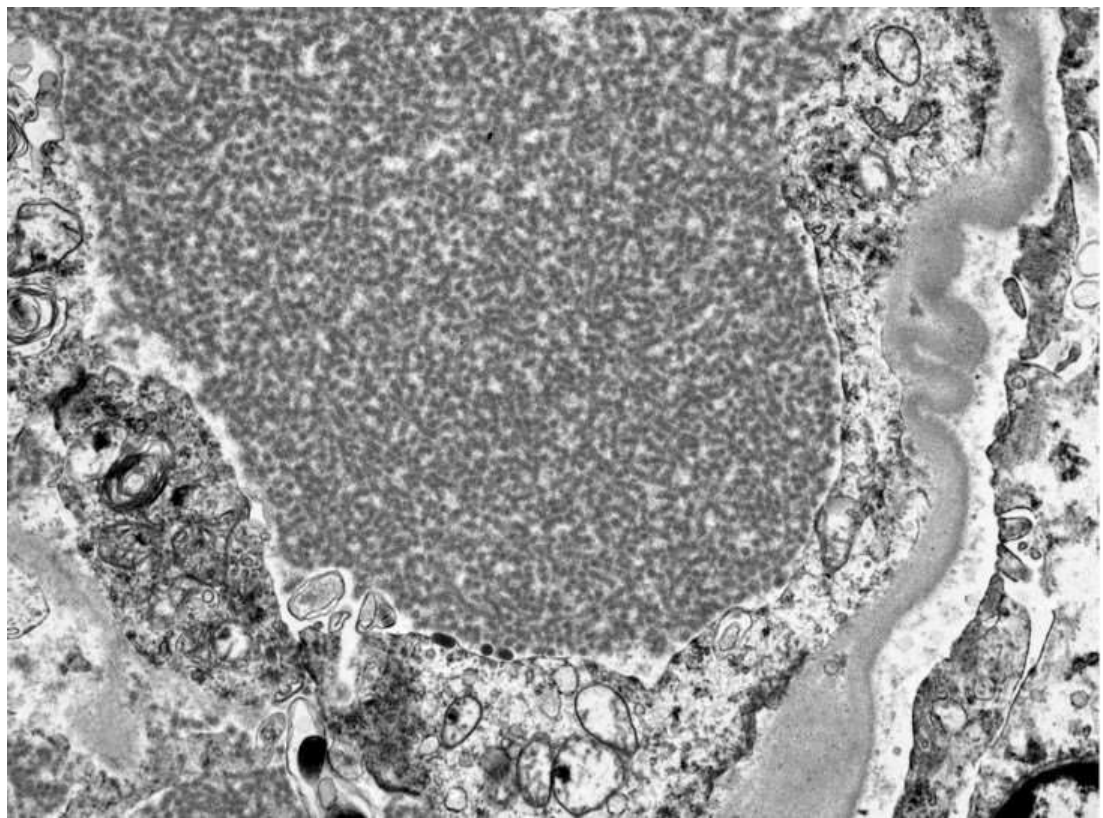
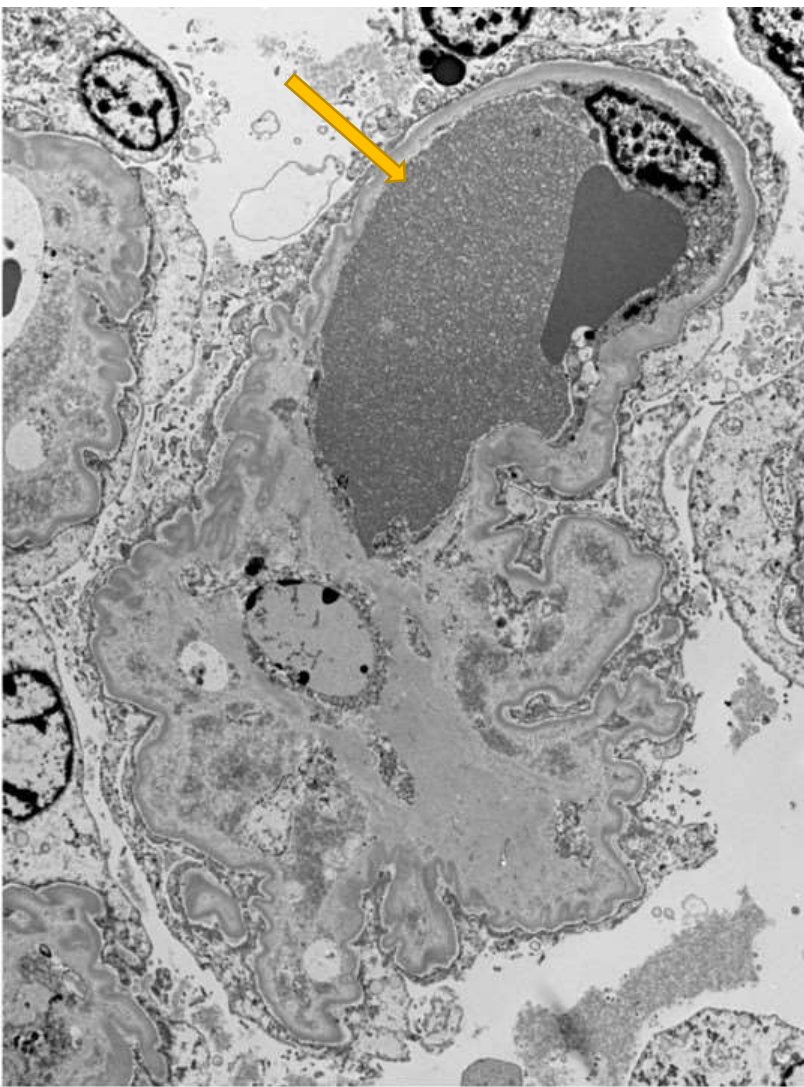


Zoom 20x 0.427 mm

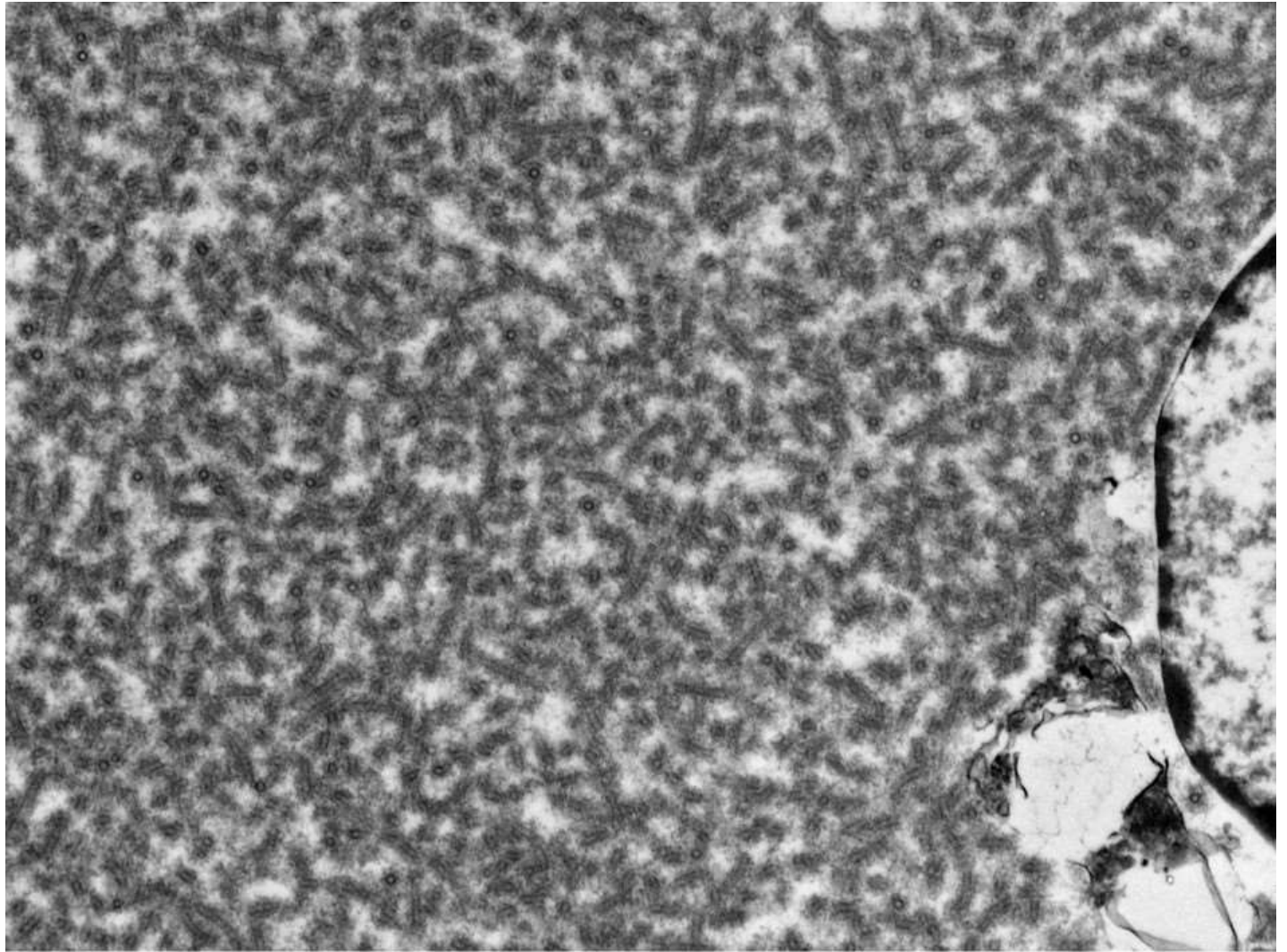
PAS

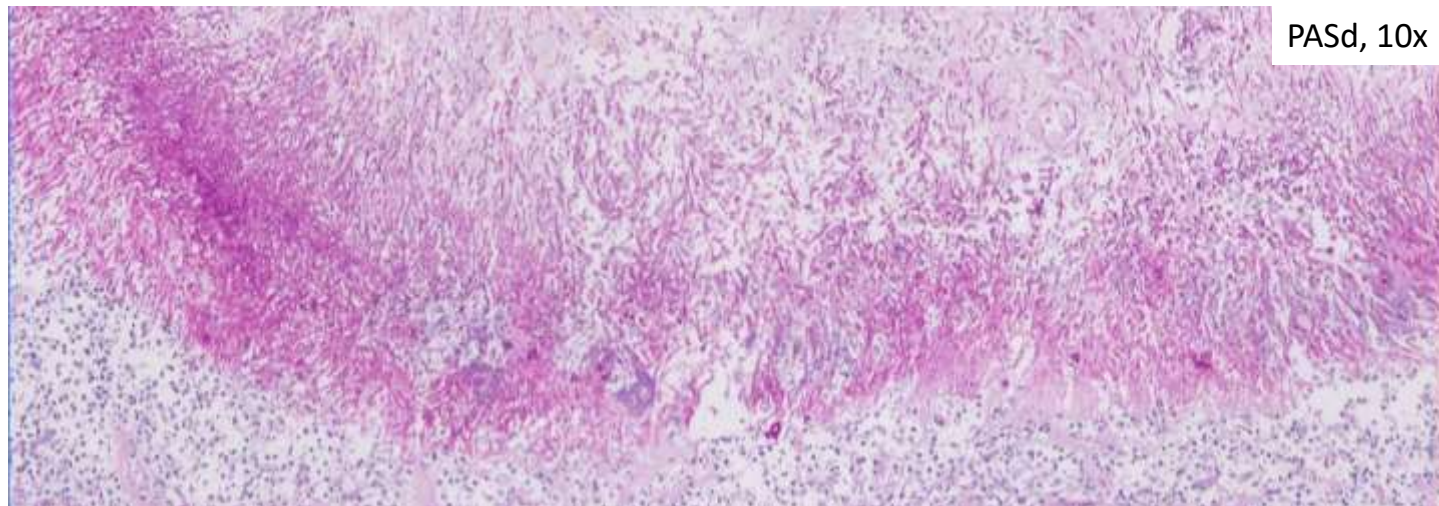
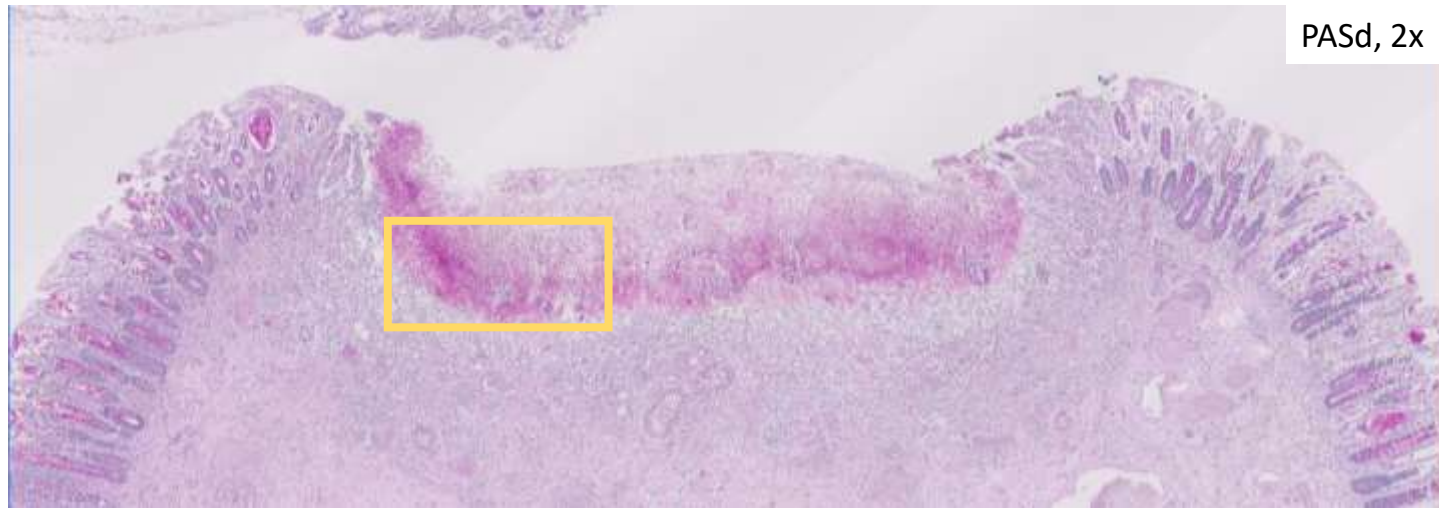






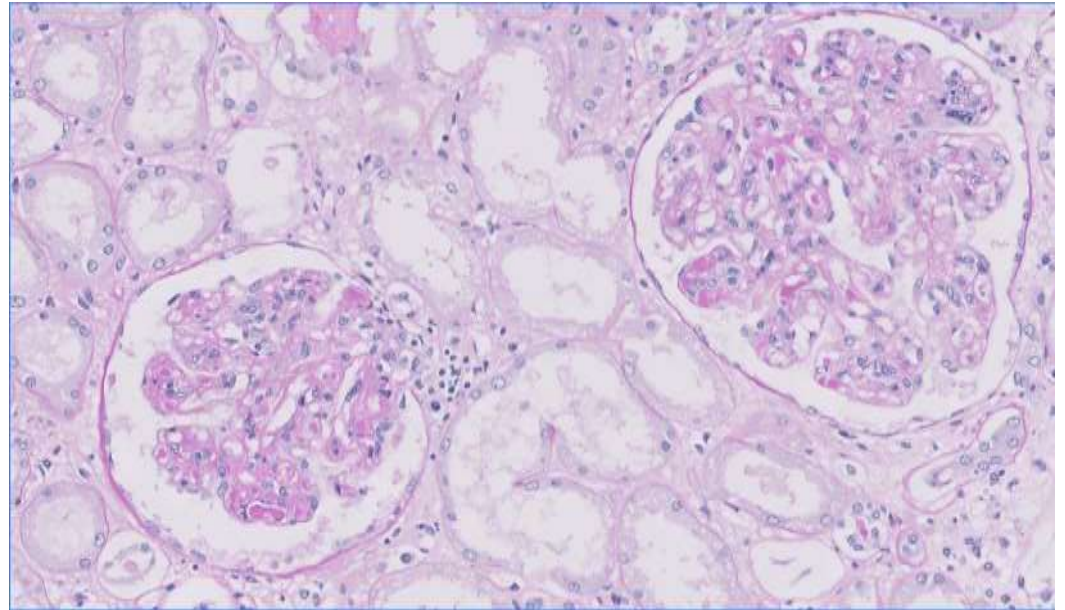
tubule diameters =
~30-50 nm





Mixed cryoglobulinemia glomerulonephritis, membranoproliferative pattern

- Cryoglobulinemia
 - associated with autoimmune, infectious, and lymphoproliferative conditions
 - may cause systemic vasculitis
- Immune complexes positive for IgG, IgM, kappa, lambda support a mixed cryoglobulinemia, type II or III
- Also deposits in small arteries --> vasculitis syndrome



Patient's rheumatoid arthritis + superimposed fungal infection



Excess immune complex formation



Acute renal failure

Thanks also to Jeff Nirschl, Darren Salmi, and Neeraja Kambham for their work on this case

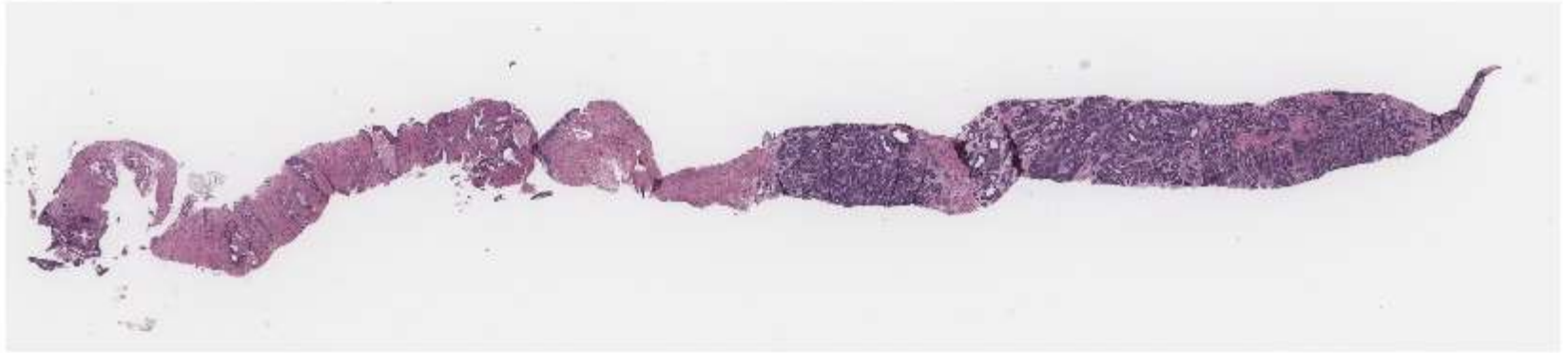
References:

- Zand L, Fervenza FC, Nasr SH, Sethi S. Membranoproliferative glomerulonephritis associated with autoimmune diseases. *J Nephrol.* 2014 Apr;27(2):165-71. doi: 10.1007/s40620-014-0049-0. Epub 2014 Feb 6. PMID: 24500888.
- Roccatello D, Saadoun D, Ramos-Casals M, Tzioufas AG, Fervenza FC, Cacoub P, Zignego AL, Ferri C. Cryoglobulinaemia. *Nat Rev Dis Primers.* 2018 Aug 2;4(1):11. doi: 10.1038/s41572-018-0009-4. PMID: 30072738.
- Terrier B, Marie I, Lacraz A, Belenotti P, Bonnet F, Chiche L, Graffin B, Hot A, Kahn JE, Michel C, Quemeneur T, de Saint-Martin L, Hermine O, Léger JM, Mariette X, Senet P, Plaisier E, Cacoub P. Non HCV-related infectious cryoglobulinemia vasculitis: Results from the French nationwide CryoVas survey and systematic review of the literature. *J Autoimmun.* 2015 Dec;65:74-81. doi: 10.1016/j.jaut.2015.08.008. Epub 2015 Aug 29. PMID: 26320984.

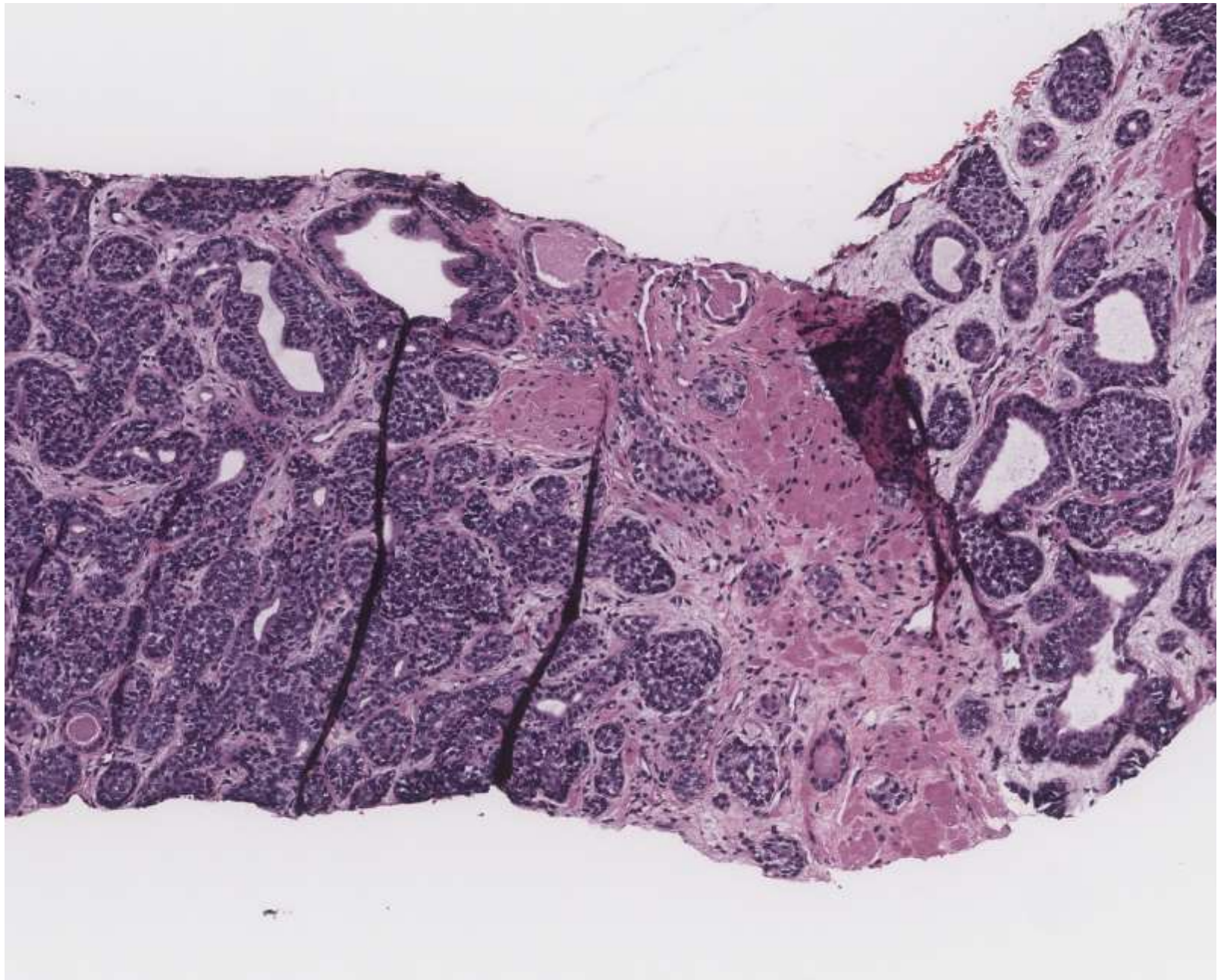
22-0105

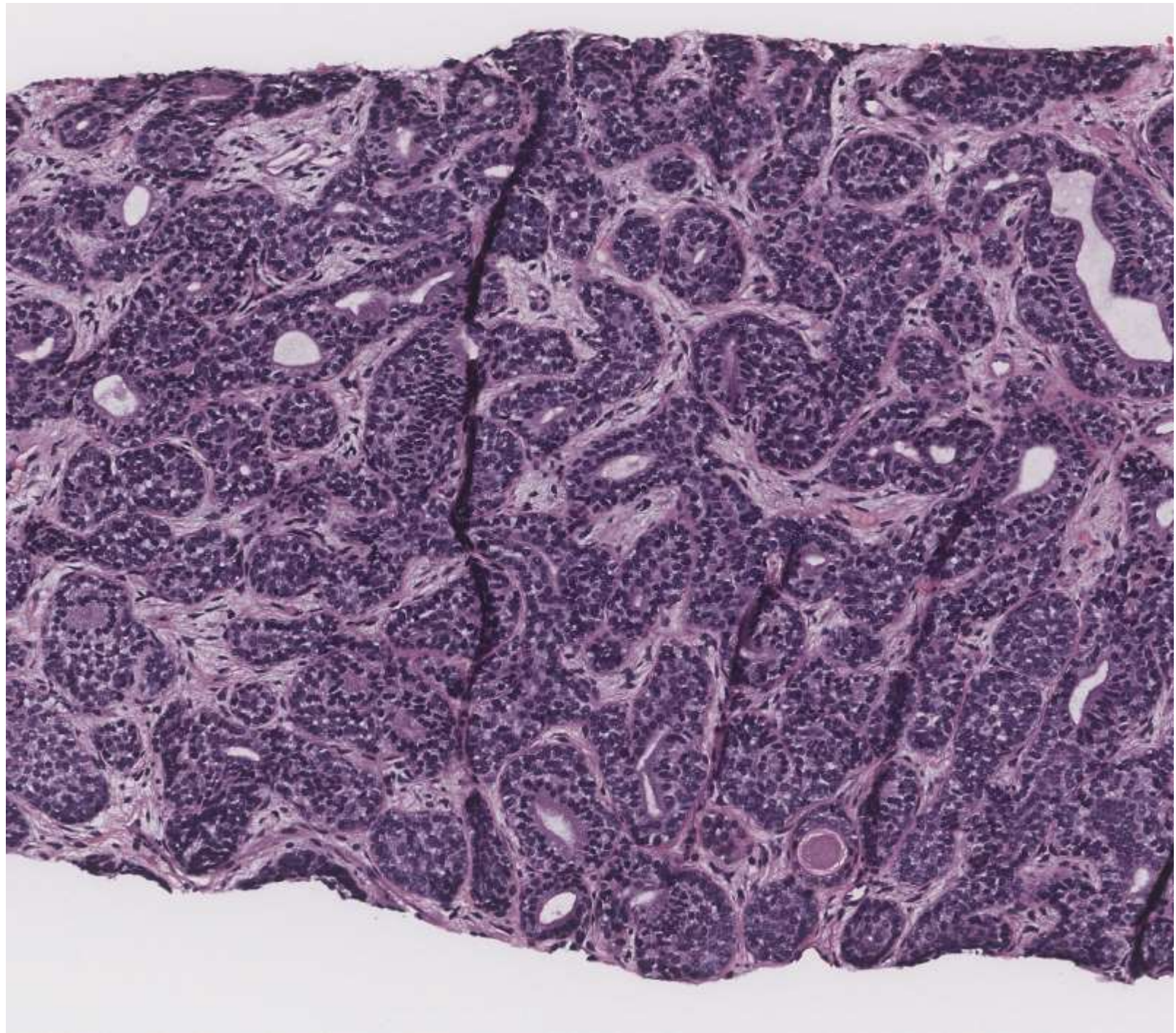
Chien-Kuang Ding/Zhen Yan/Emily Chan; UCSF

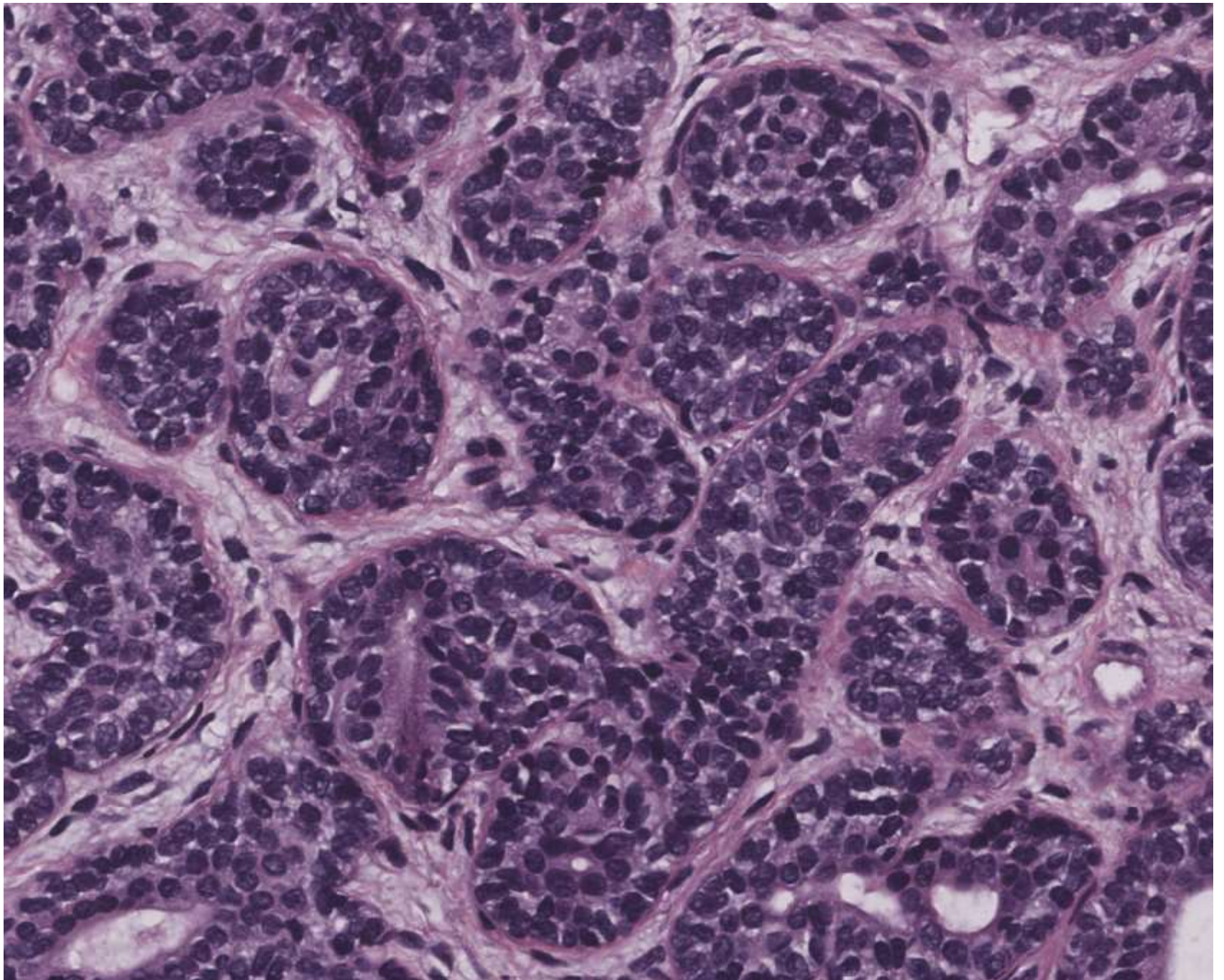
Adult M with elevated PSA, undergoes prostate biopsy.

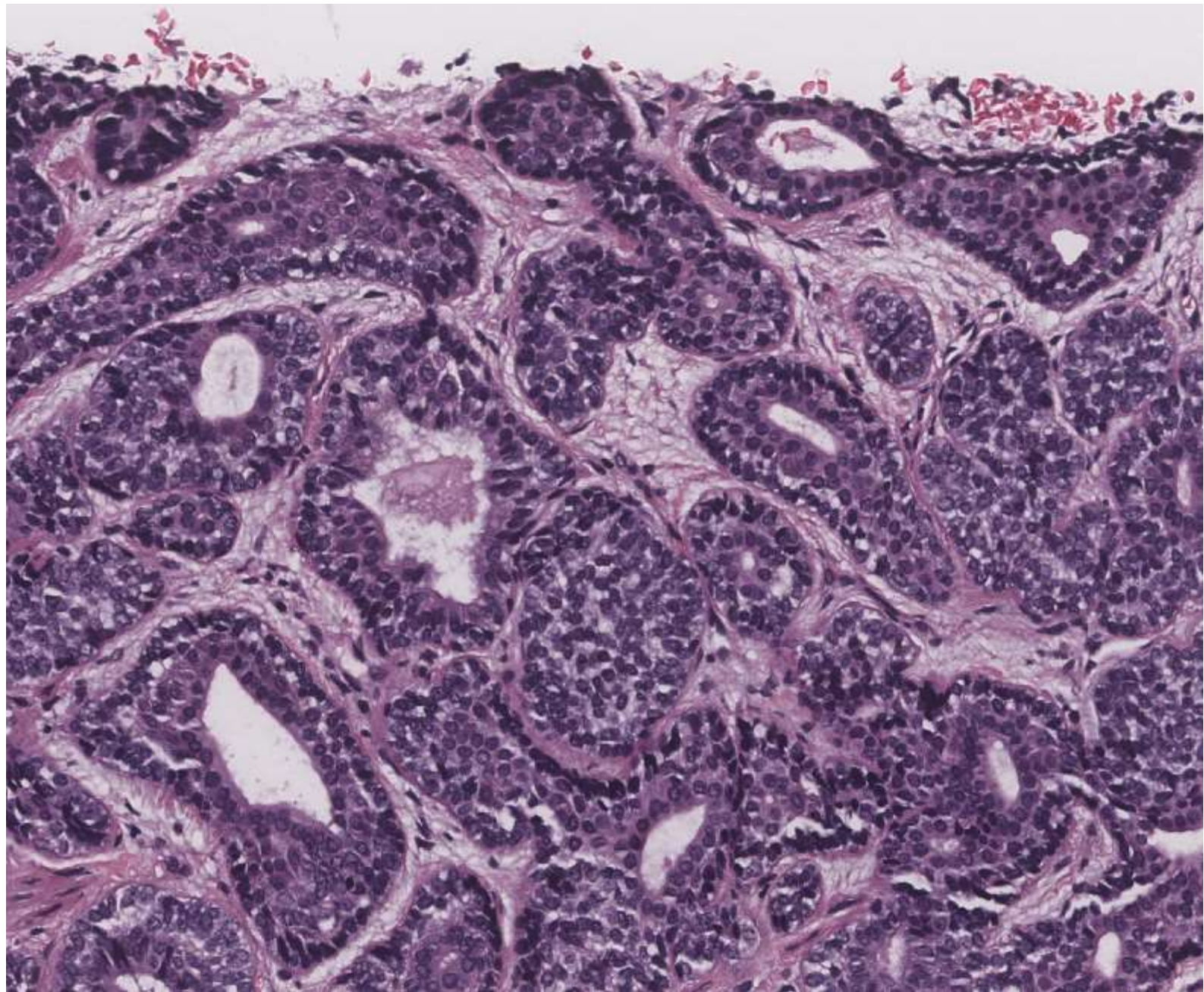




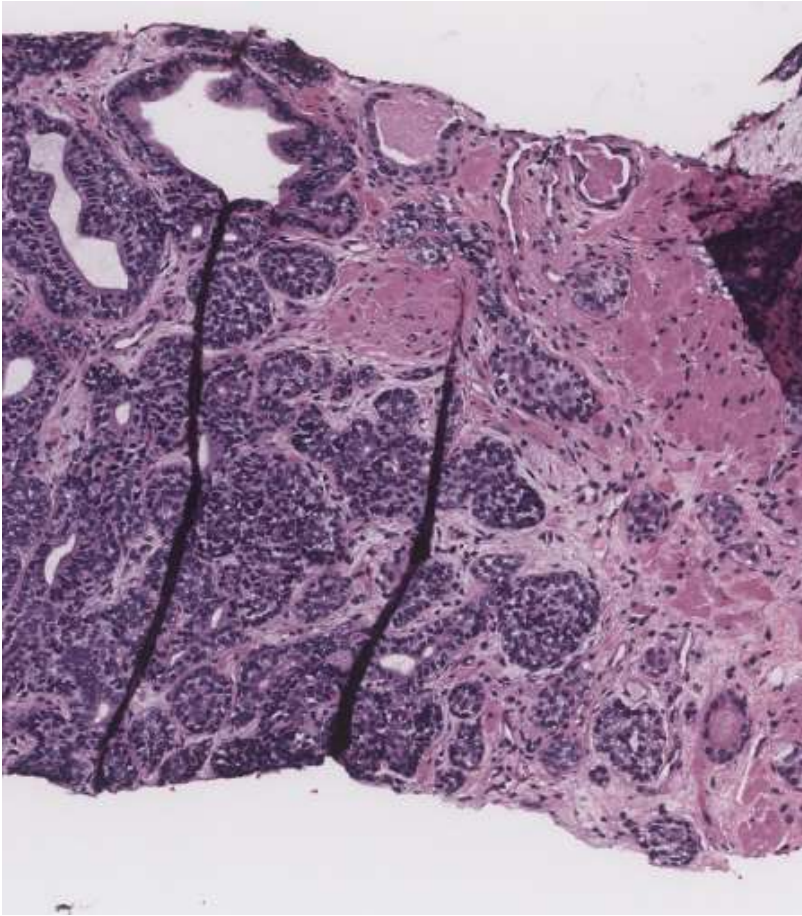








Basal cell carcinoma

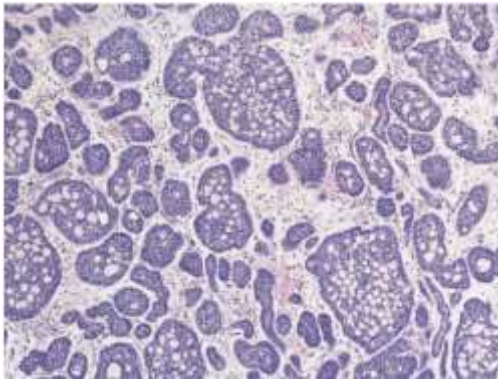


Differential diagnoses:

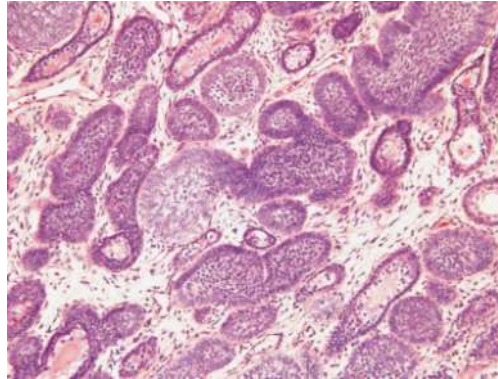
- Florid basal cell hyperplasia
- Prostatic adenocarcinoma
- Neuroendocrine tumor
- Urothelial carcinoma

Basal cell carcinoma of prostate

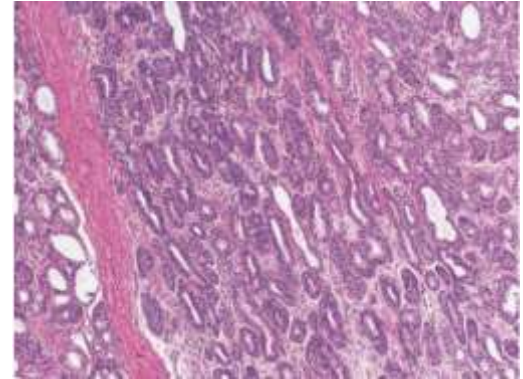
- “adenoid cystic carcinoma” or “adenoid basal cell tumor”
- Usually arise in the transition zone, low PSA
- Multiple patterns can be seen:



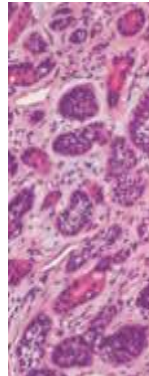
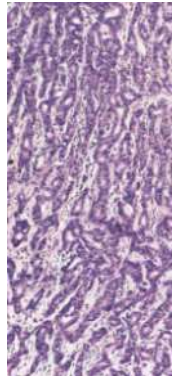
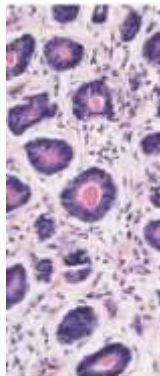
Adenoid cystic-like (AC-P)



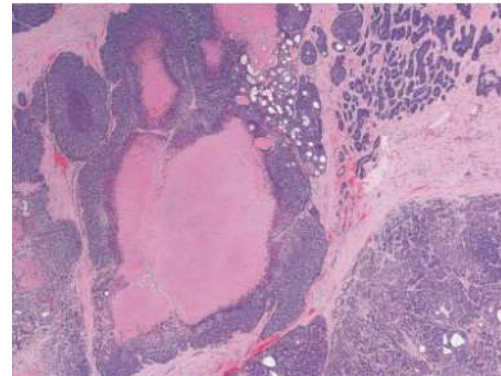
Small solid nests w/
peripheral palisading



Basal cell hyperplasia-like



Small tubules



Large nests +/- necrosis

Prostatic basal cell carcinoma IHC profile:

- Positive markers:
 - P63, HMWCK (but typically spares luminal layer)
 - CK7 will label luminal layer if present
- Negative markers: PSA/PSAP, ERG, synapto/chromo
- Not yet reported: NKX3.1, GATA3

Challenge: Basal cell hyperplasia vs. carcinoma

Hyperplasia

Morphology:

Smaller sized nests with regular shapes

Evenly and orderly arrangement of glands. (Mimics of infiltration will manifest as clusters of glands between benign glands)

IHC:

BCL-2: tend to be patchy

Carcinoma

Irregular shapes with anastomosing nests

Adenoid cystic pattern or large nests with necrosis

Infiltration between benign glands as isolated units or into bladder neck muscle

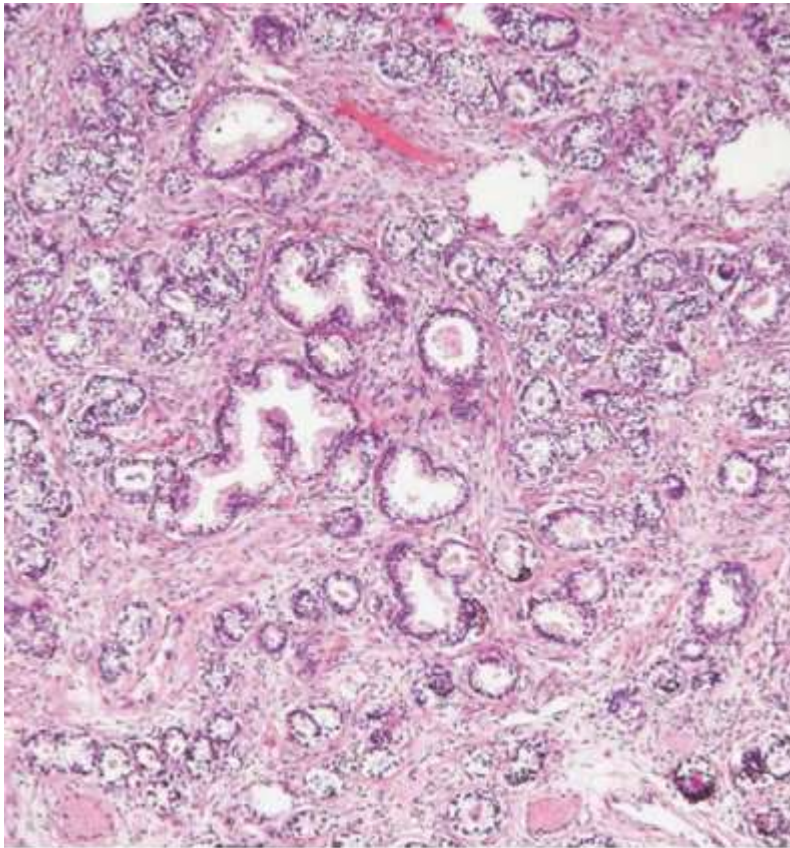
Desmoplasia

BCL-2: tend to be diffuse

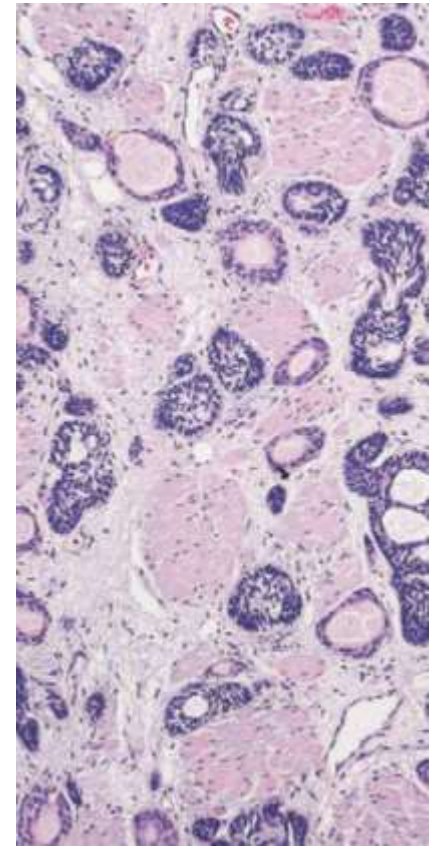
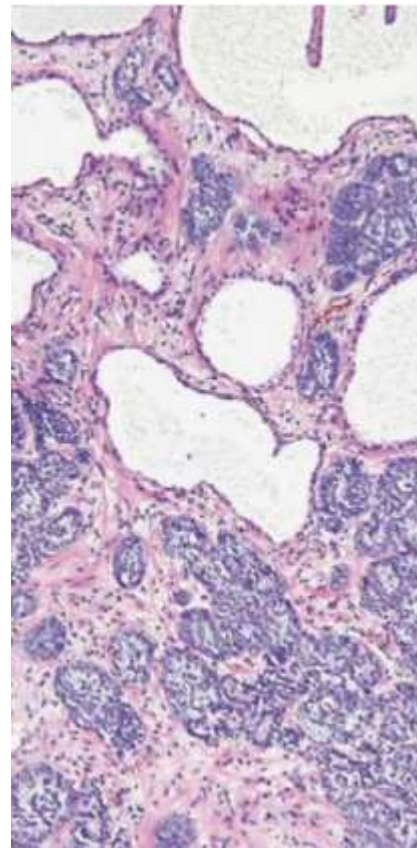
Ki-67: 2~80% (tend to be high)

Challenge: Basal cell hyperplasia vs. carcinoma

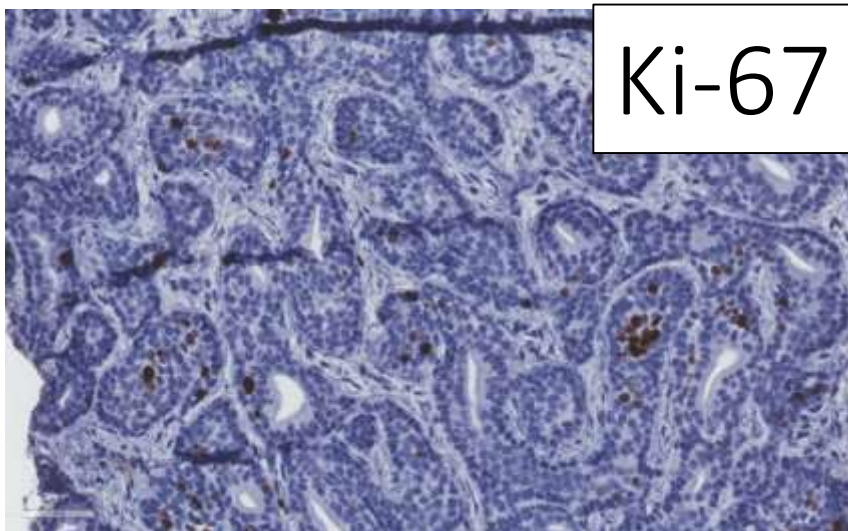
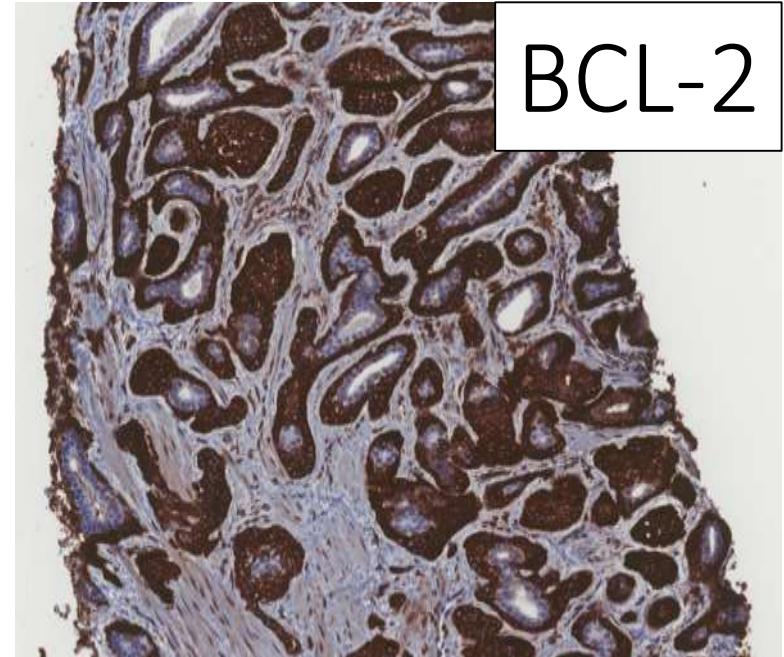
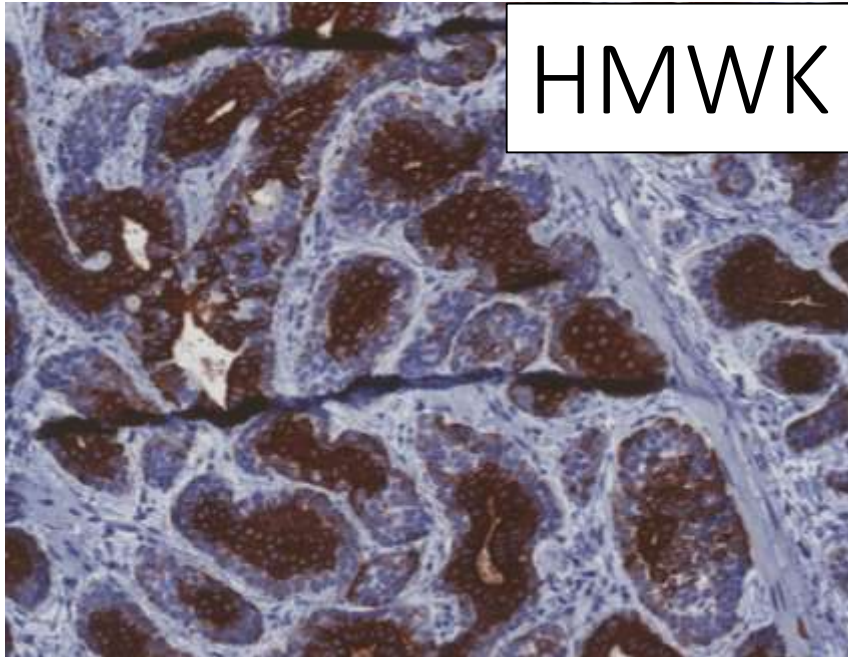
Hyperplasia



Carcinoma



Our Case: IHC



NKX3.1: focally positive in inner layer

Grading and prognosis

- No published consensus or guidelines about how to grade these tumors due to limited data
- Early studies suggest most are indolent but more recent study showed almost one half with aggressive features and showing frequent loss of PTEN and overexpression of EGFR
 - Aggressive behavior shows large solid nests with central necrosis, high Ki67 and less staining with basal cell markers

Take home message –
Basal cell carcinoma of the prostate:

- May not have high PSA
- Positive for basal cell markers (HMWCK, p63)
- D/D: basal cell hyperplasia vs. carcinoma
 - Morphology
 - IHC could be helpful -- diffuse strong BCL-2
- Aggressive behavior can occur

22-0106

Jeffrey Nirschl/Hannes Vogel; Stanford

60-year-old M with hypertension and T2DM who presented with acute-onset left-sided right gaze palsy and lip smacking. Brain MRI showed extra-dural based mass measuring 3.1cm.

Case History

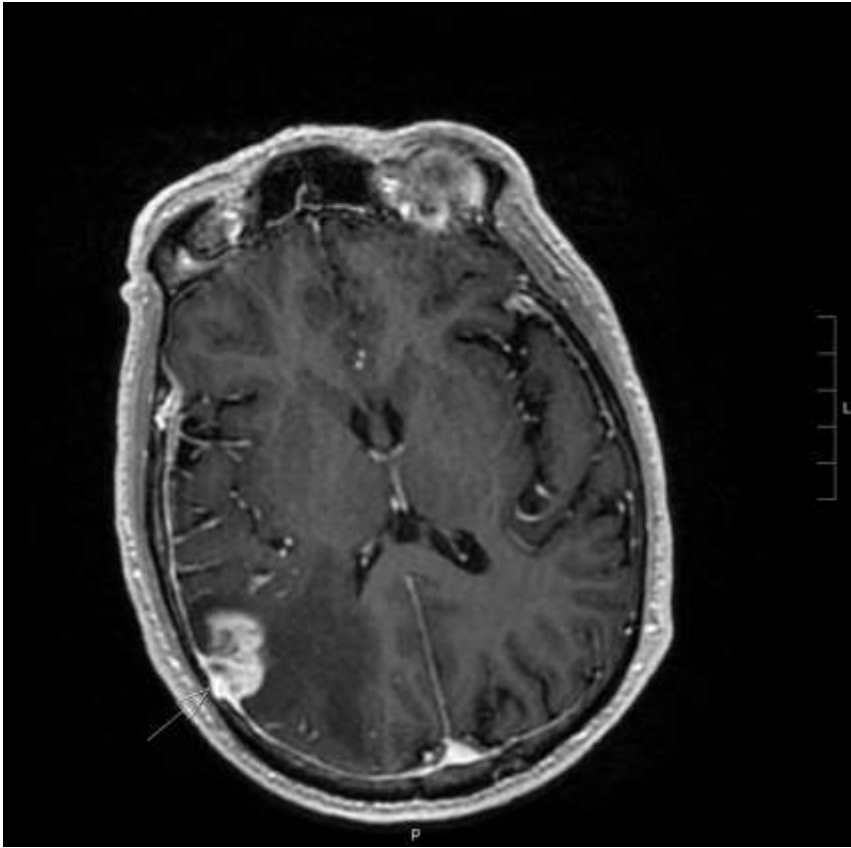
~60-year-old male with hypertension and T2DM who presented with acute-onset left sided, right gaze palsy, and lip smacking

- **Imaging data:**

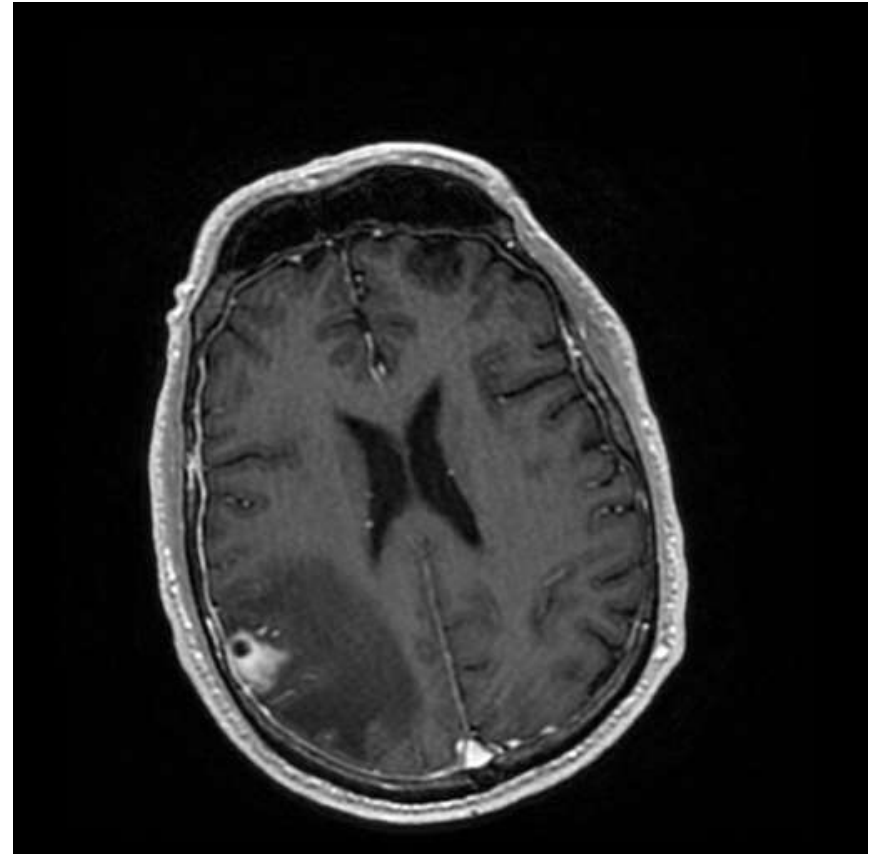
- › **Brain MRI:**

- › Heterogeneously enhancing with irregular margins
 - › Extra-axial dural-based mass with intraparenchymal extension versus a parenchymal intra-axial lesion invading the dura
 - › Located at the right parietal/parieto-occipital junction
 - › Measuring 3.1 x 1.8 x 3.7 cm

Brain MRI

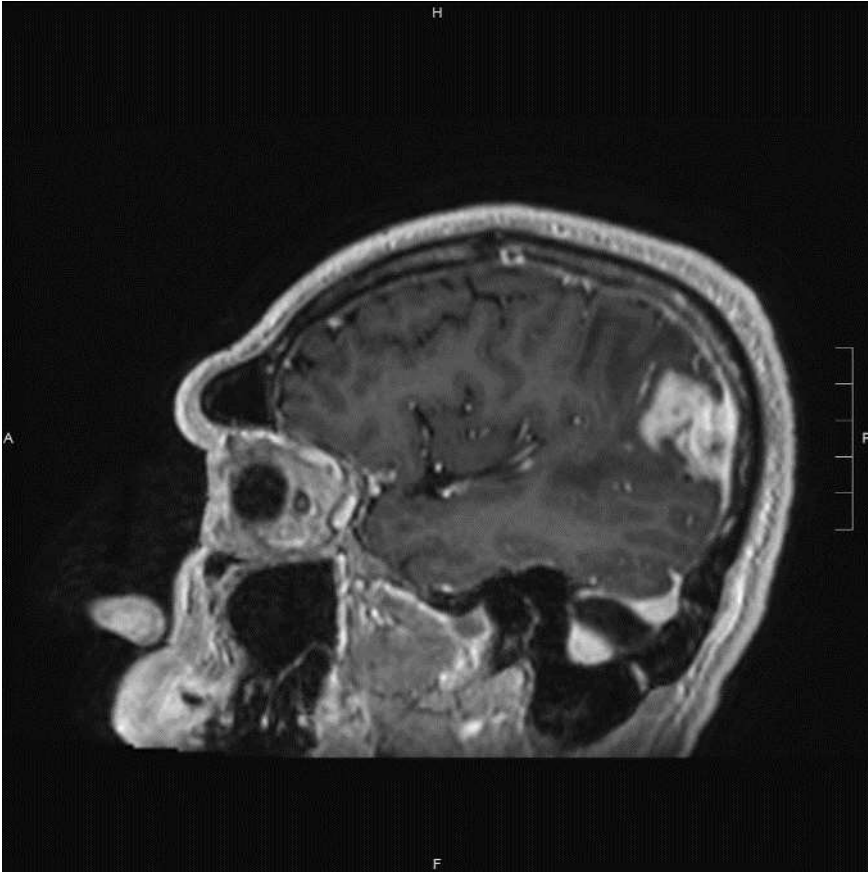


Axial T1 w/contrast

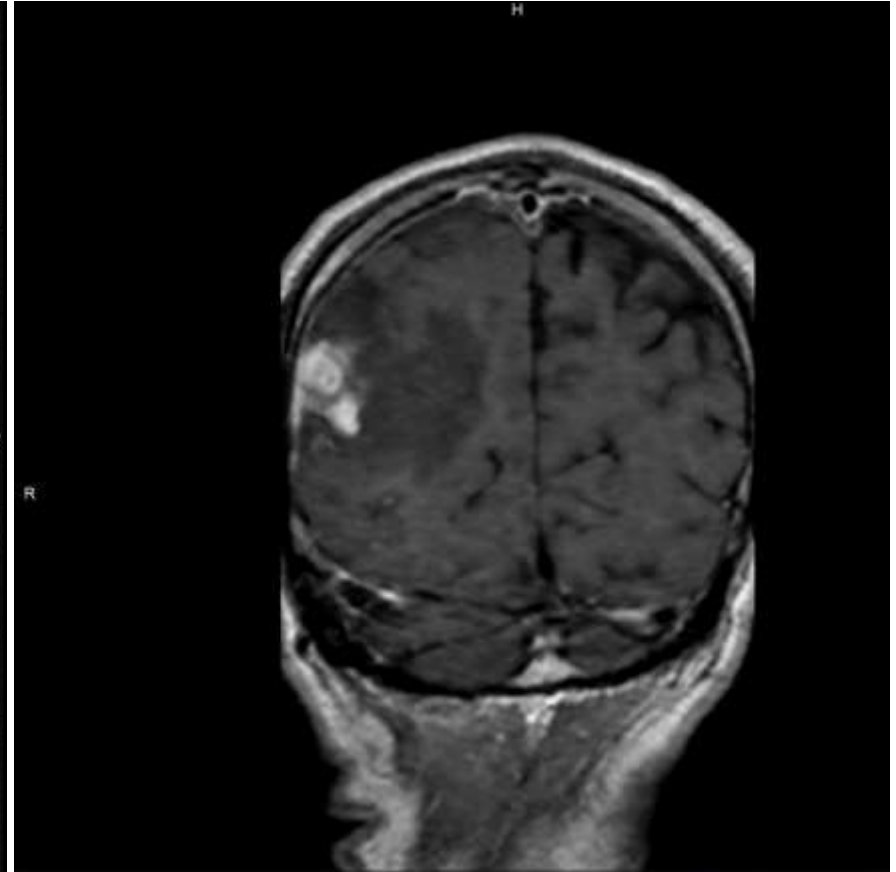


Axial T1 w/contrast

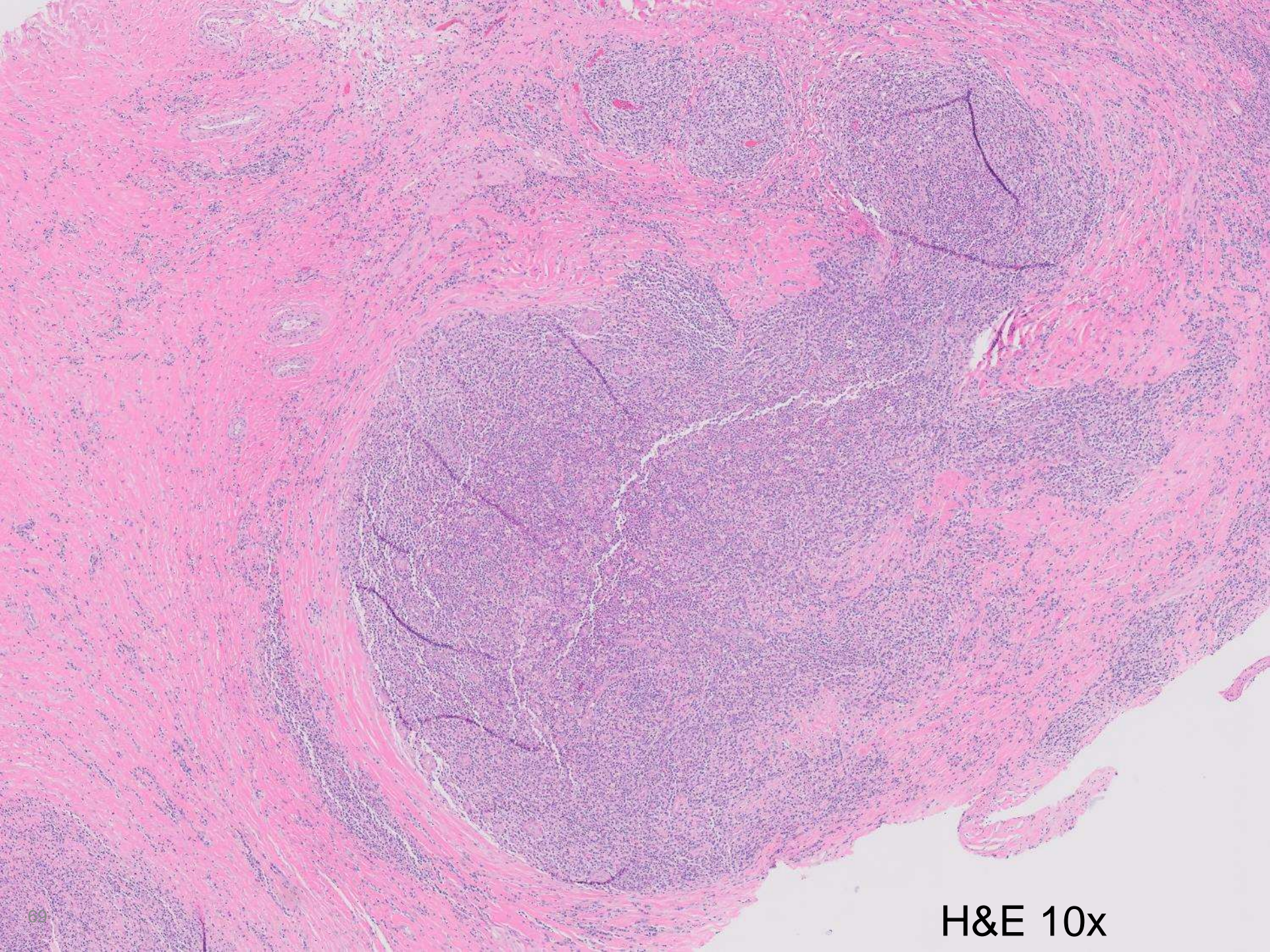
Brain MRI



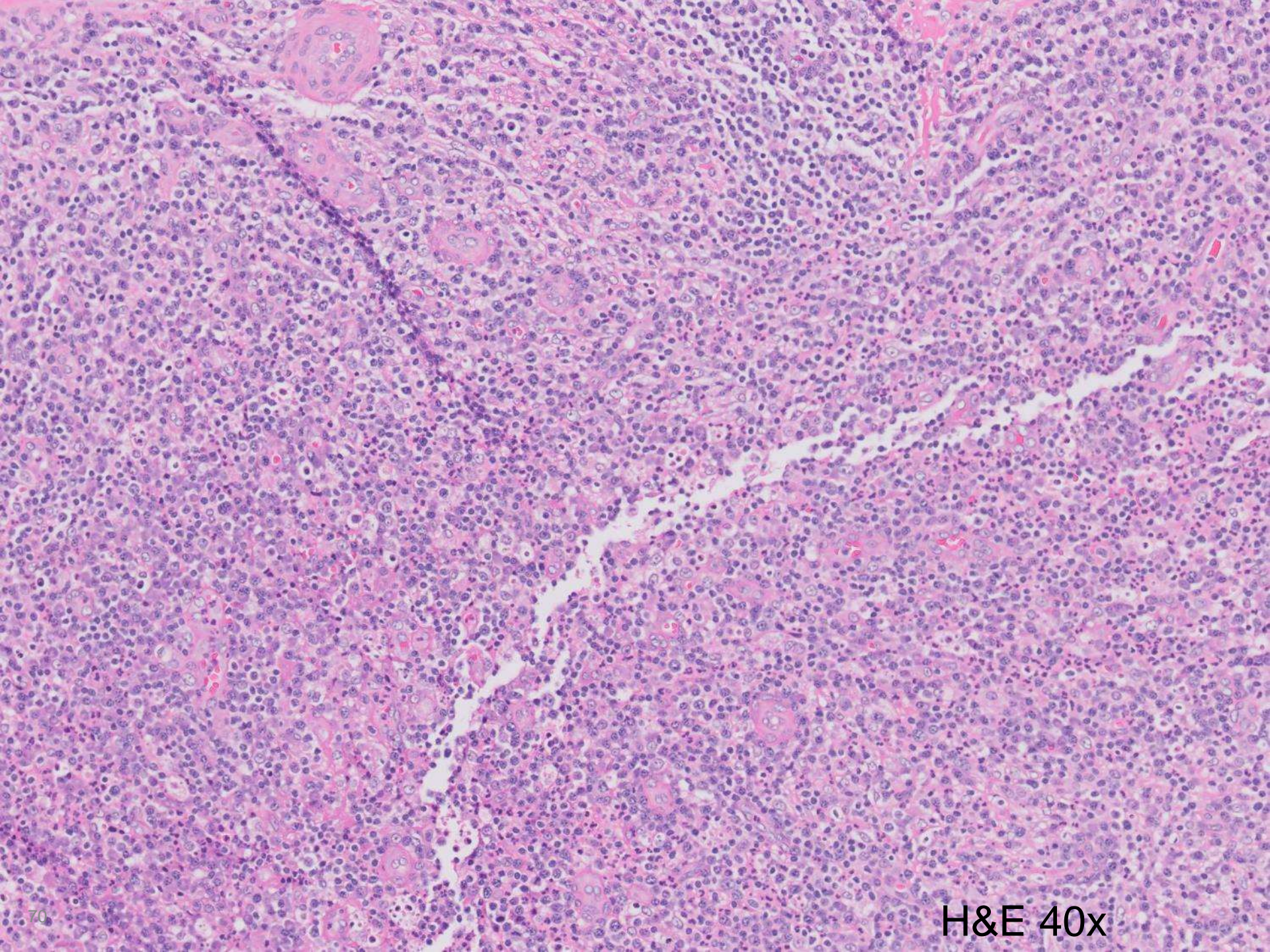
Sagittal T1 FLAIR



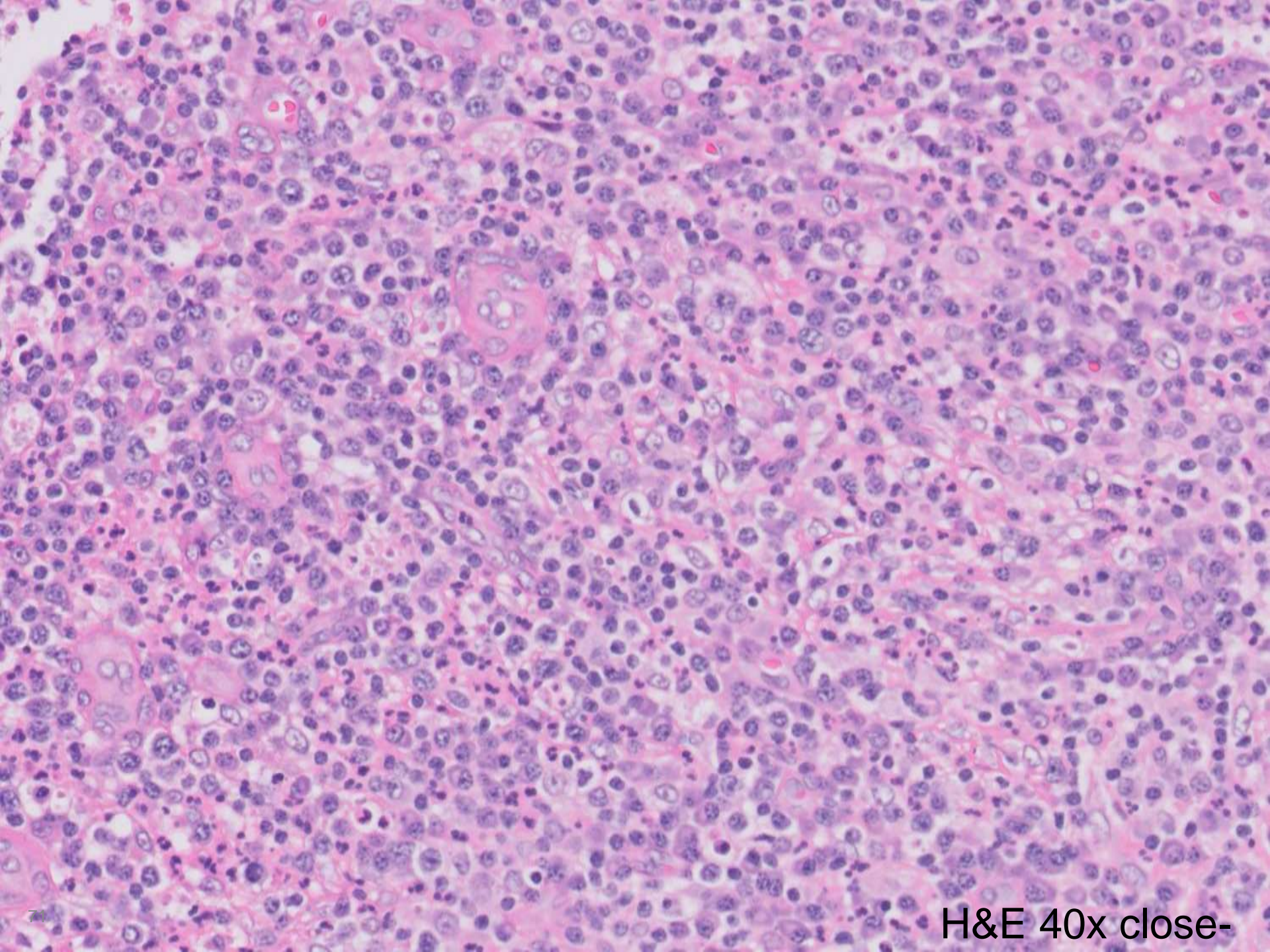
Coronal w/contrast



H&E 10x



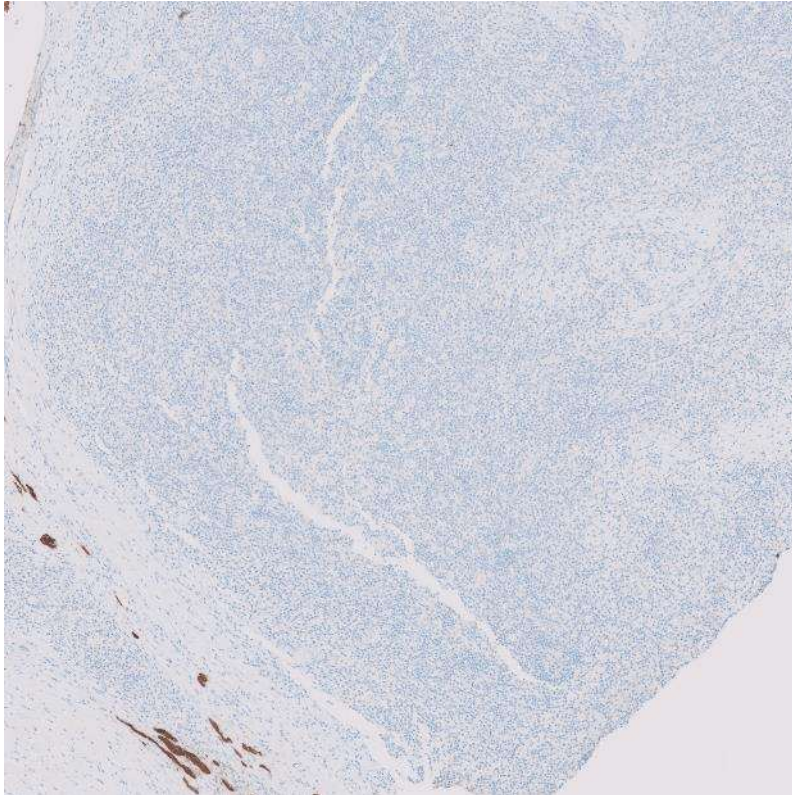
H&E 40x



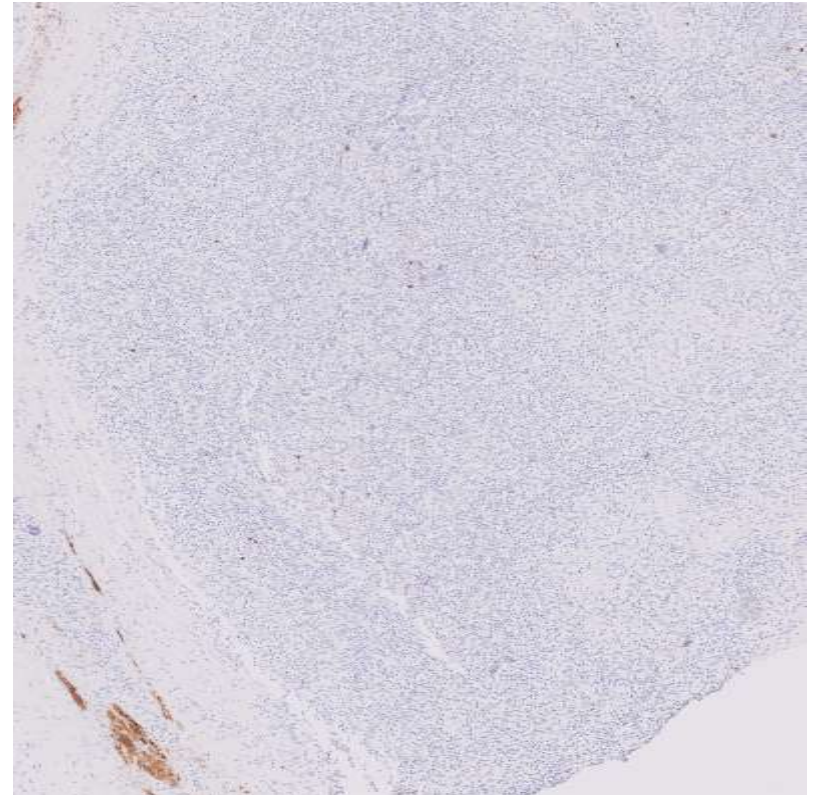
H&E 40x close-

Immunohistochemistry

GFAP

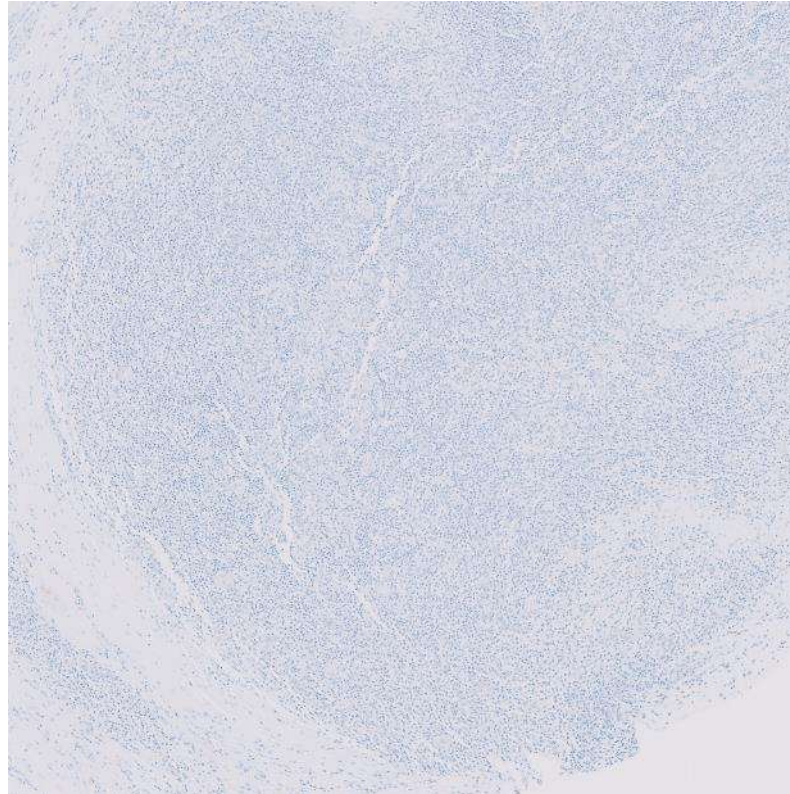


S100



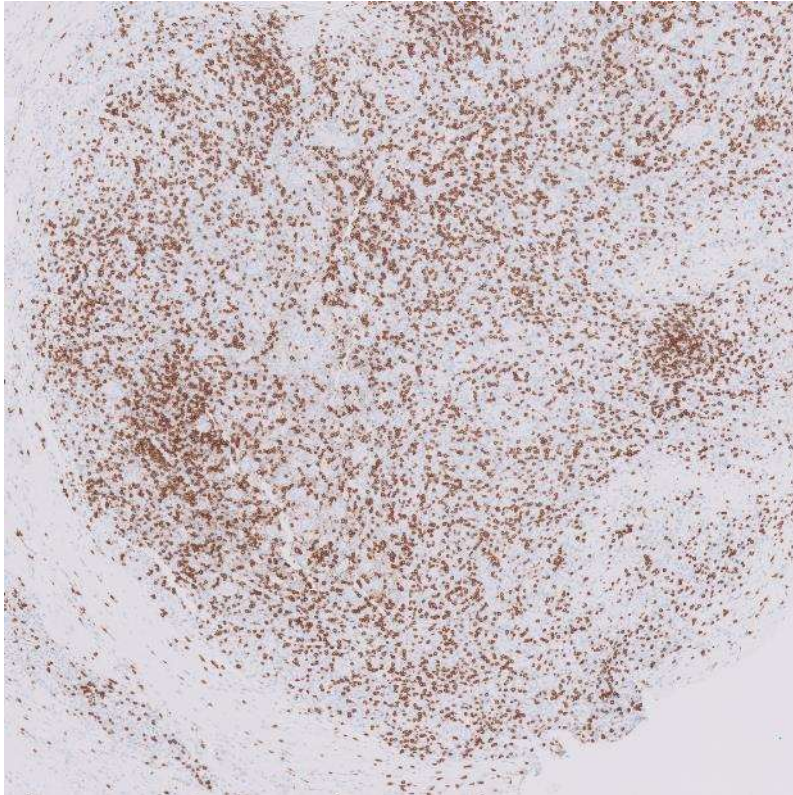
Immunohistochemistry

Mixed cytokeratins

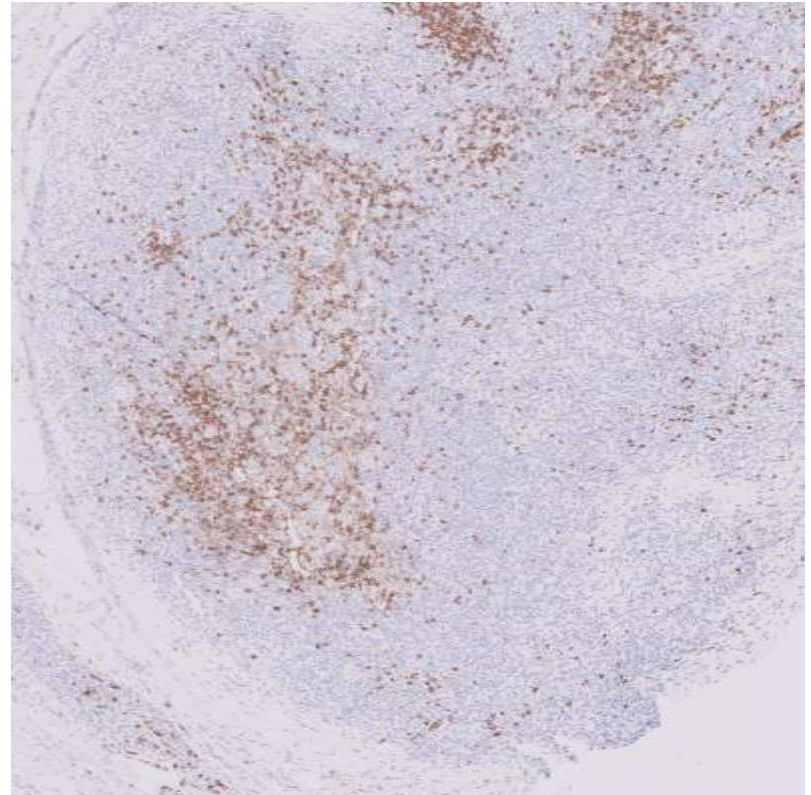


Immunohistochemistry

CD3

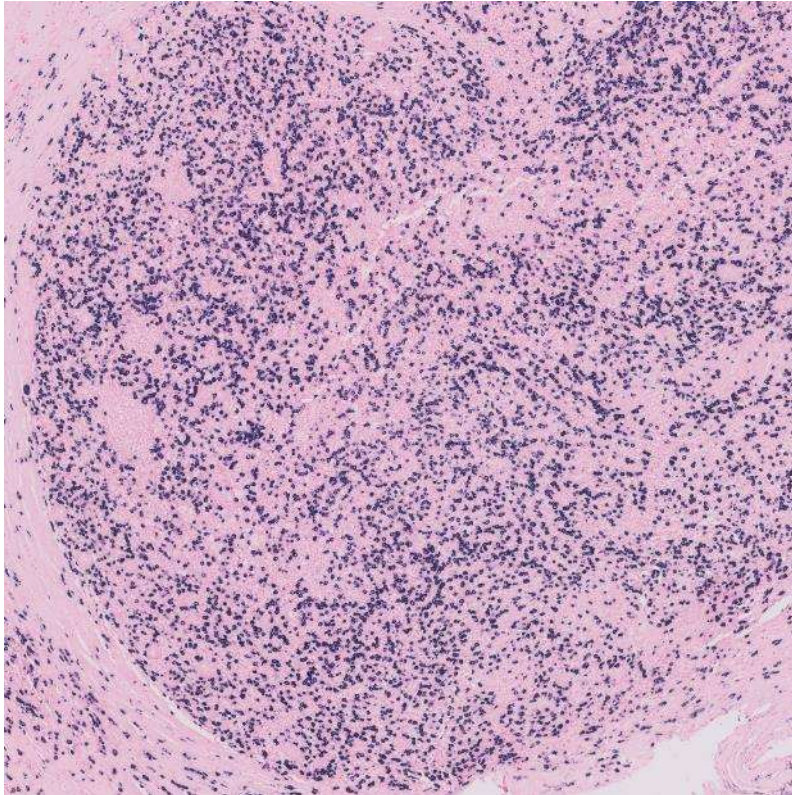


CD20

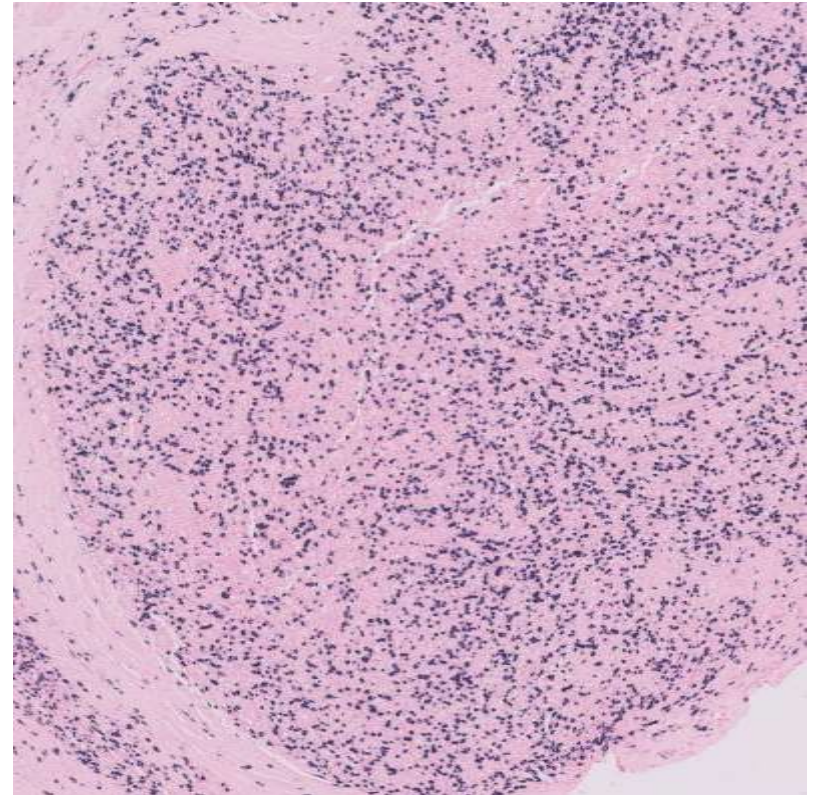


In situ hybridization

Kappa



Lambda



Select additional information & stains

No emperipolesis identified

Negative: Spirochete IHC

Negative: Warthin-Starry

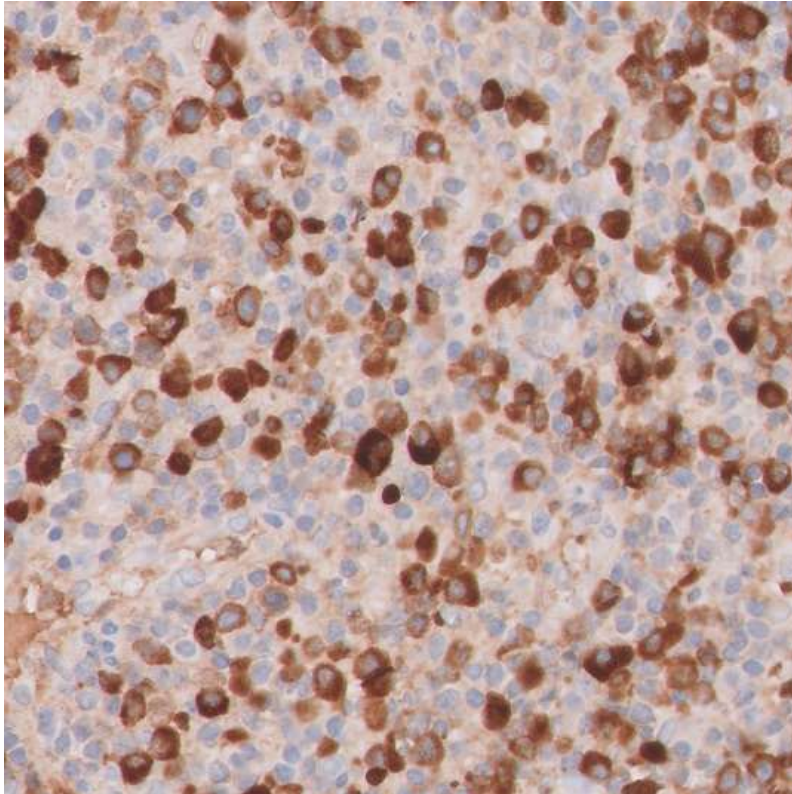
Negative: GMS, Gram, FITE

Scattered EMA in meningotheelial cells

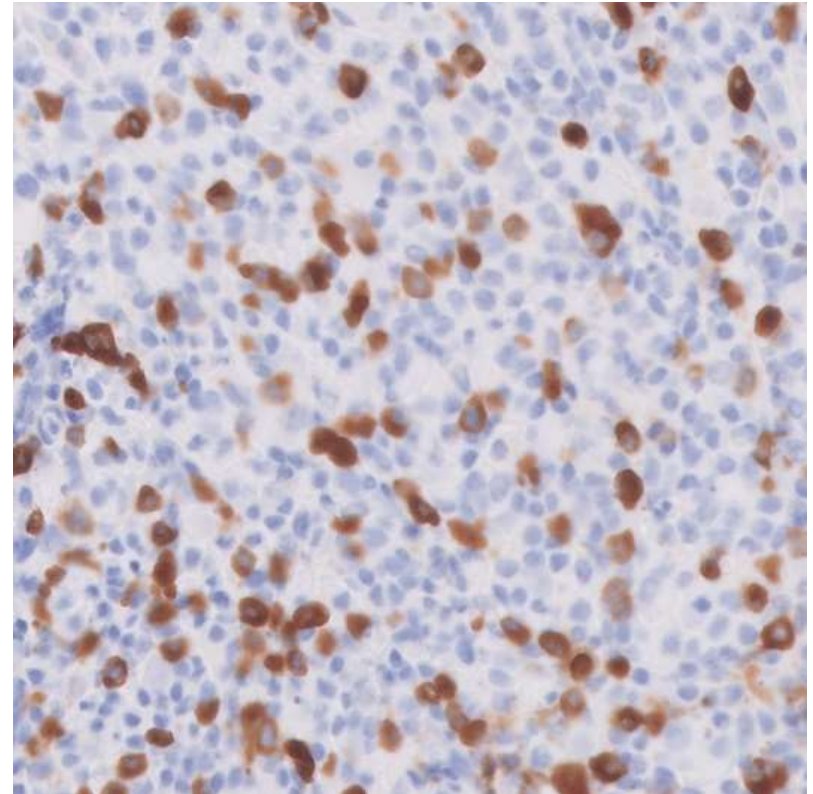
CD68 in occasional background histiocytes

IgG and IgG4 Immunohistochemistry

IgG



IgG4



Representative field: overall IgG4/IgG ratio is >50%

HISTOLOGICAL FEATURES OF PROBABLE IGG4-RELATED DISEASE

- Fibro-inflammatory condition characterized by increased IgG4 positive plasma cells. May present as an isolated or multi-organ disorder; very few cases in the CNS.
- Diagnosis requires clinical and serologic correlation (serum IgG4).
- CNS involvement reported between ages 28 - 74 years (~20 cases)
- **Histologic features:**
 - Lymphoplasmacytic infiltrate rich
 - Enriched for IgG4-positive plasma cells
 - Storiform fibrosis
 - Obliterative phlebitis
- **Treatment:**
 - Usually good response to steroids.
 - Rituximab is an emerging therapy.

Acknowledgements

Drs. Toland, Wheeler, and Vogel

Drs. Xu, Menke, and Natkunam (Hematopathology)

Dr. Fischbein (Neuroradiology)

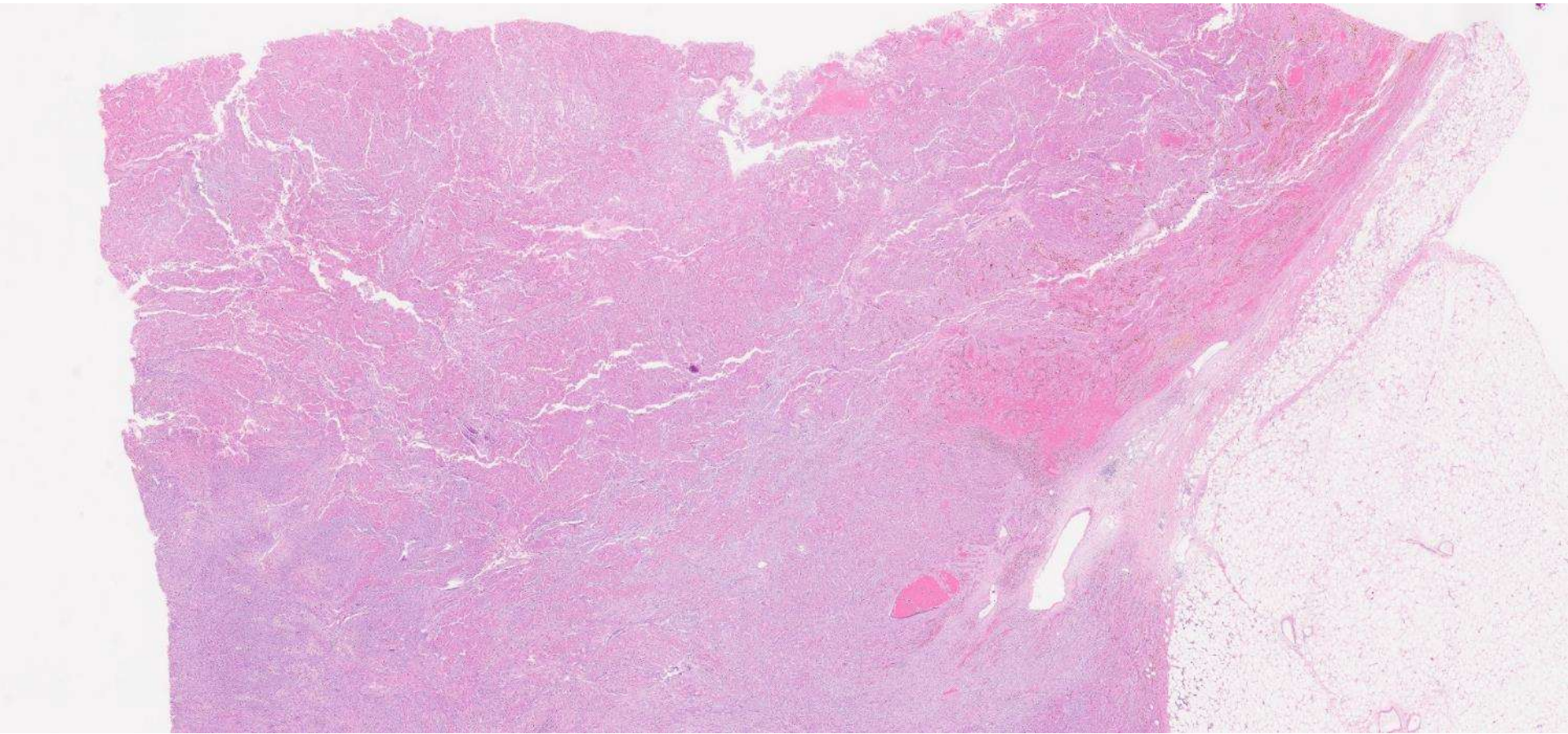
References

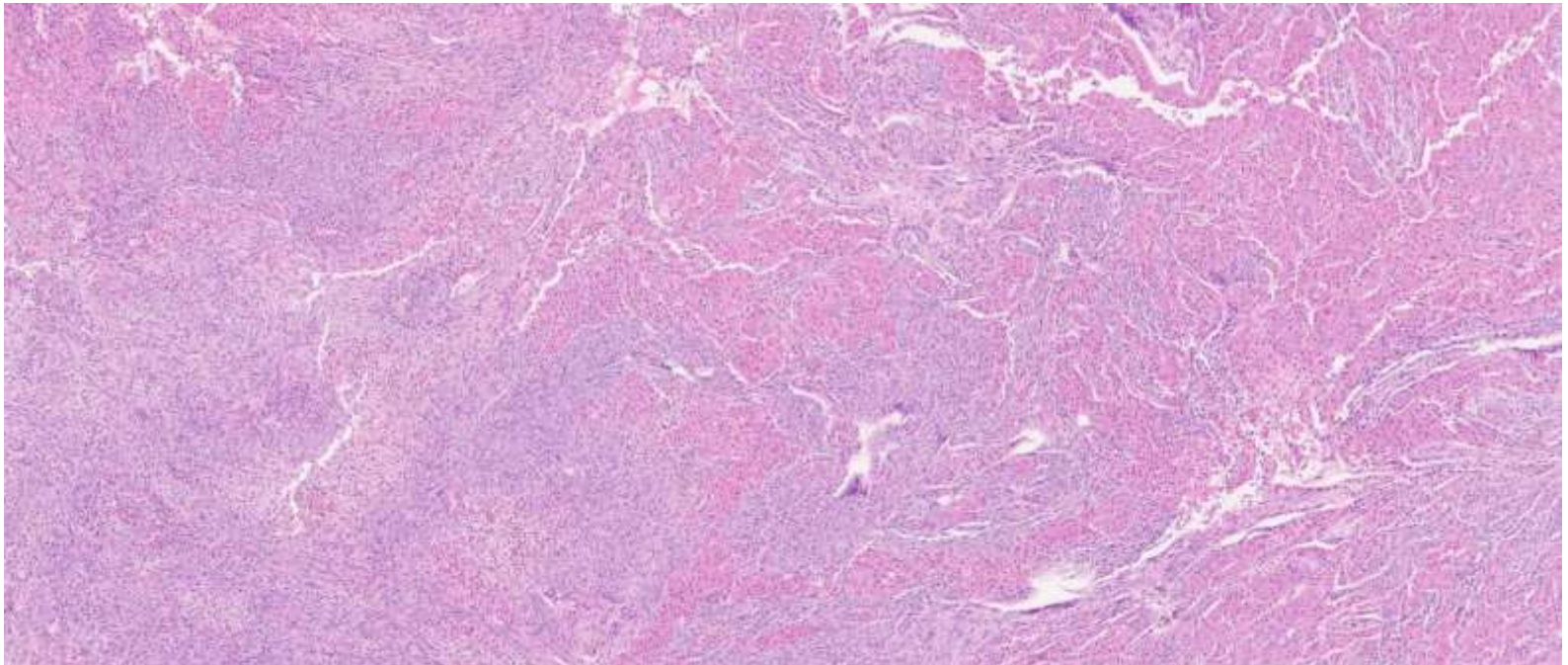
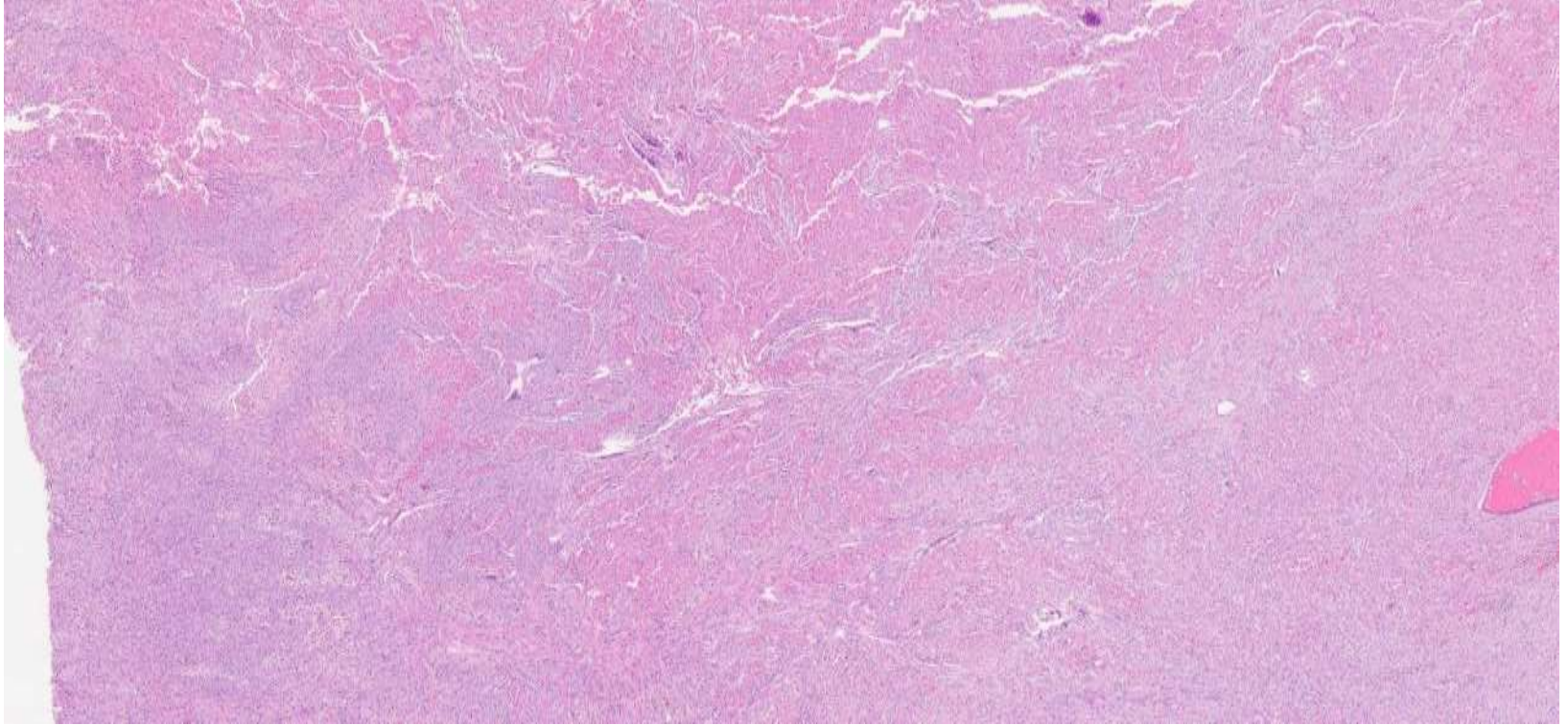
1. Deshpande, et al. "Consensus statement on the pathology of IgG4-related disease." *Modern Pathology* 25, (2012): 1181–92.
2. Regev K, et al. Central nervous system manifestation of IgG4-related disease. *JAMA Neurol.* 2014;71:767–770.
3. Goulam-Houssein S, et al. IgG4-related intracranial disease. *Neuroradiol J.* 2019;32:29-35
4. Lindstrom KM, et al. IgG4-related meningeal disease: clinico-pathological features and proposal for diagnostic criteria. *Acta Neuropathol.* 2010;120:765-76.
5. Tanboon J, Felicella MM, Bilbao J, Mainprize T, Perry A. Probable IgG4-related pachymeningitis: a case with transverse sinus obliteration. *Clin Neuropathol.* 2013 Jul-Aug;32(4):291-7. doi: 10.5414/NP300575. PMID: 23320997.

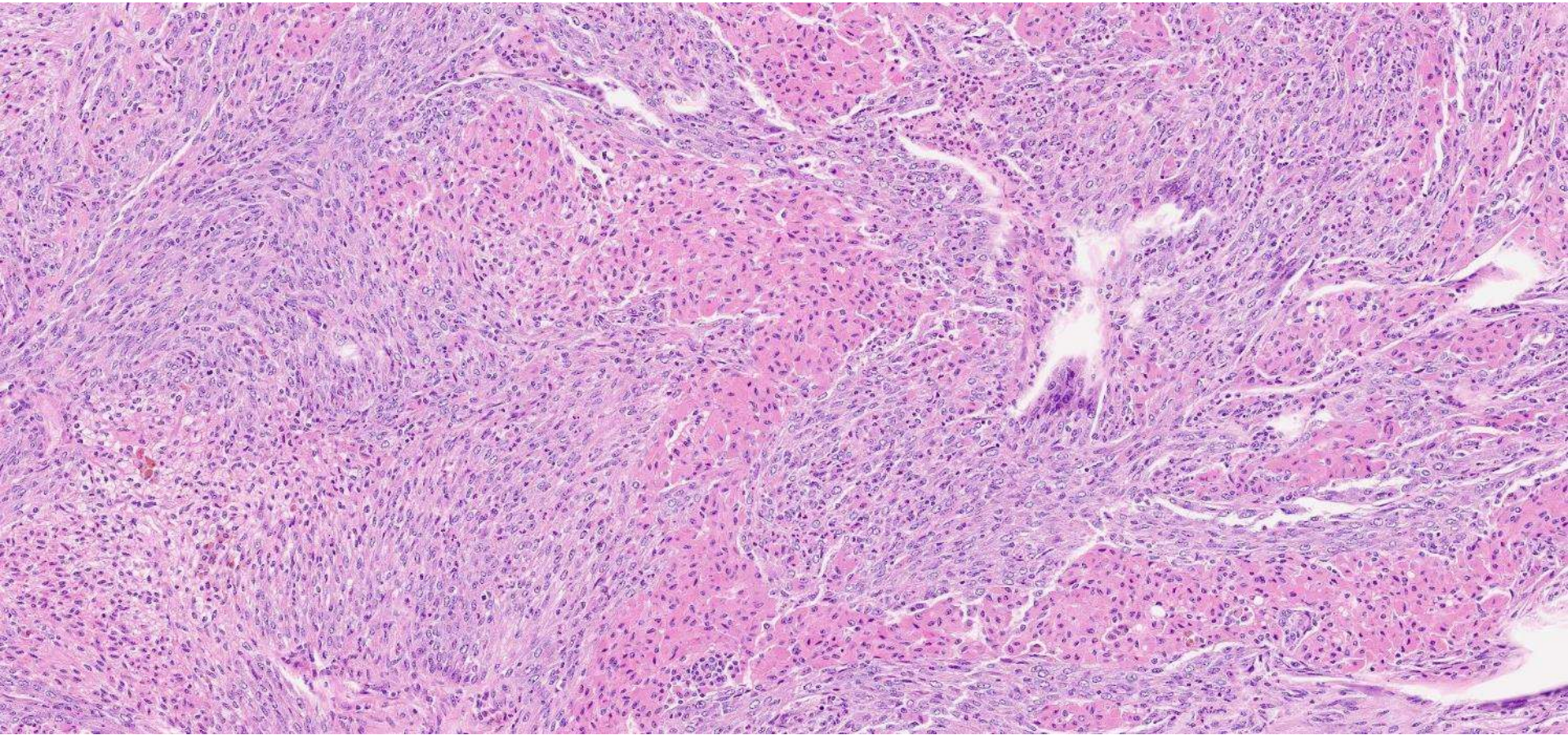
22-0107
scanned slide avail!

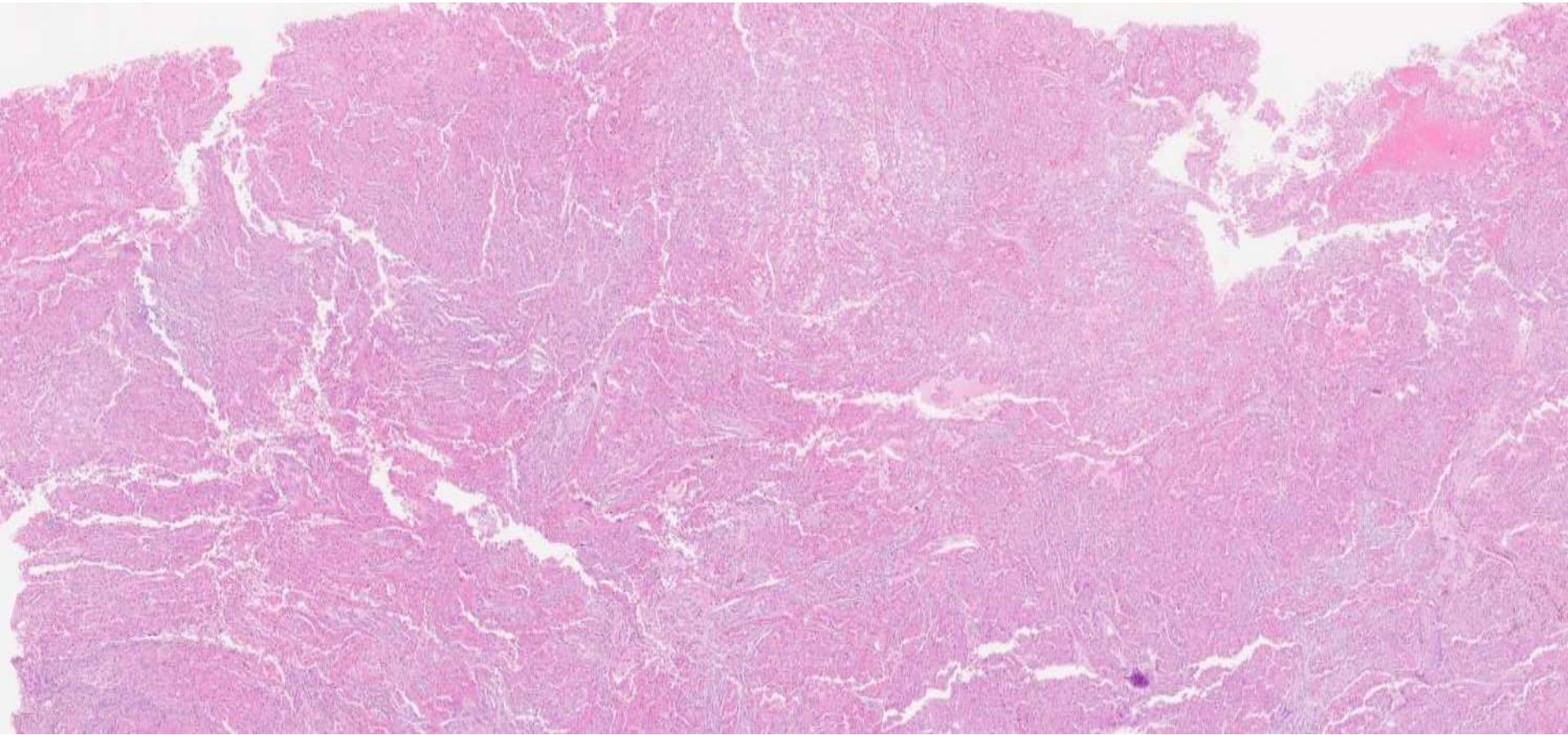
Ankur Sangoi; El Camino Hospital

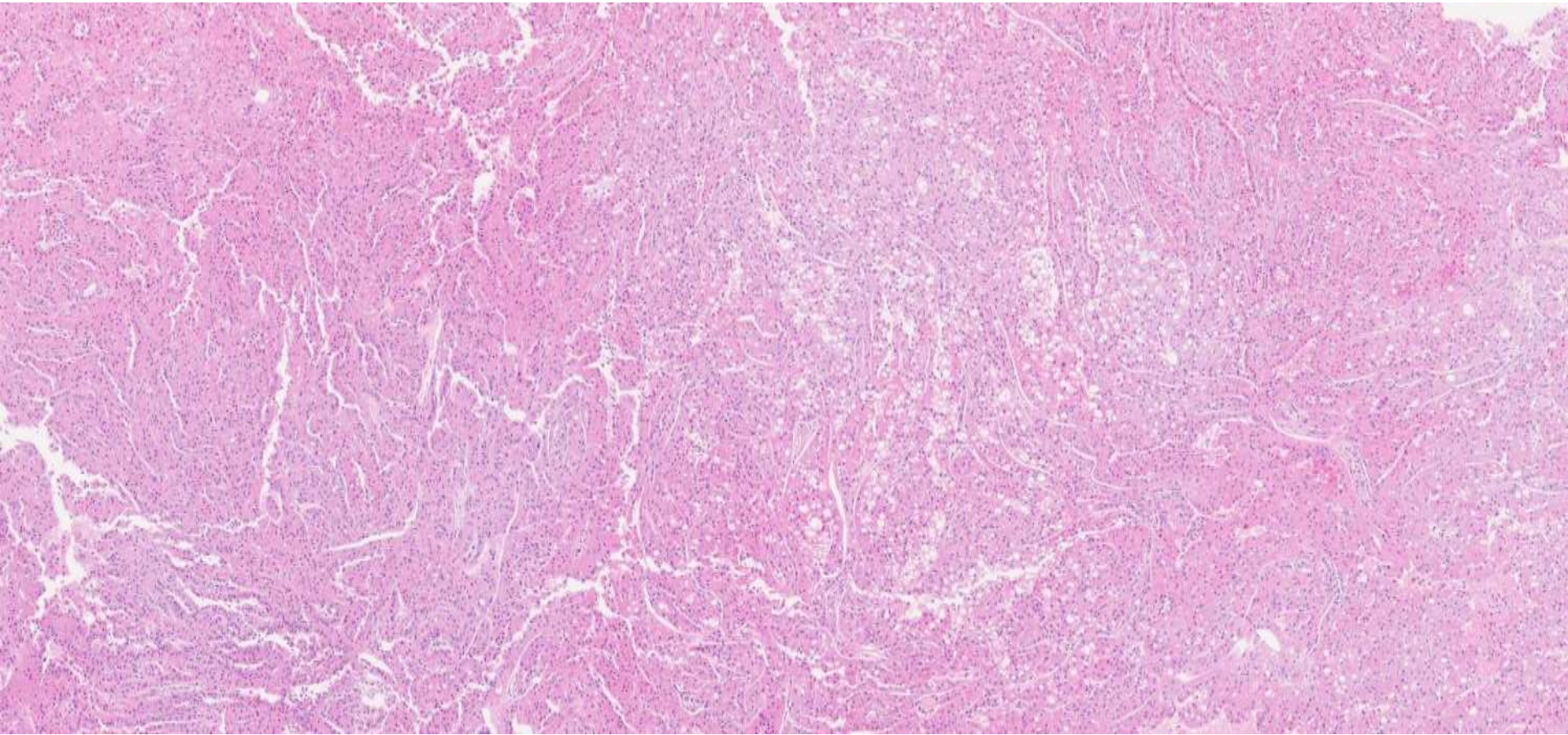
50-year-old M with renal mass, radical nephrectomy
performed.

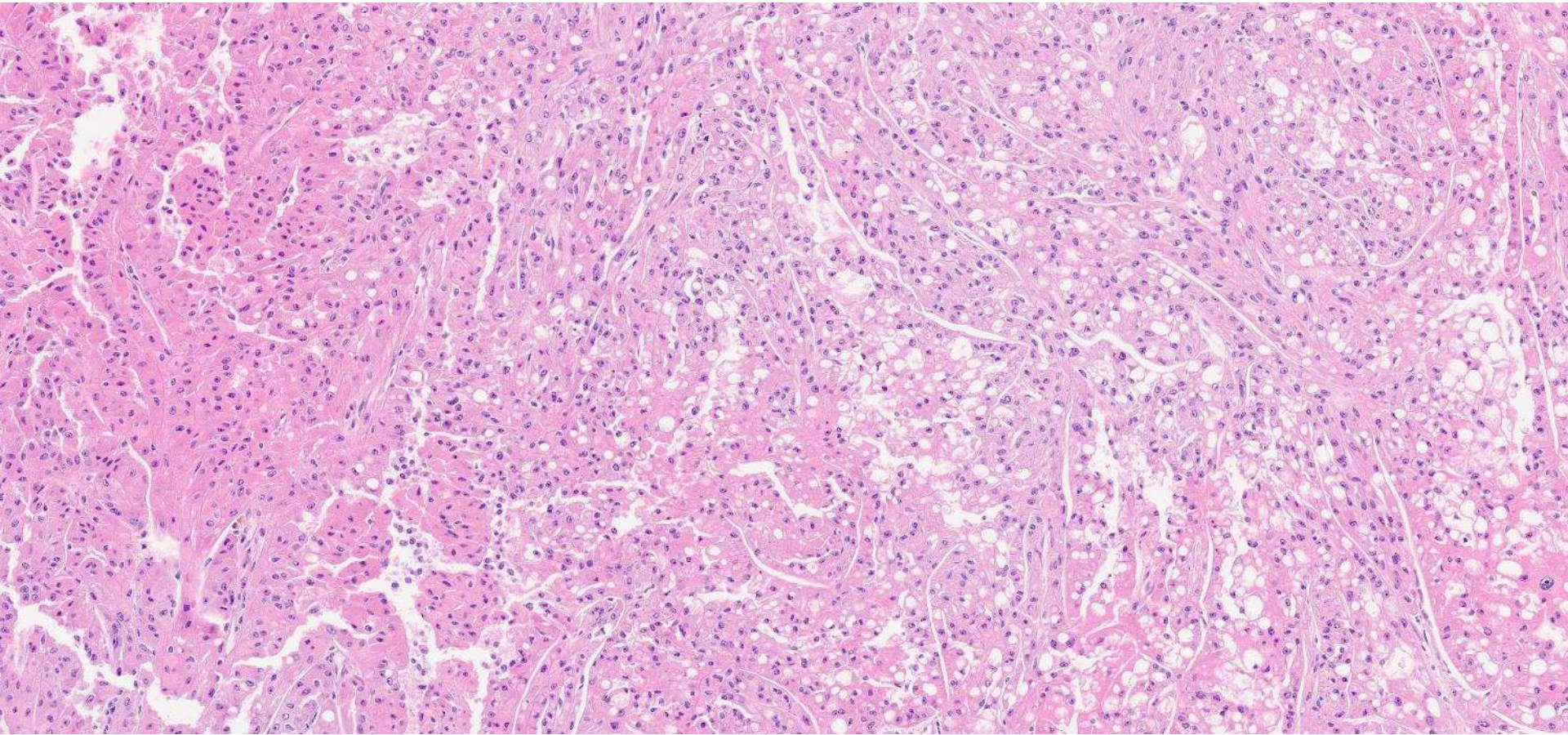


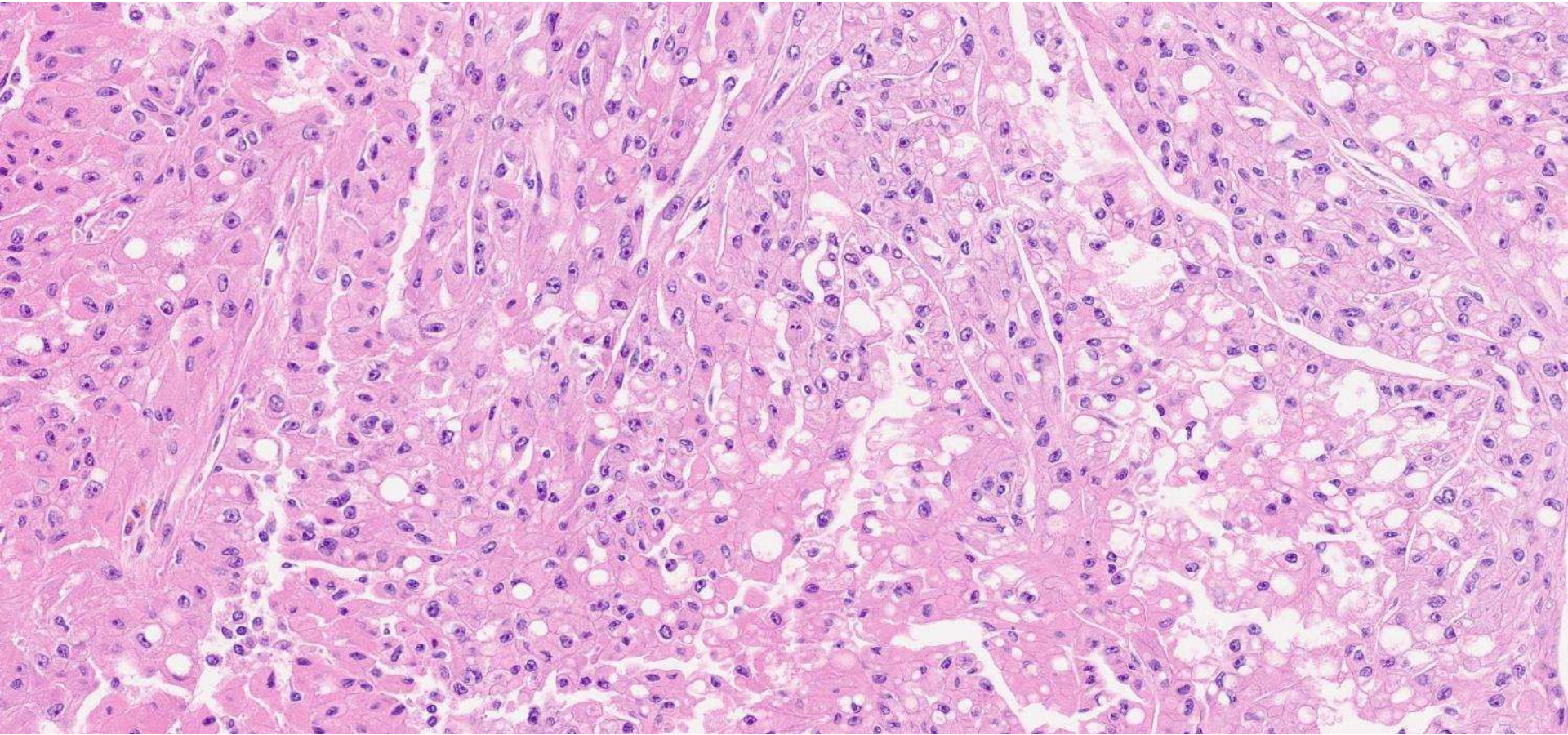


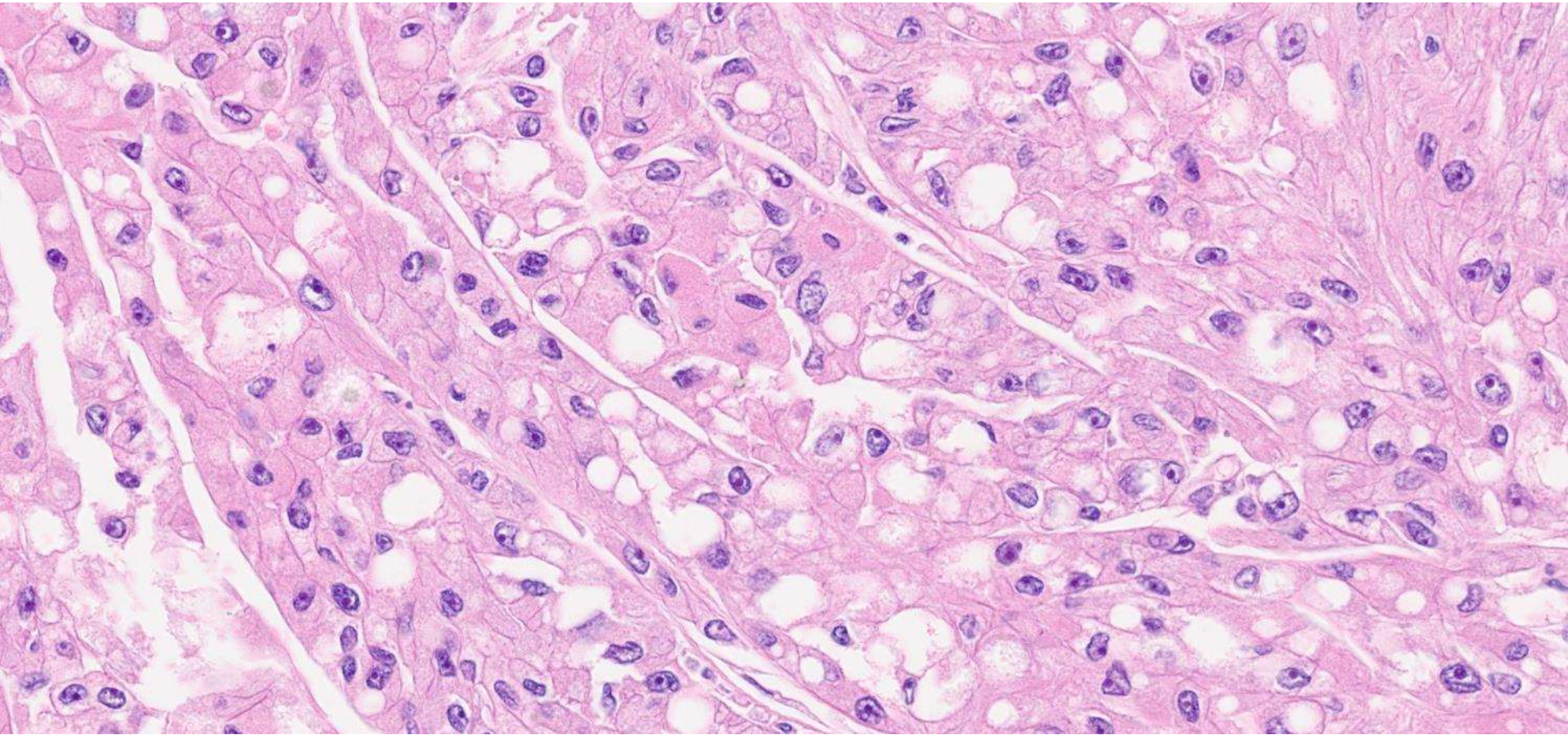


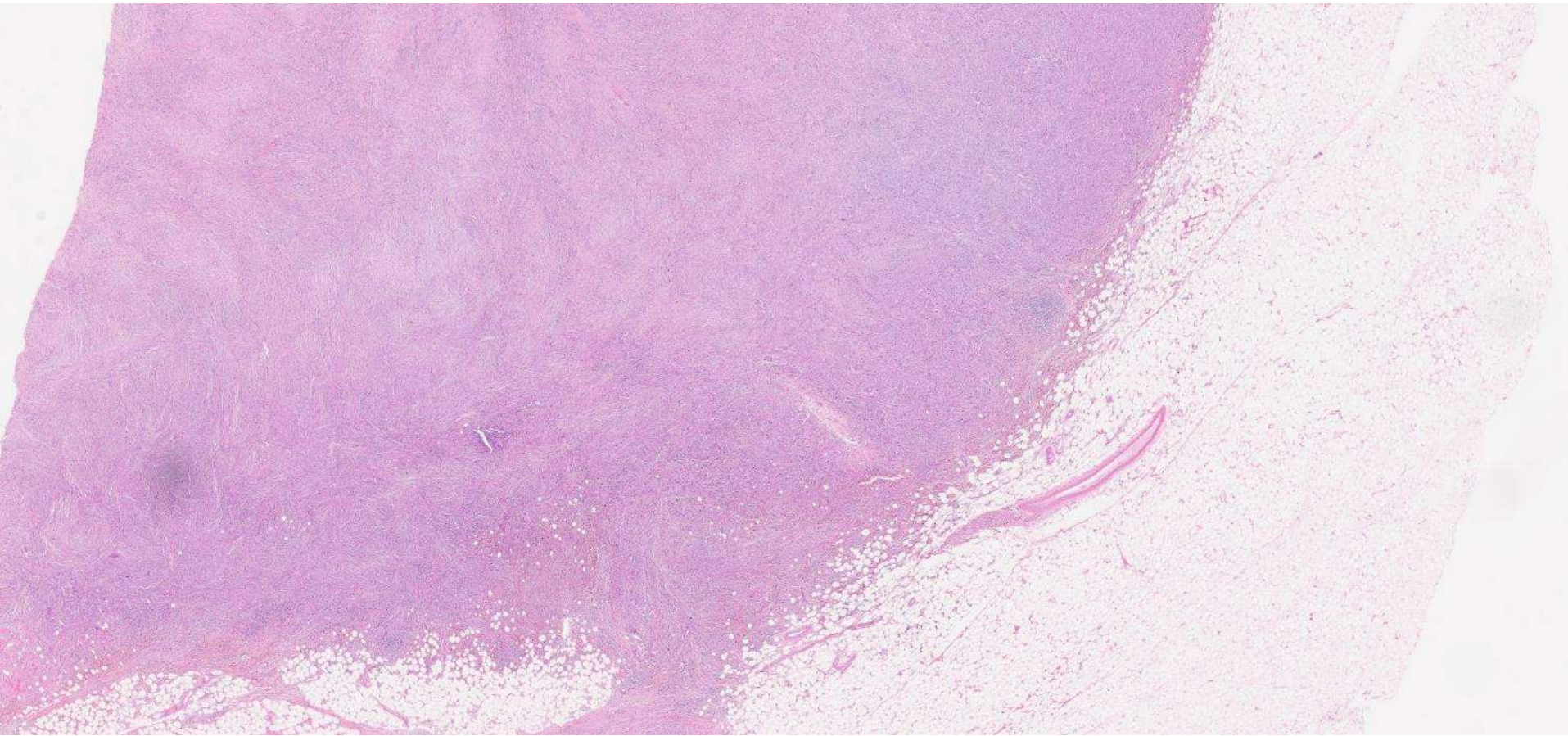


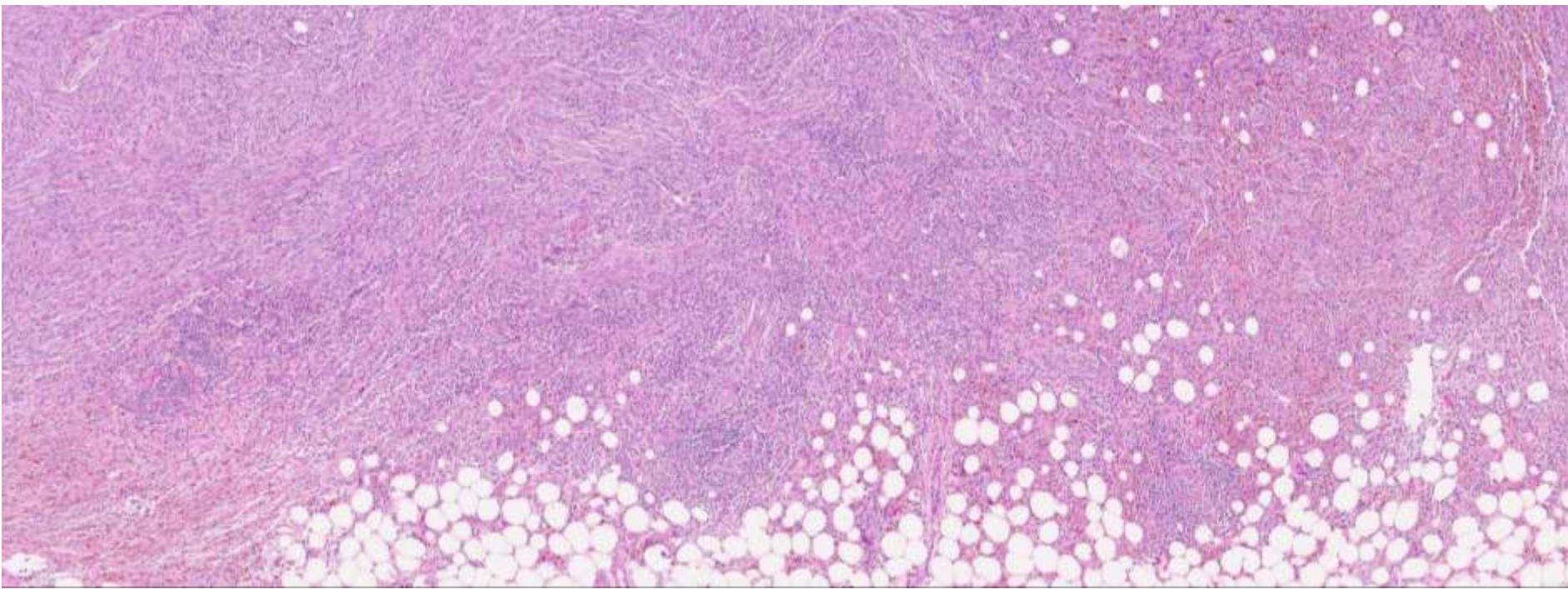
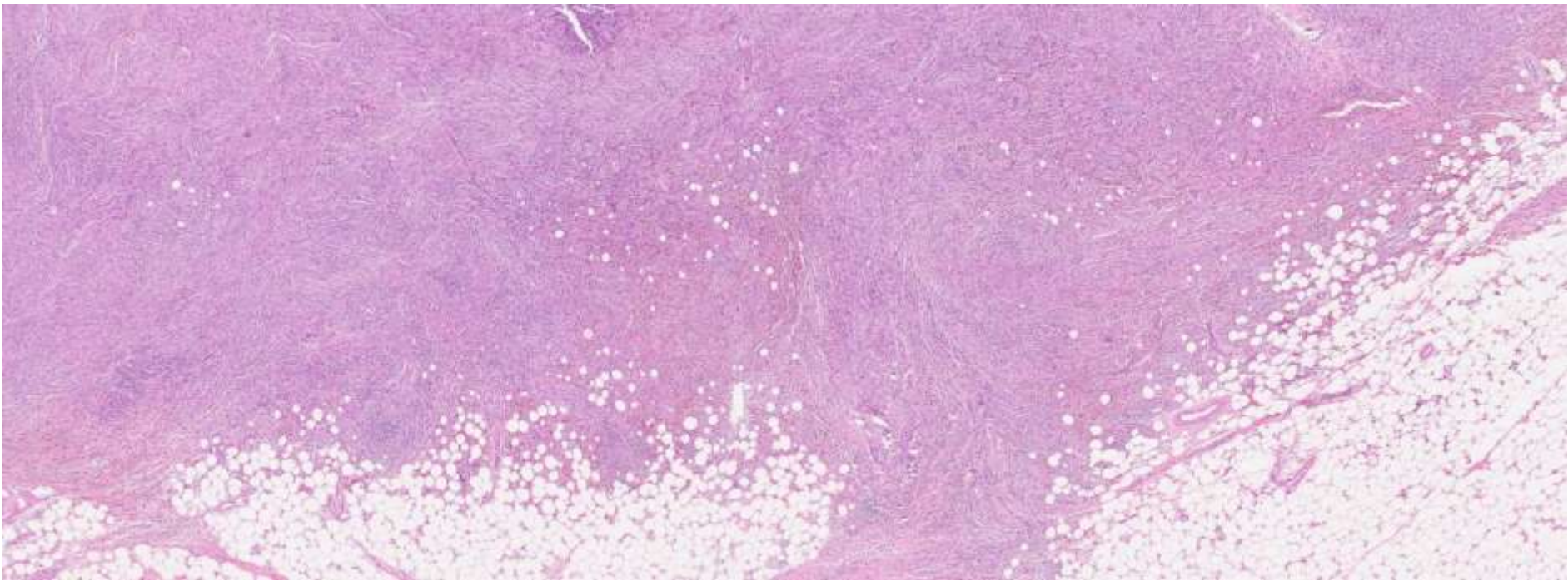


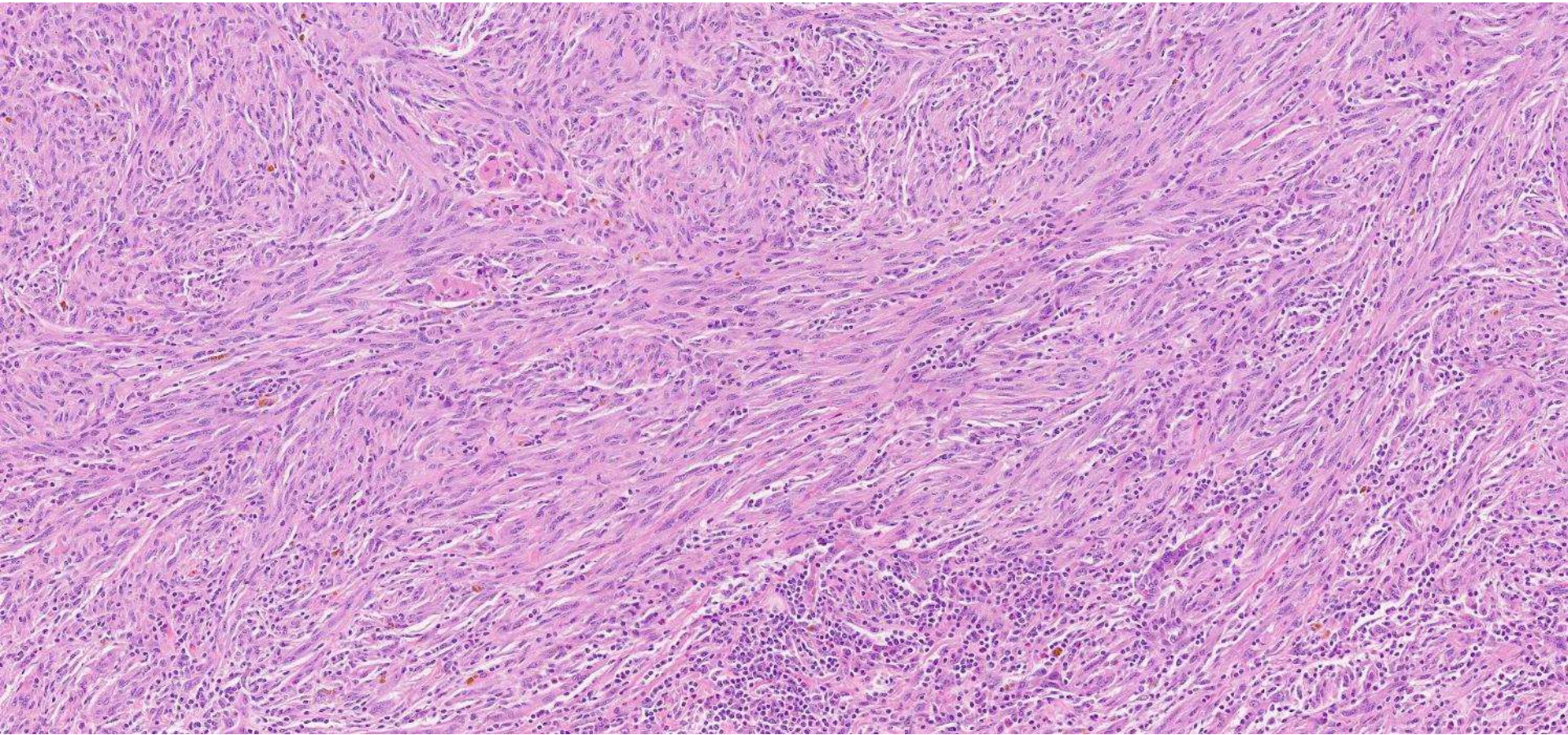


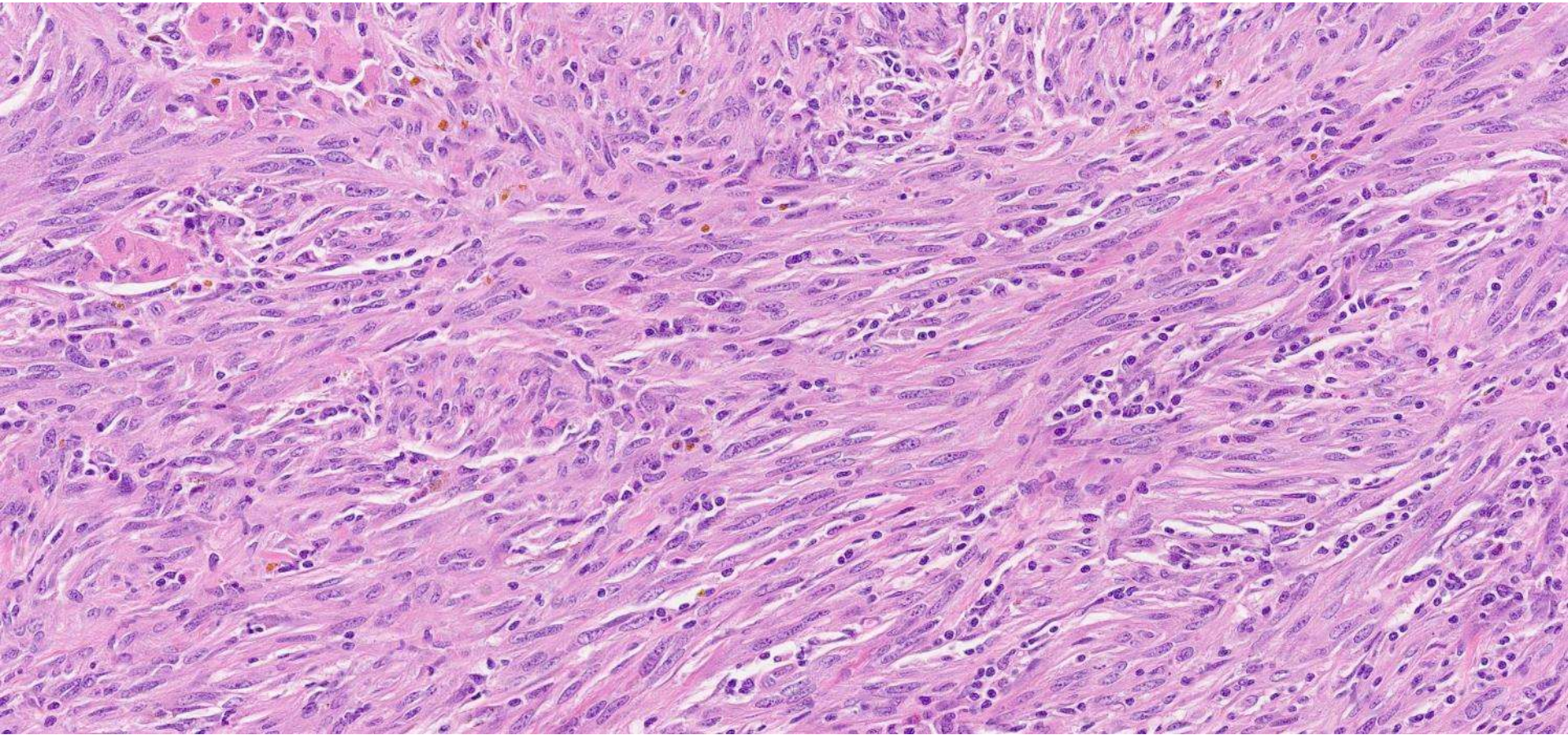


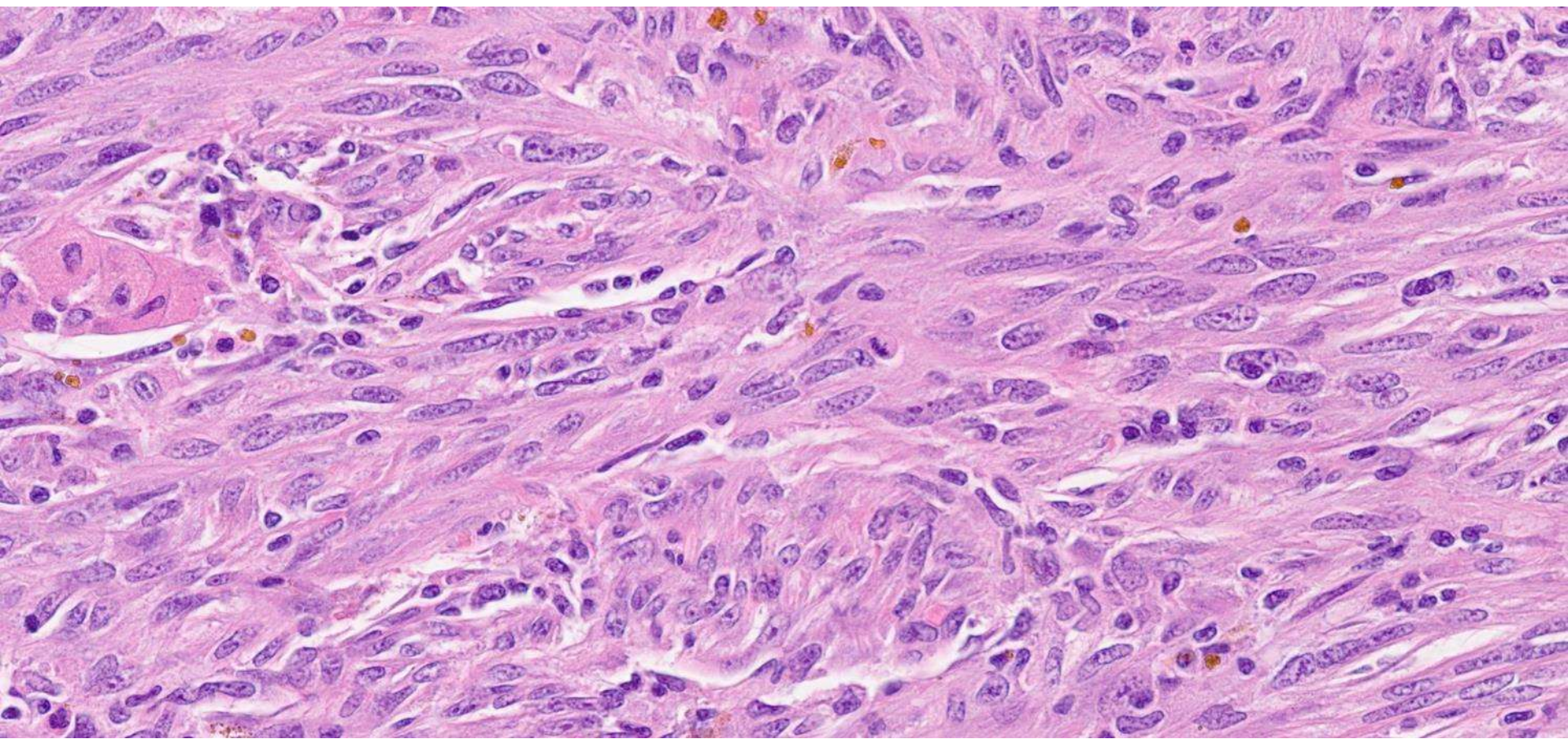












DDx

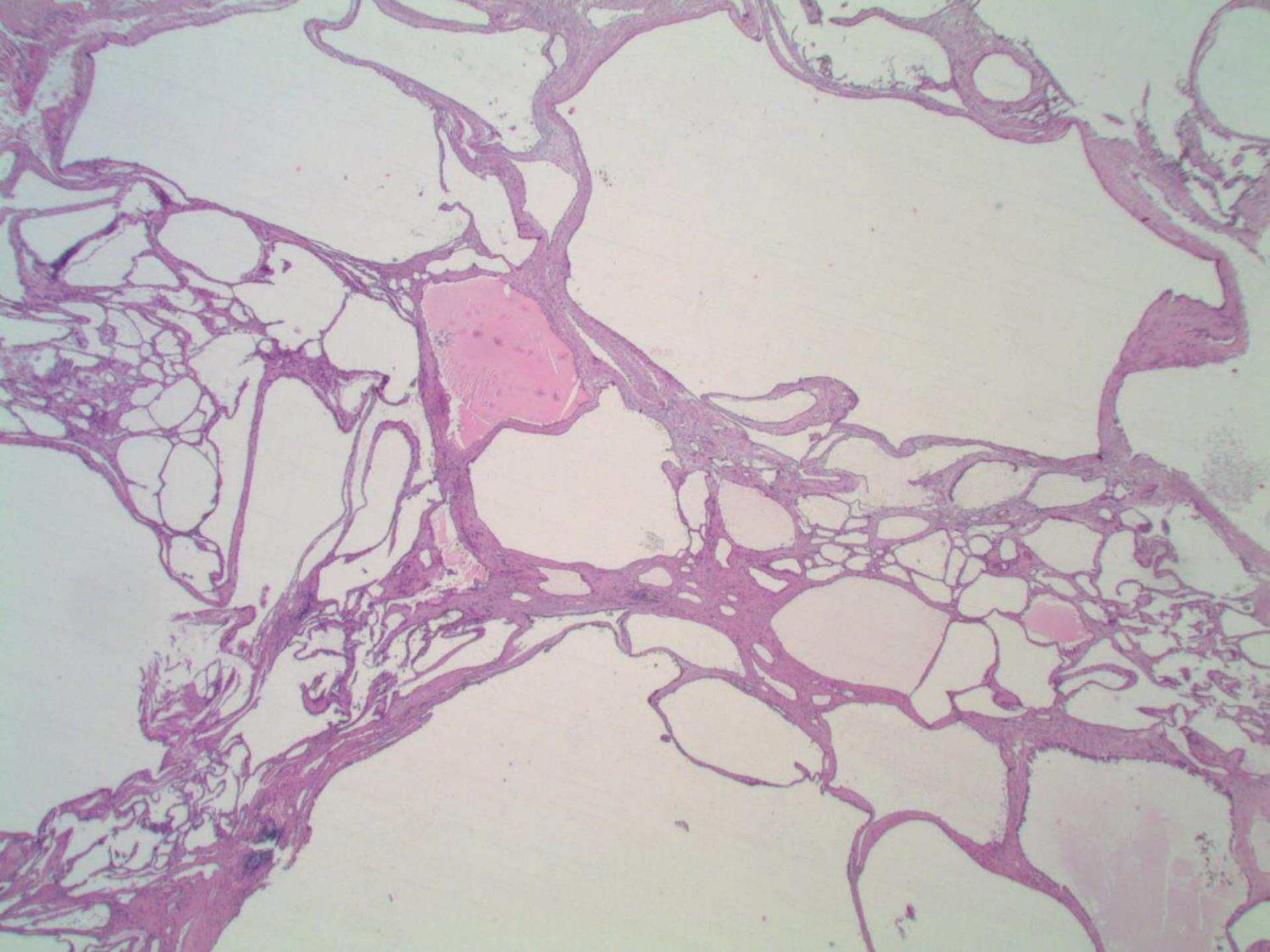
- **Acquired cystic disease-associated RCC**
- **SDHB-deficient RCC**
- **Chromophobe RCC**
- **MITF RCC**
- **Clear cell RCC**
- **Tubulocystic RCC**
- **FH-deficient RCC**
- **ALK RCC**
- **ESC RCC**
- **SMARCB1-deficient RCC/medullary carcinoma**
- **Eosinophilic vacuolated tumor**
- **Urothelial carcinoma**
- **Leiomyosarcoma**
- **Metastasis**
- **Metastasis to renal tumor**

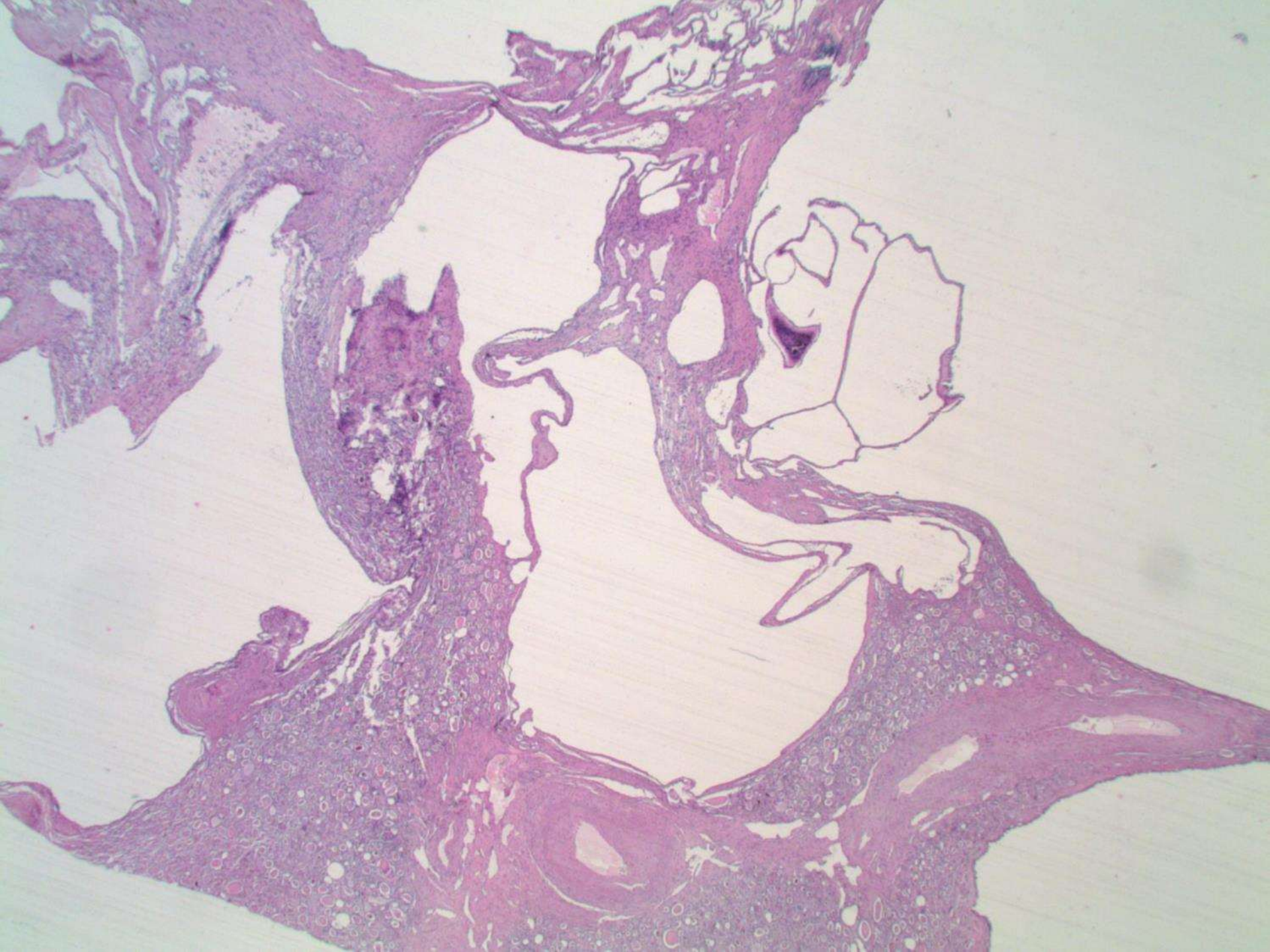
IHC summary

- **Positive: PAX8 (strong), AMACR (strong), CD10 (weak), CAIX (patchy)**
- **Negative: CK7, CK20, CD117, CAIX, cathepsinK, GATA3, NKX3.1**

**what's the background
kidney look like?**







Final Dx

- **SARCOMATOID Acquired cystic disease-associated RCC**
- SDHB-deficient RCC
- Chromophobe RCC
- MiTF RCC
- Clear cell RCC
- Tubulocystic RCC
- FH-deficient RCC
- ALK RCC
- ESC RCC
- SMARCB1-deficient RCC/medullary carcinoma
- Eosinophilic vacuolated tumor
- Urothelial carcinoma
- Leiomyosarcoma
- Metastasis
- Metastasis to renal tumor

Spectrum of Epithelial Neoplasms in End-Stage Renal Disease

An Experience From 66 Tumor-Bearing Kidneys With Emphasis on Histologic Patterns Distinct From Those in Sporadic Adult Renal Neoplasia

Satish K. Tickoo, MD,* Mariza N. dePeralta-Venturina, MD,†‡ Lara R. Harik, MD,*
Heath D. Worcester, MD,§ Mohamed E. Salama, MD,‡ Andrew N. Young, MD,§ Holger Moch, MD,||
and Mahul B. Amin, MD§

Abstract: Most (up to 71%) of renal cell neoplasms occurring in patients with end-stage renal disease (ESRD), particularly with acquired cystic disease of the kidney (ACDK), have been reported to be papillary renal cell carcinoma (RCC). Our initial experience with tumors in such a setting indicated that many tumors were histologically difficult to classify into the known subtypes of RCC or had features that were different from those in sporadically occurring RCCs. In this study on 66 ESRD kidneys (52 of which showed features of ACDK) removed because tumors were detected in them, we found two major groups of RCC. Overall, there were 261 grossly identified tumors in these kidneys, and many additional tumors were observed on microscopic evaluation in some. Of the two major groups of RCCs, one consisted of tumors similar to those seen in sporadic settings (ie, clear-cell, papillary, and chromophobe RCC), and these formed the dominant mass in 12 (18%), 10 (15%), and 5 (8%) of the 66 kidneys, respectively. The other group consisted of two subtypes of RCC that appear quite unique to ESRD. The more common tumor that we have designated as "acquired cystic disease-associated RCC" was seen as the dominant mass in 24 (36%) of 66 of the kidneys, and it formed the most common tumor type among the smaller nondominant masses, as well. It was characterized by a typical microcystic architecture, eosinophilic cytoplasm with Fuhrman's grade 3 nuclei, and frequent association with intratumoral oxalate crystals. Additionally, these tumors frequently, but usually focally, exhibited papillary architecture, and clear cytoplasm. These tumors occurred only in kidneys with ACDK, and not in noncystic ESRD. The other category was "clear-cell papillary RCC of the end-stage kidneys," present as the dominant mass in 15 (23%) of the 66 kidneys and occurring in both the ACDK and noncystic ESRD. These predominantly cystic tumors showed prominent papillary architecture with purely clear-cell cytology. Immunohistochemical studies in

tumors with histology similar to the known subtypes of sporadic RCC showed immunoprofiles similar to that reported in sporadically occurring tumors. The two subtypes of RCC unique to ESRD had distinctive immunoprofiles supporting their separate morphologic subcategorization. Only the acquired cystic disease-associated RCC showed lymph node metastases in 2 cases and sarcomatoid features in 2 more cases. One of the latter 2 died with widespread metastatic disease within 34 months of nephrectomy. Thus, a broad spectrum of renal cell tumors exist in ESRD, only some of which resemble the sporadic RCCs. Acquired cystic disease-associated RCC is the commonest tumor subtype in ESRD, and biologically it appears to be more aggressive than the other tumor subtypes in ESRD.

Key Words: end-stage renal disease, acquired cystic disease of kidney, acquired cystic disease-associated renal cell carcinoma, clear-cell papillary renal cell carcinoma of the end-stage kidneys, papillary renal cell carcinoma, immunohistochemistry

(*Am J Surg Pathol* 2006;30:141–153)

TABLE 4. Tumors Occurring in Kidneys With End-Stage Renal Disease

A) Those resembling sporadic renal tumors
Clear cell (conventional) renal cell carcinoma
Papillary renal cell carcinoma
Type 1
Type 2
Chromophobe renal cell carcinoma
B) Tumors distinct from sporadic renal tumors
Acquired cystic disease-associated renal cell carcinoma
Clear cell-papillary renal cell carcinoma of the end-stage kidneys
C) Other tumor-like lesions
Cysts
Putative precursor lesions
Clustered microcystic lesions
Papillary adenomas

Acquired Cystic Disease-associated Renal Cell Carcinoma (ACD-RCC)

A Multiinstitutional Study of 40 Cases With Clinical Follow-up

Christopher G. Przybycin, MD, Holly L. Harper, MD,† Jordan P. Reynolds, MD,* Cristina Magi-Galluzzi, MD, PhD,* Jane K. Nguyen, MD, PhD,‡ Angela Wu, MD,§ Ankur R. Sangoi, MD,|| Peter S. Liu, MD,¶ Saleem Umar, MD,# Rohit Mehra, MD,§ Xiaochun Zhang, MD, PhD,* Roni M. Cox, MD,* and Jesse K. McKenney, MD**

Abstract: The incidence of renal cell carcinoma (RCC) is known to be higher in patients with end-stage renal disease, including those with acquired cystic kidney disease due to dialysis. Acquired cystic disease (ACD)-associated RCC was recently incorporated into the 2016 WHO Classification of Tumors of the Urinary System and Male Genital Tract as a distinct entity and is reportedly the most common RCC arising in end-stage renal disease. In this study, we sought to further describe clinicopathologic findings in a large series of ACD-RCC, emphasizing histologic features, immunophenotype, clinical outcome, and patterns of disease spread. We collected 40 previously unpublished cases of ACD-RCC with mean clinical follow-up of 27 months (median, 19 mo; range, 1 to 126 mo). Mean tumor size was 2.7 cm (median, 2.4 cm), and 32 tumors (80%) were confined to the kidney (pT stage less than pT3a). International Society of Urological Pathology grade was 3 in 37 cases (92.5%), grade 2 in 1 case (2.5%), and grade 4 in 2 cases (5%). Architectural variability among ACD-RCC was common, as 39 cases (98%) showed varying combinations of tubular, cystic, solid, and/or papillary growth. ACD-RCC frequently occurred in association with other renal tumor subtypes within the same kidney, including papillary RCC (14 patients), papillary adenomas (7 cases), clear cell papillary RCC (5 cases), clear cell RCC (1 case), and RCC, unclassified type (1 case). A previously undescribed pattern of perinephric and renal sinus adipose tissue involvement by dilated epithelial cysts with minimal or absent intervening capsule or renal parenchyma was identified in 20 cases (50%); these cysts were part of the tumor itself in 5 cases (25%) and were part of

the non-neoplastic acquired cystic change in the background kidney in the remaining 15 cases (75%). Of the 24 cases (60%) with tissue available for immunohistochemical stains, 19 (79%) were positive for PAX8, 20 (83%) showed negative to patchy expression of cytokeratin 7, and 24 (100%) were both positive for AMACR and negative for CD117. Fumarate hydratase expression was retained in all tumors, including those with nuclear features resembling fumarate hydratase-deficient RCCs. Of the 36 patients (90%) with available follow-up information, 4 (11%) experienced adverse events: 2 patients developed a local recurrence, 1 patient experienced multiple visceral metastases and subsequently died of disease, and 1 patient developed metastases to regional lymph nodes only. One local recurrence and the lymph node only metastasis both had an unusual, exclusively cystic pattern of growth. In summary, we present the largest clinicopathologic series of ACD-RCC to date and describe previously unreported cystic patterns of local soft tissue involvement and recurrence/metastases.

Key Words: renal cell carcinoma, acquired cystic disease, end-stage renal disease

(*Am J Surg Pathol* 2018;42:1156–1165)

The use of dialysis to aid or replace kidney function, though essential for many patients, is not without consequence. Among the potential drawbacks is the development of acquired cystic kidney disease (ACKD), defined as ≥ 3 cysts per kidney, or cysts accounting for $\geq 25\%$ of the total renal parenchyma, in patients without

TABLE 1. Characteristics of ACD-Associated RCC

Tumor Characteristics	No. Cases	% of Total (n = 40)
Cytoplasmic characteristics		
Sieve-like vacuoles	40	100
Eosinophilic	40	100
Cytoplasmic clearing	28	70
Hemosiderin	34	85
Nuclear features		
HLRCC-like nuclei	4	10
Architectural features		
No. architectural patterns*		
1 pattern	1	2.5
2 patterns	12	30
3 patterns	18	45
4 patterns	9	22.5
Intracystic growth	35	88
Cysts involving fat	20	50
Presence of oxalate crystals		
Intratumoral	34	85
Peritumoral	33	83
Tumor features		
Necrosis	2	5
Rhabdoid	2	5
Sarcomatoid	1	2.5
Additional features		
Organizing hemorrhage	32	80
Intratumoral histiocytes	20	50
Psammoma bodies	21	53
Atypical cysts	31	78

Comprehensive Clinicopathologic Analyses of Acquired Cystic Disease–associated Renal Cell Carcinoma With Focus on Adverse Prognostic Factors and Metastatic Lesions

Fumiyoshi Kojima, MD, PhD,* Jatin S. Gandhi, MD,† Ibu Matsuzaki, CT, IAC,*
Akinori Iba, MD,‡ Scott Collier, MD,† Takanori Yoshikawa, ME,§ Yuichi Kinoshita, CM, IAC,||
Kenji Warigaya, MD,* Masakazu Fujimoto, MD, PhD,* Naoto Kuroda, MD, PhD,¶
Eiichi Morii, MD, PhD,# Isao Hara, MD, PhD,‡ Shin-ichi Murata, MD, PhD,*
and Mahul B. Amin, MD†

Abstract: Acquired cystic disease of kidney-associated renal cell carcinoma (ACD-RCC) is a distinct subtype of renal cell carcinoma with unique morphologic and clinicopathologic features. Generally, ACD-RCC is regarded as an indolent tumor; however, prognostic and outcomes data have been conflicted by the limited and relatively low number of cases with patient follow-up or adverse events. In this study, we focused on the histology of metastatic lesions and identifying prognostic factors associated with metastatic progression. From 32 cases in the cohort, 9 patients had metastasis [ACD-RCC (M+)] and 23 patients were without metastasis [ACD-RCC (M–)]. The median age of patients was 52 years; right side, n=10; left side, n=18; bilateral, n=4; median tumor size=2.6 cm; median hemodialysis duration=17 y; and the median duration of follow-up was 50 mo. Immunohistochemistry showed ACD-RCC to be racemase positive and CK7 negative to focally positive within tumor cells, with consistent positivity for renal histogenesis-associated markers (PAX8 and RCC antigen); S100A1 was a less reliable marker at metastatic sites. All metastatic ACD-RCC except 2 cases involved lymph nodes (para-aortic, renal hilar, subclavicular). Overall, 6/9 (67%) had visceral metastasis to sites including lung (n=3), liver (n=3), bone (n=5),

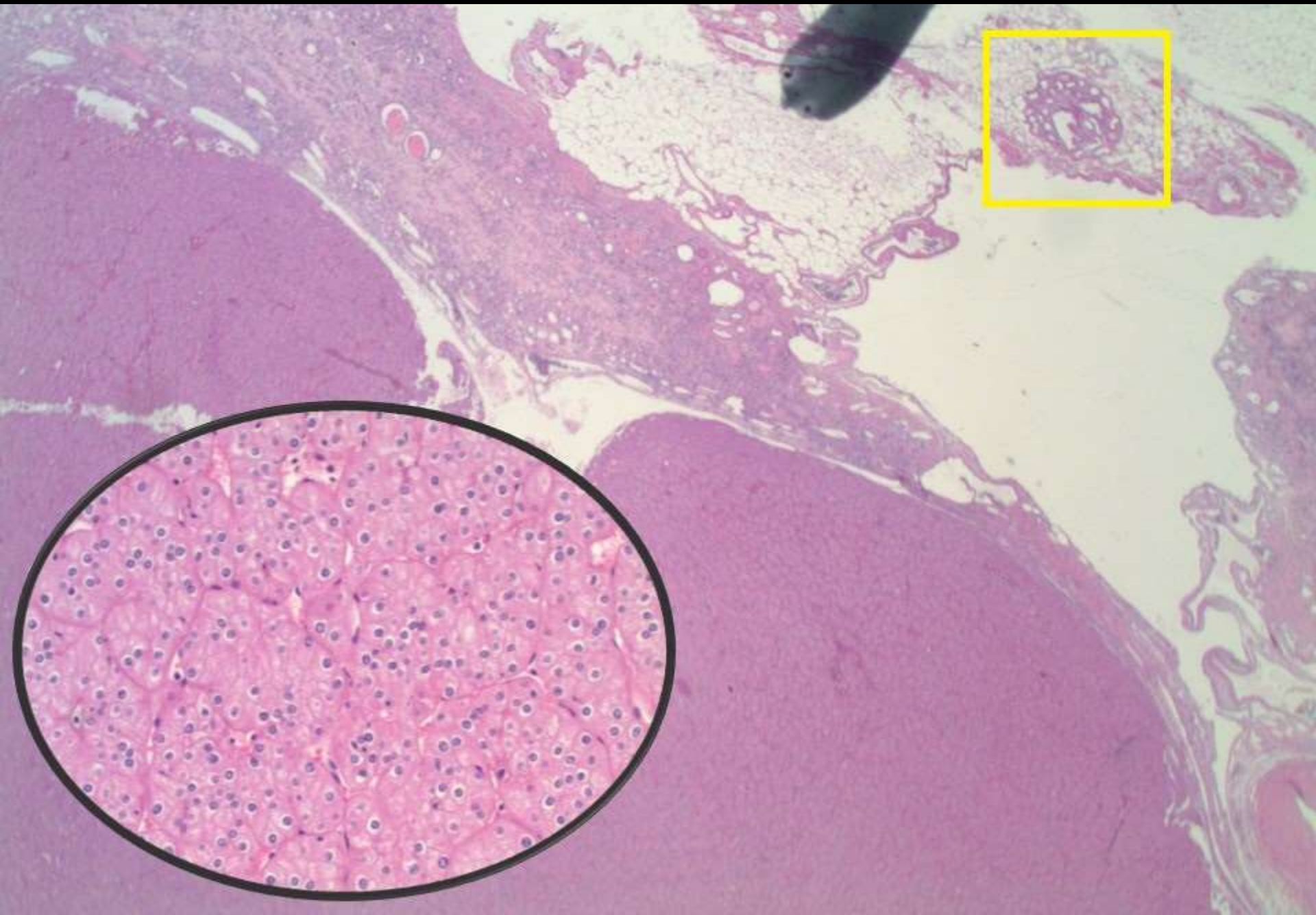
stomach (n=1), and brain (n=1). In total, 5/9 (56%) metastatic tumors had distinctive cystic growth pattern at the metastatic site; intriguingly metastatic tumors had intrametastatic oxalate crystal deposition, a pathognomonic feature associated with primary tumors. Four of nine (44%) patients with ACD-RCC (M+) had fatal outcomes due to metastatic disease. Clinically significant adverse prognostic features associated with metastasis [median follow-up 47 mo, ACD-RCC (M+) vs. ACD-RCC (M–), 50 mo] included: duration of hemodialysis (≥ 20 vs. <20 y, $P=0.0085$) and tumor necrosis ($P=0.049$). Because of sufficient overlap between these parameters, the study was not able to identify parameters that would be reliable in further management strategies, in clinical settings. Our data indicate that ACD-RCC is a tumor which has distinct metastatic potential with nodal and visceral tropism and proclivity for cystic morphology at metastatic sites; this is the first report of the presence of oxalate crystals in metastatic tumors. Our data suggest that ACD-RCC patients with prolonged hemodialysis and tumoral coagulative necrosis require additional surveillance in view of the association of these parameters with metastatic progression.

Key Words: acquired cystic disease–associated renal cell carcinoma, acquired cystic kidney, S100A1, prognosis, metastasis

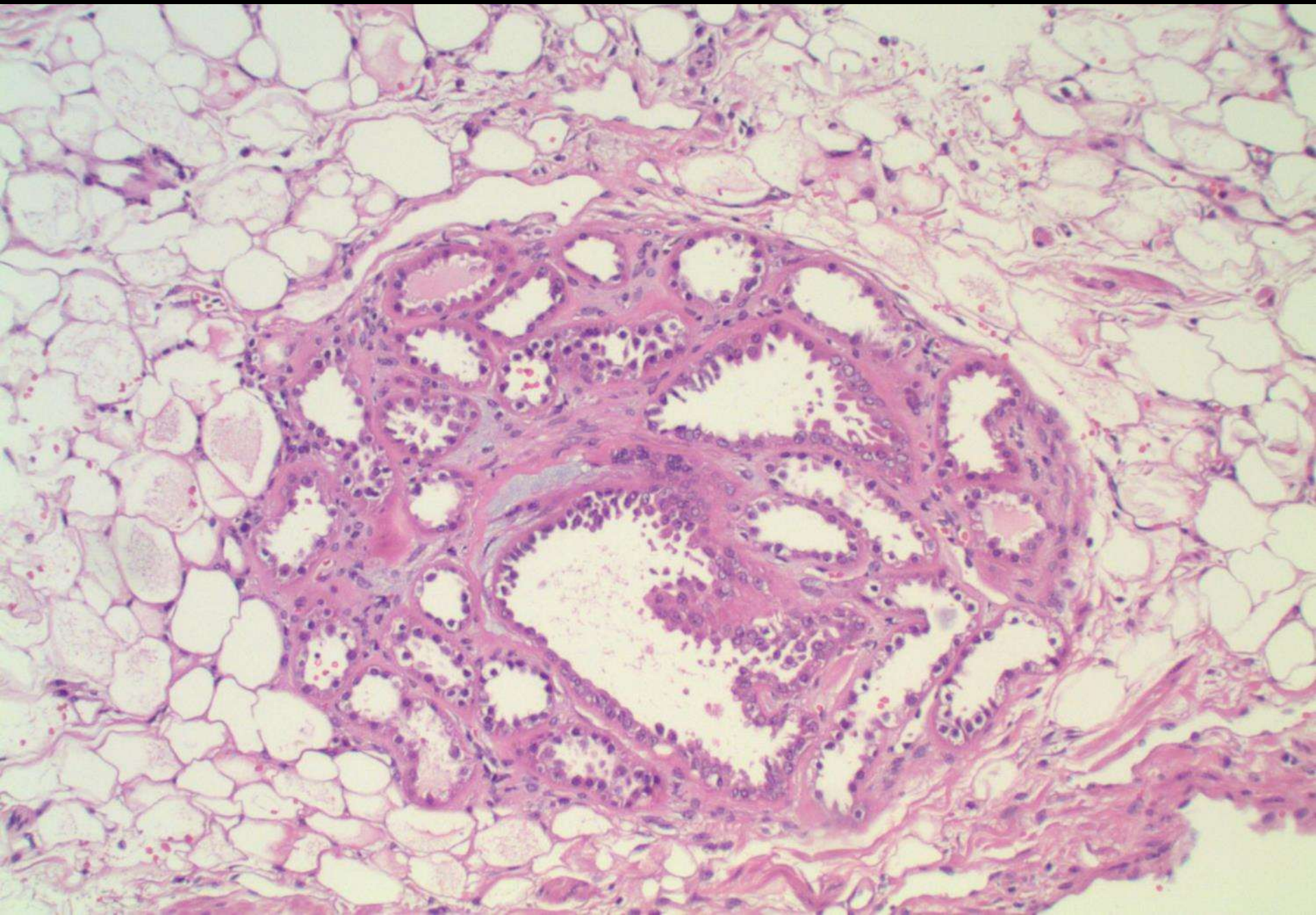
TABLE 3. Pathologic Findings of ACD-RCC

	ACD-RCC (M+) (N = 9)	ACD-RCC (M-) (N = 23)	<i>P</i>
Size			
Average	4.0	2.9	0.146†
Median	2.8	2.6	
Range	2.0-8.5	1.2-7.5	
pT category			
1a	5	19	0.1839‡
1b	1	3	
2a	1	0	
2b	0	0	
3a	1	1	
3b	1	0	
4	0	0	
Perinephric extension			
+	2	1	0.184
-	7	22	
Infiltrative pattern			
inf	3	1	0.0572
exp	6	22	
Coagulative necrosis			
+	6	6	0.0493
-	3	17	
LVI			
+	2	0	0.0726
-	7	23	
Oxalate crystal			
+	5	12	1.00
-	4	11	
Sarcomatoid change			
+	2	2	0.5568
-	7	21	
Grade (WHO)			
2	4	12	1.00§
3	3	8	
4	2	3	

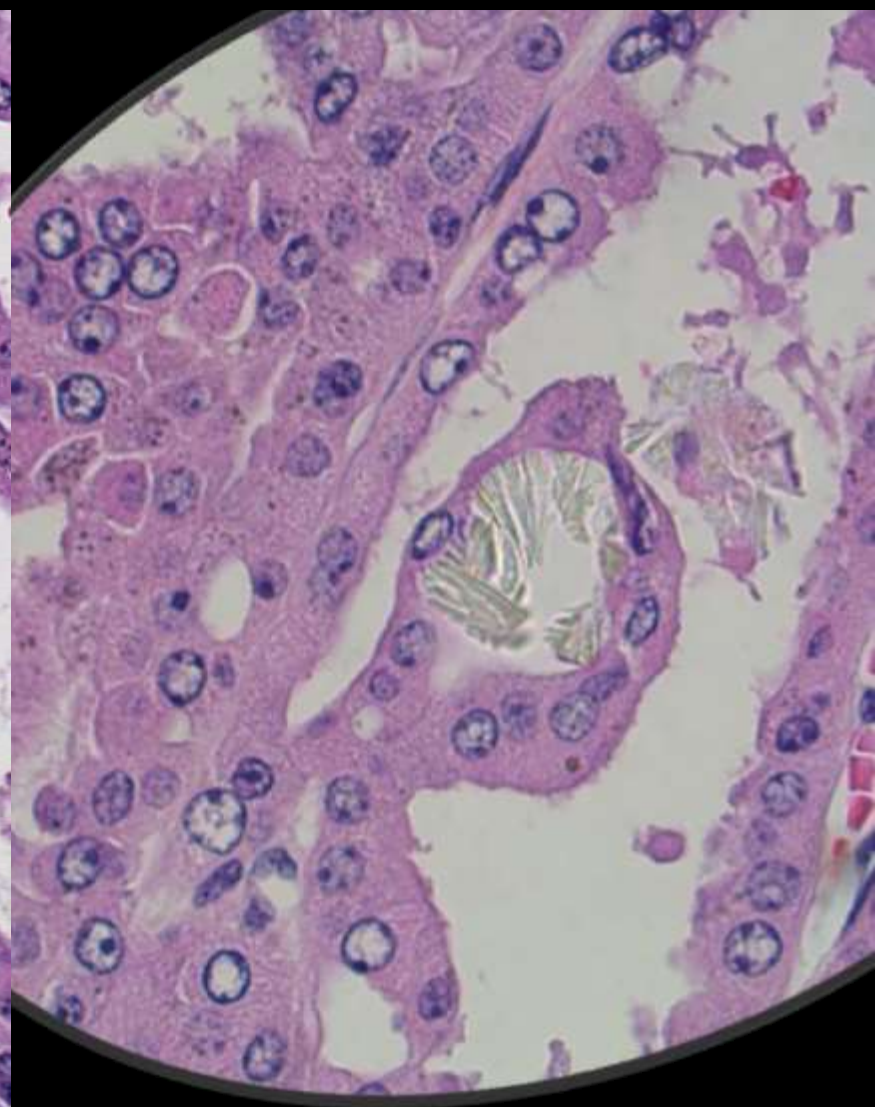
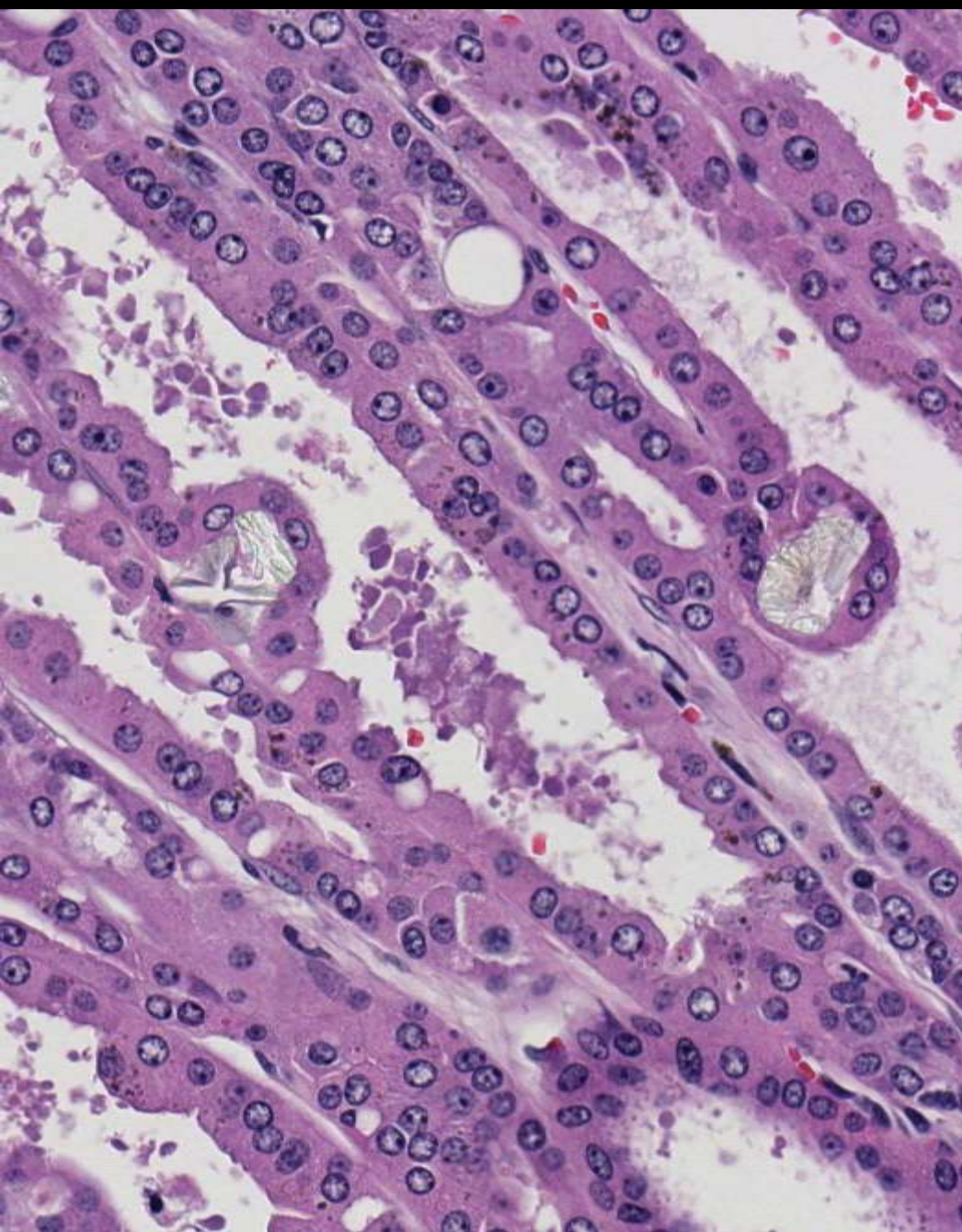
DIFFERENT CASE: chromo-RCC in end-stage kidney



not pT3a!



Calcium oxalate crystals in another ACD-RCC



TAKE HOME POINTS

- **Check the background kidney!**
- **ACD-RCC specific to end-stage kidney, but other tumor types can occur**
 - Calcium oxalate helpful in some cases
 - IHC of limited use (AMACR+++?)
 - ACD-RCC can behave aggressively despite small size, low stage
 - Caution on isolated cysts within fat (not pT3a!)
- **“sarcomatoid” not an RCC subtype**